International Ocean Discovery Program Expedition 392 Scientific Prospectus

Agulhas Plateau Cretaceous Climate: drilling the Agulhas Plateau and Transkei Basin to reconstruct the Cretaceous–Paleogene tectonic and climatic evolution of the Southern Ocean basin

Gabriele Uenzelmann-Neben
Co-Chief Scientist
Department of Geosciences, Geophysics Section
Alfred Wegener Institute
Helmholtz Center for Polar and Marine Research
Germany

Steven M. Bohaty
Co-Chief Scientist
School of Ocean and Earth Science
University of Southampton
United Kingdom

Denise K. Kulhanek
Expedition Project Manager/Staff Scientist
International Ocean Discovery Program
Texas A&M University
USA

IODP
INTERNATIONAL OCEAN DISCOVERY PROGRAM

Publisher's notes

This publication was prepared by the *JOIDES Resolution* Science Operator (JRSO) at Texas A&M University (TAMU) as an account of work performed under the International Ocean Discovery Program (IODP). This material is based upon work supported by the JRSO, which is a major facility funded by the National Science Foundation Cooperative Agreement number OCE1326927. Funding for IODP is provided by the following international partners:

National Science Foundation (NSF), United States
Ministry of Education, Culture, Sports, Science and Technology (MEXT), Japan
European Consortium for Ocean Research Drilling (ECORD)
Ministry of Science and Technology (MOST), People's Republic of China
Korea Institute of Geoscience and Mineral Resources (KIGAM)
Australia-New Zealand IODP Consortium (ANZIC)
Ministry of Earth Sciences (MoES), India
Coordination for Improvement of Higher Education Personnel (CAPES), Brazil

Portions of this work may have been published in whole or in part in other IODP documents or publications.

This IODP *Scientific Prospectus* is based on precruise *JOIDES Resolution* Facility advisory panel discussions and scientific input from the designated Co-Chief Scientists on behalf of the drilling proponents. During the course of the cruise, actual site operations may indicate to the Co-Chief Scientists, the Expedition Project Manager/Staff Scientist, and the Operations Superintendent that it would be scientifically or operationally advantageous to amend the plan detailed in this prospectus. It should be understood that any substantial changes to the science deliverables outlined in the plan presented here are contingent upon the approval of the IODP JRSO Director and/or *JOIDES Resolution* Facility Board.

Disclaimer

Copyright

Citation

Uenzelmann-Neben, G., Bohaty, S.M., and Kulhanek, D.K., 2020. *Expedition 392 Scientific Prospectus: Agulhas Plateau Cretaceous Climate*. International Ocean Discovery Program. https://doi.org/10.14379/iodp.sp.392.2020

ISSN

World Wide Web: 2332-1385

Abstract

The long-term climate transition from the Cretaceous greenhouse to the late Paleogene icehouse provides an opportunity to study changes in Earth system dynamics associated with large changes in global temperature and atmospheric CO_2 levels. Elevated CO_2 levels during the mid-Cretaceous supergreenhouse interval (~95–80 Ma) resulted in low meridional temperature gradients, and oceanic deposition during this time was punctuated by widespread episodes of severe anoxia termed oceanic anoxic events, resulting in enhanced burial of organic carbon in conjunction with transient carbon isotope and temperature excursions. The prolonged interval of mid-Cretaceous warmth and subsequent Late Cretaceous–Paleogene climate trends, as well as intervening short-lived climate excursions, are poorly documented in the southern high latitudes. International Ocean Discovery Program (IODP) Expedition 392 aims to drill five sites in the southwest Indian Ocean on the Agulhas Plateau and in the Transkei Basin, positioned at paleolatitudes of 65°–58°S during the Late Cretaceous (100–66 Ma) and in the new and evolving gateway between the South Atlantic, Southern Ocean, and southern Indian Ocean basins. Recovery of basement rocks and expanded sedimentary sequences from the Agulhas Plateau and Transkei Basin will provide a wealth of new data to (i) determine the nature and origin of the Agulhas Plateau and (ii) significantly advance the understanding of how Cretaceous temperatures, ocean circulation, and sedimentation patterns evolved as CO_2 levels rose and fell and the breakup of Gondwana progressed. Importantly, Expedition 392 drilling will test competing hypotheses concerning Agulhas Plateau large igneous province formation and the role of deep ocean circulation changes through southern gateways in controlling Late Cretaceous–Paleogene climate evolution.

Schedule for Expedition 392

International Ocean Discovery Program (IODP) Expedition 392 is based on IODP drilling Proposal 834-Full2 and 834-Add (available at **http://iodp.tamu.edu/scienceops/expeditions/agulhas_plateau_climate.html**). Following evaluation by the IODP Scientific Advisory Structure, the expedition was scheduled for the research vessel (R/V) *JOIDES Resolution*, operating under contract with the *JOIDES Resolution* Science Operator (JRSO). At the time of publication of this *Scientific Prospectus*, the expedition is scheduled to start in Cape Town, South Africa, on 4 February 2021 and to end in Cape Town, South Africa, on 6 April 2021. A total of 61 days will be available for the transit, drilling, coring, and downhole measurements described in this report (for the current detailed schedule, see **http://iodp.tamu.edu/scienceops**). Further details about the facilities aboard *JOIDES Resolution* can be found at **http://iodp.tamu.edu/labs/index.html**.

Introduction

The warmest sustained greenhouse episode of the past ~150 My occurred during the mid-Cretaceous between ~95 and 80 Ma (e.g., Clarke and Jenkyns, 1999; Friedrich et al., 2012; Huber et al., 2002, 2018). Proxy data and climate models suggest CO_2 levels during this supergreenhouse climate phase may have been as high as 3500 parts per million by volume (ppmv), which then subsequently declined to less than 560 ppmv following the Eocene–Oligocene climate transition at ~34 Ma (Berner et al., 1983; Bice et al., 2006; DeConto and Pollard, 2003; Royer et al., 2004). High-latitude temperatures were exceptionally warm during the prolonged period of elevated CO_2 levels in the mid-Cretaceous, resulting in low meridional temperature gradients (Bice et al., 2006, 2003; Forster et al., 2007; Huber et al., 1995). However, Cretaceous warmth was also interrupted by periods of rapid global climate change during oceanic anoxic events (OAEs), which were associated with widespread reduction in basin ventilation and major changes in ocean temperature and circulation (Arthur et al., 1985, 1987; Jenkyns, 2003, 2010; Schlanger and Jenkyns, 1976; Sinninghe Damsté et al., 2010). The timing, magnitude, and oceanographic and ecological consequences of the Cretaceous greenhouse warming are poorly documented in the southern high latitudes. Furthermore, greenhouse climate conditions with CO_2 levels approaching those of the Cretaceous–Paleogene interval are envisioned for the near future (e.g., Hay, 2011) calling for action to gain a better understanding of their potential impacts.

Climate models have identified significant geography-related Cenozoic cooling arising from the opening of Southern Ocean gateways, pointing toward a progressive strengthening of the Antarctic Circumpolar Current (ACC) as the major cause for cooler deep ocean temperatures (Sijp et al., 2014; Toggweiler and Russell, 2008). Analogous arguments point to a critical role for deep circulation in controlling Late Cretaceous climate evolution (e.g., Frank et al., 1999; MacLeod and Huber, 1996; Robinson and Vance, 2012; Voigt et al., 2013). The southwest Indian Ocean is a key area to retrieve high-quality basement and sedimentary records to test these models and proxy reconstructions concerning the formation of the Agulhas Plateau and the evolution of deep ocean circulation between the Indian and Atlantic Ocean basins. The proposed Expedition 392 drill sites on Agulhas Plateau and Transkei Basin were located at high latitudes during the Late Cretaceous (65°–58°S; Hay et al., 1999; Sewall et al., 2007) and positioned in the gateway between the newly opening South Atlantic, Southern Ocean, and southern Indian Ocean basins. Recovery of basement and sedimentary sequences from this region and comparison with recent results from Naturaliste Plateau drilled during IODP Expedition 369 (Huber et al., 2018) will significantly advance the understanding of large igneous province (LIP) formation and the evolution of ocean temperature, circulation, and sedimentation patterns during the Cretaceous.

Background

Tectonic history of the African–Southern Ocean gateway

During the Early Cretaceous, the African–Southern Ocean gateway was closed and the South American, African, and Antarctic continents were connected (Figure **F1**). Breakup of this region of Gondwana commenced at ~146 Ma and was associated with the formation of two oceanic plateaus (Figure **F1**): the Mozambique Ridge (~136–120 Ma) and the Agulhas Plateau (105–95 Ma) (Gohl and Uenzelmann-Neben, 2001; Gohl et al., 2011; König and Jokat, 2010; Parsiegla et al., 2008; Uenzelmann-Neben et al., 1999). These seafloor elevations constituted barriers for circulation of deep and intermediate water masses as indicated by neodymium (Nd) isotopic evidence for different water masses bathing the Falkland Plateau and the western flank of the Kerguelen Plateau between ~95 and 78 Ma (Murphy and Thomas, 2012, 2013). A deepwater connection between the South Atlantic and the Indian Ocean opened with the separation of the Falkland Plateau from Africa between ~120 and 100 Ma (König and Jokat, 2010).

The origin and development of structural units in the African–Southern Ocean gateway (including the Agulhas Plateau, Mozambique Ridge, Maud Rise, Astrid Ridge, Madagascar Ridge, and Gunnerus Ridge) are heavily debated. Seismic studies and plate tectonic reconstructions suggest that the Agulhas Plateau is a LIP that formed no earlier than 105 Ma (Parsiegla et al., 2008) in combination with the Northeast Georgia Rise and Maud Rise (Gohl and Uenzelmann-Neben, 2001; König and Jokat, 2010; Parsiegla et al., 2008; Uenzelmann-Neben et al., 1999). In contrast, Gohl et al. (2011) suggested the existence of a southeast African super-LIP between ~140 and 95 Ma, which formed as a result of an intense period of magmatism (Charvis et al., 1995; Fischer et al., 2017; Gohl and Uenzelmann-Neben, 2001; Jacques et al., 2019) and consisted of the Northeast Georgia Rise, Agulhas Plateau, Maud Rise, Astrid Ridge, Mozambique Ridge, and Transkei Rise. This southeast African super-LIP is conjectured to be the same size and age as the Kerguelen-Broken Ridge LIP (Coffin and Eldholm, 1994). It is unclear whether this super-LIP includes continental fragments, and its age of formation, as well as the timing of later separation into Mozambique Ridge, Astrid Ridge, Northeast Georgia Rise, Agulhas Plateau, and Maud Rise, remain unresolved.

African–Southern Ocean gateway circulation

In the Cretaceous greenhouse world, the role of oceanic poleward heat transport as a main driver of long-term climate change is uncertain. Low latitudinal thermal gradients and different patterns of runoff and evaporation could have shifted areas of deep convection, and constricted connections between basins could have led to largely internal circulation of deepwater masses in relatively small Cretaceous oceanic basins (120–80 Ma; Friedrich et al., 2008; MacLeod et al., 2011, 2008). Numerical simulations of Cretaceous circulation do not predict overturning circulation in the African–Southern Ocean gateway, although weak circulation connecting the Pacific, Atlantic, and Indian basins is indicated (Uenzelmann-Neben et al., 2017). Cooling due to atmospheric CO_2 reduction, probably because of enhanced carbon burial (Robinson et al., 2010; Robinson and Vance, 2012) and/or evolving tectonic barriers via the formation of oceanic plateaus (Frank and Arthur, 1999), could have resulted in circulation patterns similar to the modern with consequent feedbacks through changing ocean heat transport. Better depth-resolved, empirical constraints on circulation coupled with modeling experiments from critical regions like the southwest Indian Ocean are needed to test and refine these hypotheses.

In the Agulhas Plateau region today, surface and deep currents transport warm and salty waters through the African–Southern Ocean gateway from the Indian Ocean into the southern Atlantic via the Agulhas Current and formation of Agulhas rings, whereas cold water flows eastward into the Indian Ocean (Figure **F2**) (de Ruijter et al., 1999, 2006; Lutjeharms, 1996, 2006; Lutjeharms and Ansorge, 2001; Mantyla and Reid, 1995; Read and Pollard, 1999; Tomczak and Godfrey, 1994; Toole and Warren, 1993; van Aken et al., 2004; You et al., 2003). Water mass exchange in this region is controlled by seafloor topography, requiring a deep and wide gateway. Lutjeharms (1996, 2006) observed that the Agulhas Current hugs the shelf break of the Agulhas Passage and the path of Agulhas rings is influenced by the Agulhas Ridge topography. Both the Agulhas Current and Agulhas rings maintain the energy transfer between the Indian and Atlantic Oceans (Biastoch et al., 2008, 2009). Seafloor elevations, such as the Mozambique Ridge and Agulhas Plateau, constitute barriers for the flow of these oceanic currents and lead to modifications in flow paths.

In the Cretaceous, the presence of large magmatic obstructions likely caused constriction of the African–Southern Ocean gateway and hence were a hindrance to water mass exchange between the Atlantic and Indian basins. Two hypotheses suggest that LIP formation complicated the opening of the African–Southern Ocean gateway: (1) a southeast African super-LIP (140–95 Ma) (Gohl et al., 2011) or (2) the formations of two LIPs between 140 and 120 Ma (Mozambique Ridge and Astrid Ridge) (König and Jokat, 2010) and 105 and 95 Ma (Northeast Georgia Rise, Agulhas Plateau, and Maud Rise) (Parsiegla et al., 2008; Uenzelmann-Neben et al., 1999). The second hypothesis allows deepwater circulation between the Tethys/Indian Ocean and Southern Ocean/South Atlantic from ~120 Ma onward. Convergence of Falkland and Kerguelen intermediate water masses may have then initiated following tectonic subsidence of the intervening barriers in the Southern Ocean basin. Therefore, instead of the African–Southern Ocean gateway slowly opening and allowing increasingly deeper water mass exchange, geophysical studies (Fischer, 2017; Gohl et al., 2011; König and Jokat, 2010; Schlüter and Uenzelmann-Neben, 2008) indicate prolonged restricted circulation in the opening gateway (e.g., Transkei Basin). In this model, only surface current flow occurred between the Tethys/Indian Ocean and the evolving Southern Ocean/South Atlantic, whereas deep and intermediate water masses were blocked by this barrier. With the full clearance of the South American plate and the separation of the Agulhas Plateau–Northeast Georgia Rise–Maud Rise LIP into three parts (Figure **F1**), changes in the seafloor topography may have allowed open-ocean circulation across the African–Southern Ocean gateway by ~94 Ma.

Recovery of Cretaceous basement and sediments from the Agulhas Plateau during Expedition 392 will provide an archive of African–Southern Ocean gateway evolution from the onset of Agulhas Plateau–Northeast Georgia Rise–Maud Rise LIP formation (<105 Ma) to a fully open gateway (~94 Ma) (König and Jokat, 2010; Parsiegla et al., 2008). The sedimentary rock sequences targeted for drilling on the Agulhas Plateau and in the Transkei Basin during Expedition 392 will provide long records of changing paleodepth, paleoceanography, and paleoclimate spanning the mid-Cretaceous through the Paleogene, documenting the formation of the plateau in presumed subaerial or shallow-water environments and its subsidence to bathyal depths.

Seismostratigraphic model

The seismostratigraphic model developed for the proposed Expedition 392 drill sites (Figures **F3**, **F4**, **F5**, **F6**, **F7**, **F8**) is tentative because the uppermost part of the sedimentary sequence of the Agulhas Plateau has previously been sampled by scientific drilling at only one location (IODP Expedition 361 Site U1475 on the southwest Agulhas Plateau; Hall et al., 2017), and therefore the interpretations for ages of reflectors should be applied with caution. The seismostratigraphic models for the Agulhas Plateau and Transkei Basin sequences are based on analysis of reflection characteristics (e.g., amplitude, frequency content of units, and continuity of reflections) and are tied to the ages of conventional gravity/piston cores (Tucholke and Carpenter, 1977; Table **T1**) where possible and to Site U1475 for the post-Miocene sequences (Gruetzner et al., 2019).

For the Agulhas Plateau, Tucholke and Carpenter (1977) and Tucholke and Embley (1984) identified four distinct seismic horizons above acoustic basement and constructed a first seismostratigraphic model (Table **T2**). An unconformity above acoustic basement was cored where it crops out high on the western flank of

the plateau and was found to be minimally Maastrichtian in age (~72–66 Ma). The underlying reflections terminate against the Upper Cretaceous reflector, thus documenting erosion (Uenzelmann-Neben, 2002, 1999).

A 9 My hiatus across the Paleocene/Eocene boundary in the Agulhas Plateau sedimentary sequence (Tucholke and Embley, 1984) is interpreted at Reflector LE, which shows strong amplitudes and is mostly conformable to bounding beds (Figures **F4**, **F5**). Intensified bottom currents (e.g., due to the formation and strengthening of the ACC [Tucholke and Embley, 1984]) led to the formation of a second regional hiatus between ~33 and 29 Ma (Reflector LO; Figures **F4**, **F5**, **F6**, **F7**) that is of medium to strong amplitude and represents an unconformity observed on the Agulhas Plateau (Uenzelmann-Neben, 2002). Reflector MM (middle Miocene) is also likely a result of deepwater erosion and redeposition (Tucholke and Embley, 1984). This reflection shows weaker amplitudes and frequent wedge-outs at the seafloor (Figures **F5**, **F7**). A regional hiatus of late Miocene–early Pliocene age (~10–6 Ma) is attributed to erosion and redeposition of sediments by Circumpolar Deep Water in the ACC (Tucholke and Embley, 1984) and represented by a strong reflection (Reflector LP), which is often found very close to, and thus indistinguishable from, the seafloor. Reflector LP is dated to 5.7 Ma (Gruetzner et al., 2019) and interpreted to represent the onset of a period of increased Atlantic Meridional Overturning Circulation. A relatively thin veneer of Pliocene–Pleistocene sediments (~0–50 m) rests on top of the lower Pliocene reflection across most areas of the Agulhas Plateau, forming thicker drift packages only in localized areas. Several reflections in the Pliocene–Pleistocene sequence have been associated with climate-induced changes in circulation (Gruetzner et al., 2019).

In the Transkei Basin, the top of the oceanic crust is imaged as a high-amplitude, partly rugged reflection (Schlüter and Uenzelmann-Neben, 2007). An undisturbed sedimentary sequence overlying basement is identified as Subunit 1A and is separated from the overlying heavily faulted Subunit 1B by Horizon K-T (Cretaceous/Paleogene boundary) of medium reflection amplitude (Table **T3**; Figure **F8**). Sedimentary Unit 1 is topped by Horizon E (late Eocene). In Subunit 1A, a reflection band with higher amplitudes is interpreted to represent black shales (Schlüter and Uenzelmann-Neben, 2008). The overlying Unit 2 marks a short transition zone and appears as a small but very high amplitude reflection band with a thickness of ~25 m. The interface between Units 2 and 3 is characterized by Reflector O and represents the Eocene/Oligocene boundary (Figure **F8**). Unit 3 indicates an increasing energy level and also thickens up to 70 m. The Unit 3/4 boundary is represented by Reflector M, which is hypothesized to be middle Miocene in age (Schlüter and Uenzelmann-Neben, 2007). In contrast to Unit 3, overlying Unit 4 thickens up to 130 m, whereas the amplitudes weaken. Units 4 and 5 are separated by the lower Pliocene Reflector P (Figure **F8**). The youngest Unit 5 shows high-amplitude reflections (Schlüter and Uenzelmann-Neben, 2007).

Seismic studies/site survey data

The supporting site survey data for Expedition 392 are archived at the IODP Site Survey Data Bank (**https://ssdb.iodp.org/SSDBquery/SSDBquery.php**; select P834 for proposal number).

Scientific objectives

The main scientific questions and objectives to be addressed by the proposed primary and alternate drill sites (Figures **F3**, **F9**; Table **T4**) for Expedition 392 are outlined below.

1. *Did Indian Ocean LIPs related to the breakup of Gondwana tap a similar source and show a similar temporal and geochemical evolution to coeval and older Pacific LIPs?*

It is hypothesized that the Agulhas Plateau, Northeast Georgia Rise, and Maud Rise initially formed a superplateau similar to the combined Ontong Java–Manihiki–Hikurangi Plateau (Davy et al., 2008; Hoernle et al., 2010; Taylor, 2006; Timm et al., 2011) before being broken up by seafloor spreading in the mid-Cretaceous. Recovery of basement rocks on the Agulhas Plateau will test whether the Agulhas Plateau–Northeast Georgia Rise–Maud Rise super-LIP formed at the Bouvet triple junction (Gohl et al., 2011; Parsiegla et al., 2008) much like the Shatsky Rise in the northwestern Pacific (Sager et al., 1999) or through interactions between the Bouvet and Marion hotspots with the Southwest Indian Ridge (Georgen et al., 2001). Continuous, 15–20 km long reflections observed in Agulhas Plateau basement structures are similar to lava flow sequences drilled at Shatsky Rise (Tamu Massif) that rapidly accumulated at inferred melt production rates of 0.63–0.84 km^3/y over a time interval of 3–4 My (Geldmacher et al., 2014; Gohl and Uenzelmann-Neben, 2001; Expedition 324 Scientists, 2010; Sager et al., 2013; Uenzelmann-Neben et al., 1999). These rates imply the involvement of a mantle plume.

A fundamental question concerning Cretaceous LIPs is whether they tapped a common reservoir in the lower mantle, and if so, what is the composition of this reservoir and its homogeneity/heterogeneity (e.g., Jackson and Carlson, 2011; Jackson et al., 2010). Most lavas from Ontong Java Plateau show a homogeneous isotopic composition, characterized by the Kwaimbaita/Kroenke component similar to the composition of proposed common mantle components with intermediate isotopic compositions compared to oceanic intraplate volcanic rocks (e.g., Prevalent Mantle [PREMA], Focal Zone [FOZO], and Common Component [C]; Hanan et al., 2004; Stracke et al., 2005; Zindler and Hart, 1986). However, the stratigraphically youngest plateau lavas in some areas display a compositionally distinct (Enriched Mantle 1 [EM1] type; e.g., Zindler and Hart, 1986) Singgalo composition. On the other hand, recent studies of lavas from the Manihiki Plateau (Timm et al., 2011), Shatsky Rise (Heydolph et al., 2014), and Mozambique Ridge (Jacques et al., 2019) show considerably more compositional variation, suggesting that even single LIP events tap heterogeneous sources similar to ocean island basalts.

Another important question about LIPs concerns their longevity: Do they represent single short-term events occurring over a few million years, or are these volcanic provinces active over longer time periods (e.g., Bryan and Ernst, 2008)? Although the main Tamu Massif of Shatsky Rise formed between ~144 and 143 Ma, magnetic data suggest the three massifs formed over a longer time interval from M20 to M4 (146–127 Ma). The uppermost lava group at the Tamu Massif (Shatsky Rise) yielded an age (133 Ma) ~10 My younger than the main sequence of lavas (144–143 Ma) (Geldmacher et al., 2014), providing evidence for volcanic rejuvenation.

These lavas are geochemically identical to the main plateau stage lavas and therefore appear to have tapped the same source. At Ontong Java Plateau, the stratigraphically youngest Singgalo lavas have a distinct trace element and isotopic composition from the main Kwaimbaita/Kroenke lavas (Tejada et al., 2004, 1996, 2002). The uppermost lavas at Manihiki Plateau drilled at Deep Sea Drilling Project (DSDP) Site 317 have a distinct Singgalo-type chemical composition compared to the main low-Ti plateau lavas with Kwaimbaita/Kroenke-type compositions (Hoernle et al., 2010; Timm et al., 2011). Alkalic rejuvenated lavas with distinct (high μ [HIMU] type) incompatible element and isotopic compositions occur on Ontong Java, Hikurangi, and Manihiki Plateaus (e.g., Hoernle et al., 2010; Timm et al., 2011). Seismic data from the Manihiki Plateau revealed several formation stages: the initial phase forming the nucleus (>125 Ma), the extension (125–116 Ma), and the secondary phase (100–65 Ma) (Pietsch and Uenzelmann-Neben, 2015). Seismic and geochemical data from Mozambique Ridge indicate a rapid, partly contemporaneous formation of the four segments and later postsedimentary magmatism (Fischer et al., 2017; Jacques et al., 2019). These observations pose the question of whether rejuvenated volcanism is a common feature on oceanic plateaus, and if so, what is its origin?

Key questions regarding Agulhas Plateau volcanism include the following:

- What are the age, origin, and temporal and geochemical evolution of the uppermost Agulhas Plateau volcanic sequences?
- Do the uppermost Agulhas Plateau lavas show evidence for subaerial volcanism?
- Does the Agulhas Plateau show geochemical affinities and melt production rates similar to other LIPs (e.g., Shatsky, Ontong Java, Manihiki, Hikurangi, and Kerguelen Plateaus), requiring elevated mantle temperatures and/or lower mantle source (high $^3He/^4He$ and solar Ne isotope ratios) and thus the presence of a mantle plume from the lower mantle?
- Is there evidence for late-stage volcanism on the Agulhas Plateau as has been observed at Shatsky Rise and the Ontong Java, Manihiki, and Hikurangi Plateaus? How much younger is it compared to the main plateau stage, and does it show compositional differences in major (alkalic vs. tholeiitic) and trace element and isotopic (e.g., more enriched) composition?
- Does Agulhas volcanism coincide with the separation of Africa and Antarctica and the formation of other plateaus in the African–Southern Ocean gateway (e.g., Mozambique Ridge)?

We intend to determine the nature of the basement at the Agulhas Plateau (continental, oceanic, or LIP) to understand the origin of the plateau and its role in the break-up history of Gondwana. Assessing the age and geochemistry of the basement will provide information on the geodynamic development of the South Atlantic/South Indian domain. This information will provide insight into when the plateau started to influence the paths of deep oceanic currents. We intend to drill well into basement (as deep as 200 m) at two sites to allow complete characterization of the material, in particular to assess if there is low-volume rejuvenated volcanism. At two additional sites, we will restrict basement penetration to ~50 m to save time, but basement recovery at these additional sites will allow us to test the spatial compositional variability of the plateau. Four proposed primary sites target the tectonic/basement objectives: Sites AP-07A (up to 200 m into basement) and AP-08A (~50 m into basement) on the northern Agulhas Plateau and Sites AP-09B (up to 200 m into basement) and AP-10A (~50 m into basement) on the southern Agulhas Plateau (Figures **F3**, **F4**, **F5**, **F6**, **F7**, **F9**, **F10**). These four drill sites form a transect along the north–south elongated Agulhas Plateau, allowing us to evaluate temporal and compositional variation across the plateau's axis (Figures **F3**, **F9**). Basement highs at Sites AP-07A (northern Agulhas Plateau) and AP-09B (southern Agulhas Plateau), which we intend to sample with deeper (up to 200 m) basement penetration, could reflect late-stage plateau or even rejuvenated (alkalic?) volcanism. Recovery of an extended interval of basement cores from these sites will therefore help to reconstruct the termination of Agulhas Plateau volcanism. In contrast, the sites with less basement penetration (Sites AP-08A [northern Agulhas Plateau] and AP-10A [southern Agulhas Plateau]) will penetrate the main plateau edifice. According to the LIP/plume head model, the edifice is believed to have formed by widespread contemporaneous volcanism within a relatively short time interval and thus could record the beginning of Agulhas Plateau formation. Obtaining age information from these two sites that are 335 km apart will enable us to test this classical model. By combining age and geochemical results from all four sites, we should be able to reconstruct the full cycle of Agulhas Plateau formation.

2. *Did sedimentation on the Agulhas Plateau start immediately after crustal emplacement at ~100 Ma under subaerial conditions?*

Following the separation of the Falkland Plateau from southern Africa during the breakup of Africa, South America, and Antarctica (Figure **F1**), the onset of free water mass exchange between the Tethys/Indian Ocean and evolving South Atlantic/Southern Ocean emerged. However, the emplacement of LIPs appears to have obstructed the opening of this gateway. König and Jokat (2010) suggested that the Mozambique Ridge formed between 140 and 122 Ma and parts of the Astrid Ridge (Antarctica) were possibly still attached to the Mozambique Ridge (Gohl et al., 2011). It is still unclear whether this LIP was submarine or emplaced subaerially, but it was likely an obstacle for the flow of intermediate- and deepwater masses (Fischer and Uenzelmann-Neben, 2018). Another barrier for oceanic circulation was created with the formation of the Agulhas Plateau–Northeast Georgia Rise–Maud Rise LIP between 105 and 95 Ma, after which the Northeast Georgia Rise and Maud Rise detached from the Agulhas Plateau by seafloor spreading (Figure **F1**) (Gohl and Uenzelmann-Neben, 2001; Gohl et al., 2011; Parsiegla et al., 2008), leading to a widening and deepening of the gateway. Based on crustal thickness and estimated subsidence, Parsiegla et al. (2008) speculated that the central part of the Agulhas Plateau (present water depths <3000 m) formed subaerially. The Transkei Basin formed between the Mozambique Ridge and Agulhas Plateau–Northeast Georgia Rise–Maud Rise LIPs and the African continent. Plate tectonic reconstructions (König and Jokat, 2010; Parsiegla et al., 2008) show that this basin may have been a restricted subbasin until 80 Ma (Schlüter and Uenzelmann-Neben, 2008; Uenzelmann-Neben, 2010), which resulted in anoxic conditions and led to the deposition of black shales (Figure **F8**).

Key questions regarding initial sedimentation on the Agulhas Plateau include the following:

- Under what environmental conditions were sediments deposited shortly after formation of the Agulhas Plateau—subaerial, shallow or deep water, or warm or cool conditions?
- How did emplacement of the plateau influence the climate, oceanic environments, and Earth's biota?
- What can we deduce about water mass changes during early stages of the plateau's evolution? Did emplacement of the Agulhas Plateau LIP interrupt an already incipient circulation?

The deep opening of Southern Ocean gateways (African–Southern Ocean, Tasman, and Drake Passage), which took place over a prolonged period of time from the Cretaceous to mid-Cenozoic, had a significant effect on the cooling of the deep ocean and hence global climate (Sijp et al., 2014). Drilling on the Agulhas Plateau will provide further constraints on this early history and the African–Southern Ocean gateway opening with respect to timing, subsidence, and the initial environment. The Cretaceous sedimentary sequence at the proposed primary sites on the Agulhas Plateau is as thick as 120 m (Figure **F10**) and will allow reconstruction of paleoenvironmental evolution since formation of the plateau (100 Ma according to plate tectonic reconstructions; Parsiegla et al., 2008; Sijp et al., 2014), spanning OAE 3 (~86–83 Ma) and OAE 2 (93.6 Ma). The Cretaceous sequence in the Transkei Basin is much thicker (Figure **F10**) and has the potential to provide a higher resolution record of those OAEs.

Piston cores located near proposed alternate Site AP-05A (Core V16-55 ~13 nmi south of the site [lower Eocene surface sediments]; Core V22-124 ~2 nmi southeast of the site [upper Maastrichtian surface sediments]) (Figure **F3**) provide evidence that a moderately thick sequence of Cretaceous sediments (~100–200 m based on seismic interpretation) can be recovered on the Agulhas Plateau immediately above basement. The seismic interpretation in this area, however, is not unequivocal. Recovery of sediments containing well-preserved microfossils as old as the late Albian (~105 Ma) is possible on the southern Agulhas Plateau (proposed Sites AP-01A, AP-02A, AP-03A, AP-04B, AP-09B, and AP-14A; Figure **F3**) based on sediment ages of piston cores (Table **T1**) and clearly delineated seismic reflectors showing a thick conformable sedimentary sequence between the seafloor and the basement (Figure **F4**).

Four primary sites are selected to determine the age and paleoenvironment of the oldest sediments deposited on crust: Sites AP-07A, AP-08A, AP-09B, and AP-10A (Figures **F3**, **F4**, **F6**, **F7**, **F10**).

3. *Did bottom currents associated with deep and intermediate water masses as well as climatic events leave their imprint in the form of seismic reflections and unconformities?*

Tucholke and Carpenter (1977) and Tucholke and Embley (1984) identified five distinct horizons in their interpretation of Agulhas Plateau seismic reflection data sets, of which they dated the oldest horizon from piston cores and dredge samples as Maastrichtian (Tables **T1**, **T2**). These horizons were subsequently related to regional hiatuses resulting from local sea level highstands, initiation and spreading of the ACC, and activity of Antarctic Bottom Water (Uenzelmann-Neben, 2001, 2002). For the Transkei Basin, Schlüter and Uenzelmann-Neben (2007) presented a seismostratigraphic model tied to the model of Niemi et al. (2000) (Table **T3**) that showed the importance of dating the horizons with respect to possible erosion and the evolution of ocean circulation, which may represent significant climatic episodes (e.g., OAE 3). Black shales identified via bright spots in seismic data from the Transkei Basin (Figure **F8**) (Schlüter and Uenzelmann-Neben, 2008) form an archive of the circulation initially restricted by the emplacement and elevation of both the Mozambique Ridge and Agulhas Plateau. Dating of these sedimentary units and unconformities in the Transkei Basin and mapping their regional extent will help us to identify traces of deep and intermediate water masses, their onset, the intensification and/or weakening of the circulation, and changes to the circulation pathways. This information will provide insight into both long-term and short-lived changes in bottom water circulation through the Late Cretaceous–Paleogene interval in relation to the tectonic isolation and opening of this gateway.

Five primary sites are dedicated to determining the age and nature of the observed unconformities: Sites AP-07A, AP-08A, AP-09B, AP-10A, and TB-01A (Figures **F3**, **F4**, **F6**, **F7**, **F8**).

4. *What was the paleotemperature history at high southern latitudes across the rise and decline of the Cretaceous supergreenhouse and through the early Paleogene?*

Planktonic foraminifer oxygen isotope records from subantarctic Falkland Plateau DSDP Site 511 indicate Cretaceous sea-surface temperatures that at times exceeded 30°C (Huber et al., 2002), yet climate simulations require unrealistically high atmospheric pCO_2 levels of 6500–7500 ppm to match these extremely warm temperatures (Bice et al., 2003). Although it is unlikely that the mid-Cretaceous experienced such high pCO_2 levels, paleoceanographic and preservational explanations for the low $\delta^{18}O$ values (e.g., diagenesis and low salinity) have been ruled out. In addition, the timing and tempo of cooling following peak Turonian temperatures is debated (e.g., Ando et al., 2013; Friedrich et al., 2012), and this uncertainty compromises parallel efforts to relate changes in the tectonic configuration of gateways and geochemically inferred patterns of circulation to climate evolution. Cretaceous foraminifers recovered in a piston core from Agulhas Plateau (Figure **F11**) suggest that it will be possible to recover sediments with well-preserved Cretaceous carbonate microfossils at Agulhas Plateau and Transkei Basin sites. Such material would allow construction of oxygen isotope, Mg/Ca, and, depending on organic biomarker preservation, TEX_{86} paleotemperature estimates spanning the mid-Cretaceous supergreenhouse through the early Paleogene, providing a robust temperature history and reducing uncertainties about the climate history at high southern latitudes.

Recent advances in paleoclimate modeling offer potential avenues for reconciling model–data disparities for Cretaceous temperature and CO_2 estimates through consideration of cloud and biological feedbacks (Kump and Pollard, 2008; Poulsen and Zhou, 2013), emission of nonCO_2 greenhouse gases (Beerling and Royer, 2011), and regional increases in ocean heat transport (Poulsen and Zhou, 2013). Moreover, water isotope–enabled Earth system models are increasingly common, making direct comparisons between proxy data and simulations feasible (e.g., Zhou et al., 2008). Determining whether extreme warm conditions were localized or widespread through the Southern Ocean will provide an important test of possible warming mechanisms.

Specific questions to address include the following:

- What was the thermal history of the Cretaceous, and was this linked to changes in atmospheric CO_2, tectonic evolution, or some other forcing?
- Were surface water temperatures over the Agulhas Plateau cool enough at any time during the Cretaceous and early Paleogene to allow for growth of Antarctic ice sheets?
- Can Earth system models simulate the conditions recorded at Agulhas Plateau during the Cretaceous? What assumptions about CO_2 levels are required to reproduce these conditions?

Five primary sites are dedicated to collect sediment records for Cretaceous–Paleogene temperature reconstructions: Sites AP-07A, AP-08A, AP-09B, AP-10A, and TB-01A (Figures **F3**, **F4**, **F6**, **F7**, **F8**, **F10**).

5. *How did the progressive opening of the African–Southern Ocean gateway influence Cretaceous to early Paleogene deepwater circulation?*

Significant changes in ocean and atmospheric circulation related to evolving bathymetry in oceanic gateways are one possible driver of global-scale climate change through the Cretaceous and Cenozoic. Many studies have proposed enhanced formation and export of Southern Component Waters starting in the Campanian (e.g., Jung et al., 2013; Murphy and Thomas, 2012; Robinson et al., 2010; Robinson and Vance, 2012; Voigt et al., 2013), promoted by the opening of the South Atlantic and establishment of connections to all major oceanic basins. However, incomplete records that lack robust age control from southern high-latitude areas currently hinder deepwater circulation reconstructions for the Cretaceous and early Paleogene. The source regions for different deepwater masses in evolving southern gateways are also controversial (see **African–Southern Ocean gateway circulation**), and resolving fundamental questions on circulation history requires analyses of samples from various depths in or near gateways across which circulation may have reversed.

The proposed Agulhas Plateau and Transkei Basin drill sites, along with Ocean Drilling Program (ODP) Site 1090 (Leg 177; 3702 m) on the southern flank of Agulhas Ridge, will form an eastern counterpart to the proposed drill sites of the Maurice Ewing Bank–Georgia Basin depth transect (IODP Proposal 862-Pre) in the western South Atlantic. Integration of records across this array of sites will provide a unique opportunity to monitor surface and deepwater temperature, nutrient, and circulation changes from the Late Cretaceous through early Paleogene across the South Atlantic. This region is key for modern deepwater circulation and surface frontal systems, and new drill core records can answer questions related to the development of the ACC, the evolution of bottom water flow from the Antarctic margin into South Atlantic basins, the temperature evolution of subantarctic waters, and the global significance of Antarctic weathering inputs to the oceans during both preglacial and glacial time intervals.

Specific questions to address include the following:

- What is the role and impact of the Agulhas Plateau on the evolving communication of deep and intermediate water masses in and between ocean basins? Was there a co-development of Pacific-sourced deepwater circulation in the South Atlantic in the early Paleogene?
- When and how did the opening of Southern Ocean gateways influence Late Cretaceous and early Paleogene climate? Did early opening of the African–Southern Ocean gateway and Drake Passage cause invigorated deepwater circulation and a strengthening of surface frontal systems in the eastern South Atlantic?

Five primary sites are identified to reconstruct intermediate and deepwater circulation: Sites AP-07A, AP-08A, AP-09B, AP-10A, and TB-01A (Figures **F3**, **F4**, **F6**, **F7**, **F8**).

6. *What forcing factors caused Cretaceous OAEs and what effects did these events have on high-latitude climate, oceanography, and biota?*

Despite the nearly four decades since OAEs were discovered, no study has satisfactorily established the primary forcing factors that caused their formation. If increased organic productivity was the dominant cause for OAEs, why are biotic and geochemical indicators of nutrient upwelling generally not found in sediments deposited across those time intervals (Jenkyns, 2010)? On the other hand, if OAEs were caused by sluggish overturning circulation during times of high atmospheric CO_2 (Poulsen and Zhou, 2013) and oxygen-poor water masses in isolated basins (Poulsen et al., 2003), then why is there an offset in the timing of carbon isotope excursions that accompany each of the OAEs relative to peak phases of LIP eruptions and other major volcanic episodes (Jenkyns, 2010), and why are some peak carbon isotope excursions diachronous (Tsikos et al., 2004)? Recovery of complete OAE intervals with well-preserved organic matter and microfossils at the Expedition 392 drill sites will help resolve these controversies. Importantly, new OAE records from the Agulhas Plateau and Transkei Basin will shed light on relative variations in surface productivity and indicate whether there were cooling feedbacks associated with increased organic carbon burial during the OAEs and also whether there were significant changes in bottom circulation prior to, during, and after the OAE intervals. The presence of organic-rich shale with up to ~7% total organic carbon from upper Cenomanian–lower Turonian sequences at multiple sites in the Great Bight Basin on the southern Australian margin (Totterdell et al., 2008) provides evidence that euxinic waters may have been present elsewhere in the southern high latitudes during OAE 2. As noted above, interpretation of the seismic profiles indicates that sediments as old as late Albian may be accessible at relatively shallow burial depths on the Agulhas Plateau, which should allow for preservation of primary geochemical signals across the OAE 1d, OAE 2, and OAE 3 intervals, and a sedimentary section extending down through OAE 3 may be recovered in the Transkei Basin.

Key questions related to OAEs include the following:

- Was there an increase in C_{org} burial in the southern high latitudes during the $\delta^{13}C$ excursion intervals that define Cretaceous OAEs?
- How did surface productivity, paleotemperatures, the vertical thermal and $\delta^{13}C$ gradients, and bottom circulation change in the eastern South Atlantic across the OAE intervals?
- Did changes in Agulhas Plateau microfossil assemblages correspond to observed OAE geochemical and sedimentological shifts, and if so, can the cause for those changes be determined?

Five primary sites are dedicated to study critical OAE intervals of the Cretaceous: Sites AP-07A, AP-08A, AP-09B, AP-10A, and TB-01A (Figures **F3**, **F4**, **F6**, **F7**, **F8**, **F10**).

Drilling, coring, and downhole measurements strategy

The drilling plan for Expedition 392 includes a total of 5 primary sites and 11 alternate sites (Tables **T4**, **T5**, **T6**; Figure **F10**). The primary sites are located in three main regions: Transkei Basin (Site TB-01A), southern Agulhas Plateau (Sites AP-09B and AP-10A), and northern Agulhas Plateau (Sites AP-07A and AP-08A) (Figures **F3**, **F9**). The five primary sites were selected to satisfy key objectives in each of these three regions, and each is paired with one or more alternate sites that fulfill similar objectives.

Drilling in the Transkei Basin (Site TB-01A) aims to recover a thick sedimentary section that extends back through the Upper Cretaceous, which potentially spans a thick black shale interval (Schlüter and Uenzelmann-Neben, 2008). The interpreted black shale intervals at the proposed Transkei Basin sites are located ~900–1000 meters below seafloor (mbsf) and require the deepest penetration of the expedition. As a result, we plan to only recover a

single copy of the Transkei Basin sequence using a combination of the advanced piston corer (APC), extended core barrel (XCB), and rotary core barrel (RCB) coring assemblies (Figure **F10**).

Drilling on both the southern and northern Agulhas Plateau aims to obtain Upper Cretaceous to lower Paleogene sedimentary sequences and sample the underlying basement rocks. All sites on the Agulhas Plateau are strategically positioned at locations lacking thick Neogene drift deposits, allowing access to the Cretaceous–Paleogene sediments at shallow subseafloor depths. Based on age information from shallow piston cores from the Agulhas Plateau (Table **T1**; Tucholke and Carpenter, 1977), the lowermost marine sequences on the Agulhas Plateau will likely be calcareous oozes of Late Cretaceous age and will provide a pelagic record of oceanographic and climate evolution extending from the end of the Cretaceous through the early Paleogene. However, as discussed above, the Agulhas Plateau sedimentary sequences immediately overlying basement may have been deposited in subaerial or shallow-water environments, which we also intend to sample.

Time and weather permitting, double-coring of the Cretaceous–Paleogene sedimentary sequences is planned to achieve more complete recovery of key intervals at the Agulhas Plateau sites (Figure **F10**). Basement penetration of ~50–200 m is planned at all Agulhas Plateau sites to obtain igneous rocks with minimal alteration suitable for determining the age and origin of the Agulhas Plateau. As recommended by several ODP/IODP workshops, a drilling depth of >20 m into the igneous basement should be sufficient to retrieve relatively fresh samples for age and geochemical and geochronological studies (Duncan et al., 2007). Deeper basement penetration of ~150–200 m at two primary sites will likely provide the best opportunity to obtain fresh material for constraining the late-stage evolution of the Agulhas Plateau, which is critical for reconstructing its role in constricting water masses of the African–Southern Ocean gateway.

Wireline logging is planned in the RCB holes at four of the five primary sites (Figure **F10**) to aid in core-log-seismic integration, fill in lithologic information across poorly recovered intervals, and obtain orientated structural measurements. Logging is a particular priority for the thick sedimentary sequences in the Transkei Basin (Site TB-01A) and the two sites on the Agulhas Plateau with up to 200 m of basement penetration (Sites AP-07A and AP-09B).

Transkei Basin sites

Proposed Sites TB-01A (primary) and TB-02A (alternate)

Located on the deep, flat part of the Transkei Basin, the uppermost sections of proposed Sites TB-01A and TB-02A are composed of Pliocene–Pleistocene Agulhas Drift sequences. Below this sediment drift, Miocene to Cretaceous sequences are characterized by parallel reflections (Figure **F8**). The lower part of the interpreted Cretaceous sequence levels out basement topography. A distinctive bright reflection in the Cretaceous sequence is interpreted to image a black shale horizon deposited during OAE 3 (Schlüter and Uenzelmann-Neben, 2008) and constitutes the target depth (~900–1050 mbsf) of those two sites. The sites thus have the potential to sample material from the Neogene, Paleogene, Late Cretaceous, and possibly OAE 3, thereby providing information on the transition of climate and circulation from the Cretaceous greenhouse and through the Paleogene into the Neogene icehouse.

The coring plan for the Transkei Basin site includes drilling a single APC/XCB hole to ~700 mbsf (Table **T5**; Figure **F10**). Hole B will consist of an RCB hole that will be drilled without coring to 690 mbsf and then cored to 950 mbsf. We estimate APC refusal at 250–300 mbsf; however, this depth will be dictated by coring conditions. We do not plan to deploy the half-length APC (HLAPC) system if piston core refusal occurs in Neogene sediments. If we are able to use the APC system into Paleogene sediments, deployment of the HLAPC system will depend on core quality and time available. We may continue to deepen Hole A with the XCB system if core recovery and quality are good. If core quality or recovery is poor, we may opt to terminate coring in Hole A before reaching 700 mbsf and begin coring in Hole B at least 10 m above the termination depth of Hole A. Similarly, we may spot core in Hole B with the RCB drill string to obtain duplicate copies of key or poorly recovered intervals of interest in Hole A. Our goal at this site is to drill through the bright reflector (estimated at ~950 mbsf in proposed primary Site TB-01A) interpreted to represent OAE 3. After we reach our coring objective, we will displace the hole with mud and conduct downhole logging operations, hole and weather conditions permitting. The first tool string will be the triple combination ("triple combo"), which will include natural gamma radiation (NGR), density, resistivity, and magnetic susceptibility measurements. The second logging run will include NGR (to depth match to the other logging runs), sonic velocity, and resistivity images of the borehole using the Formation MicroScanner (FMS). The last logging run will use the Versatile Seismic Imager (VSI) to conduct a vertical seismic profile experiment. The VSI can only be used during daylight hours to allow for marine mammal observation; therefore, we may opt to run this tool as the second logging run depending on timing. If we expect weather to deteriorate or poor hole conditions that may preclude multiple logging runs, we may opt to run the sonic velocity tool on the triple combo (in place of either the resistivity or magnetic susceptibility tools). The coring and logging plan for alternate proposed Site TB-02A is similar except that the target RCB depth is deeper (1050 mbsf) to reach the bright reflector (Table **T6**).

Southern Agulhas Plateau sites

Proposed Sites AP-09B and AP-10A (primary) and AP-01A, AP-03A, AP-04B, AP-05A, AP-11A, and AP-13A (alternate)

Proposed primary Site AP-09B (alternate Sites AP-01A, AP-03A, and AP-13A) is located on the flank of a basement high interpreted to be a volcanic edifice (Uenzelmann-Neben et al., 1999) with up to 340 m of Upper Cretaceous to Paleogene sedimentary sequences (Figure **F4**), which will be sampled to determine paleodepth and paleoenvironment of the plateau across critical intervals of ocean and climate transitions from the Cretaceous greenhouse into the Paleogene. Additionally, basement sampling of ~150–200 m (to bit destruction) is planned to study the nature and age of the Agulhas Plateau's crustal development. Proposed primary Site AP-10A (alternate Sites AP-04B, AP-05A, and AP-11A) is located in a depression on the central part of the plateau with up to 700 m of Paleogene to lower Miocene sequences and ~100 m of interpreted Maastrichtian sedimentary rocks on top of basement (Figure **F7**). Approximately 50 m of basement will be sampled to contribute to a better understanding of the age and formation process of the plateau. Furthermore, the site will allow the sampling of Upper Cretaceous and Paleogene sequences spanning OAE 3, the Cretaceous/Paleogene (K/Pg) boundary, the Paleocene/Eocene Thermal Maximum (PETM), and possibly Oligocene–Miocene glaciations.

We plan to double-core the sedimentary section at both southern Agulhas Plateau sites with two APC/XCB holes, followed by single RCB holes into basement (Tables **T5**, **T6**; Figure **F10**). The sedimentary section coring plan for Hole B may be modified de-

pending on what is recovered in Hole A at both sites. At proposed Site AP-10A, we will use the APC system to refusal (estimated at 300 mbsf but likely shallower) followed by the XCB system to 620 mbsf (top of basement) in both Holes A and B. In Hole C, we will drill without coring to 610 mbsf and then RCB core to ~50 m into basement (total depth estimated at 670 mbsf). We will then displace that hole with mud and log with a modified triple combo ("quad combo") tool string that will include the sonic tool, together with the standard triple combo tools (NGR, density, resistivity, and magnetic susceptibility).

At proposed Site AP-09B, we will use the APC system to refusal (estimated at 300 mbsf) and then the XCB system to basement (at ~340 mbsf) in both Holes A and B. However, the stratigraphy of the uppermost sedimentary section at this location is likely complex. If the uppermost sediments in Hole A are older than anticipated, we are approved to core at any location along Seismic Line AWI-98015 from Common Depth Point (CDP) 5750 (original position of Site AP-09B) to CDP 5665, which is 3 km east-southeast along the seismic line (Figure **F4**), to core younger strata. We would most likely only core the younger sequence at an offset location, returning to the original position to core into basement. In Hole C, we will drill without coring to approximately 10 m above basement (330 mbsf) and then RCB core into basement. We plan RCB coring until bit destruction at this site, which we estimate to be at least 150 m into the basement section. However, if core recovery and quality warrant, we will drop a free-fall funnel (FFF) after ~40 h of rotating time on the RCB bit to allow for a bit change. We will then deploy the subsea camera to reenter the hole via the FFF and continue RCB coring the basement section. The final depth of the hole (and total amount of basement cored) will depend on recovery and be based on collection of relatively unaltered basalt and sufficient flows to document secular variation that will allow us to achieve the expedition objectives. After we terminate coring, the hole will be displaced with mud and we will log with the triple combo and FMS-sonic tool strings. The last logging run will use the Ultrasonic Borehole Imager (UBI) in the basement section to collect an acoustic image of the entire borehole wall.

Northern Agulhas Plateau sites

Proposed Sites AP-07A and AP-08A (primary) and AP-06A, AP-02A, AP-12A, and AP-14A (alternate)

Proposed primary Site AP-07A (alternate Sites AP-06A and AP-14A) is located on top of a basement high that is overlain by only a thin cover (100 m) of Cretaceous–Paleogene sedimentary rocks (Figure **F6**), which will be sampled to provide information on the sedimentary environment following plateau formation. Sampling of 200 m of basement is planned at this site to study the nature and age of the plateau's crustal development. The thicker (400 m) sedimentary column at proposed primary Site AP-08A (Figure **F6**) (alternate Sites AP-02A and AP-12A) located ~20 km southwest of proposed Site AP-07A will allow sampling of Upper Cretaceous and Paleocene material to contribute to a better understanding of the paleodepth and paleoenvironment of the plateau, as well as critical climate and oceanic events. The sampling of ~50 m of basement at primary Site AP-08A is planned to study the nature and age of the plateau's crust.

The coring plan for primary proposed Site AP-07A includes a single RCB hole to a total depth of 300 mbsf with 200 m penetration into basement (Table **T5**; Figure **F10**). We anticipate that core recovery with the RCB system will be lower in the uppermost sedimentary section; however, recovery of sediments is of lower priority at this site because the sequence is very thin (~100 m). The primary objective at this site is to core ~200 m of basement. To ensure this, the operations plan includes dropping a FFF for a bit change after 40 h of rotating time on the bit. The final drilling depth into basement will depend on recovery of relatively unaltered basalt and sufficient flows to document secular variation, which will allow us to achieve the expedition objectives. This hole will also be logged with the triple combo and FMS-sonic followed by the UBI in the basement section. If time is limited, the UBI is of higher priority than the FMS-sonic.

At proposed Site AP-08A, we plan to double-core the sedimentary section in Holes A and B, which will include using the APC system to refusal (estimated at 300 mbsf) followed by the XCB system to basement (at ~400 mbsf). In Hole C, we will drill without coring to 390 mbsf and then RCB core to 450 mbsf (~50 m into basement) (Table **T5**; Figure **F10**). If time permits, we intend to log this hole with the triple combo and FMS-sonic. However, this is not included in the operations plan (Table **T5**) because we anticipate that not enough operational time will be left to do so. The sedimentary section is the highest priority at this site; therefore, if time is short, we will not core basement at Site AP-08A.

Risks and contingency

A number of challenges are associated with the planned Expedition 392 operations in deep water that could impact the drilling, coring, and logging operations strategy for this expedition. One of the main challenges is the time available to conduct the planned coring and logging operations for this expedition. The primary operations plan includes 62 days, which is 1 day longer than scheduled for the expedition (Table **T5**). Time estimates for XCB and RCB coring are based on average penetration rates because sediments and rock of this age have not be cored in this region. Actual penetration rates may vary significantly from predicted rates, which could result in excess time or (more likely) less time to complete operations. If operational time becomes an issue, we can reduce operations at the remaining sites by (1) only double-coring key intervals in Hole B where complete double-coring is planned, (2) reducing basement penetration provided that enough good quality basalt has been obtained to achieve expedition objectives, and/or (3) reducing the number of downhole logging runs at one or more sites. Below we outline additional risks and present possible alternatives should operations be impacted by these or other challenges.

Weather conditions

Weather is always a potential issue because sea state and the resulting heave can have adverse effects on drilling, coring, and downhole logging. To help mitigate weather risks, Expedition 392 is scheduled during the Southern Hemisphere summer and early autumn when the risk for bad weather is lower. The southern Agulhas Plateau sites are the most likely to be impacted by weather. During the expedition, we will monitor weather forecasts and can adjust the order in which we occupy sites (e.g., coring at Site TB-01A in the middle of the expedition rather than at the beginning) based on the potential for inclement weather with a relatively small impact on the total amount of transit required for the expedition. Despite this, the expedition could experience some weather delays depending on conditions and operations. If we need to make up for lost time waiting on weather, we can reduce operations at some sites by reducing the amount of double-coring of the sedimentary section, reducing basement penetration (provided we have recovered enough mate-

rial to meet the expedition objectives), or reducing the number of downhole logging runs conducted.

Operational risks

The proposed penetration depth at some sites (as much as 1050 mbsf, including alternate sites) and coring dense basement material present several challenges. Hole stability is always a risk during coring operations, and the risk increases with longer open hole sections. Casing long open hole sections (especially over intervals of unconsolidated sediment) is the best way to mitigate this risk, but we do not plan to case any holes during this expedition. Casing adds a significant amount of operational time and is also more likely to be impacted by inclement weather than coring operations. Instead, we will use drilling mud to help stabilize the open hole, although lower annular velocities will make hole cleaning more challenging in the deeper sections of these holes. Increasing flow rates to clean the hole could result in washing out unconsolidated sections in the upper part of the hole. This could lead to hole stability problems toward the end of drilling and during logging operations.

We plan to deploy a FFF for some holes to allow reentry capability so that we can change drill bits for deeper penetration into basement or in case we need to temporarily leave a site because of inclement weather. There are several risks associated with FFF deployment. The FFF can be dislodged while pulling out of the hole, and the FFF can become buried or impossible to use for reentry. The use of a FFF also leaves the open hole section open for a longer duration, which can contribute to hole stability problems. If we are unable to reenter a hole, the only option is to start a new hole and drill down to just above the total depth of the previous hole to continue coring. This decision will depend on the expedition time left and whether or not the scientific objectives can be reasonably achieved with the sediment and basement already collected at that site.

A stuck drill string is always a risk during coring operations and can consume expedition time while attempting to free the stuck drill string. If the drill string cannot be extracted, then additional time is spent to sever the stuck pipe. This can result in the complete loss of the hole, lost equipment, and lost time while starting a new hole. *JOIDES Resolution* carries sufficient spare drilling equipment to enable the continuation of coring, but the time lost to the expedition can be significant.

Chert layers may occur in sedimentary sequences targeted for Expedition 392, particularly in the Campanian sequences on the Agulhas Plateau, and present unique difficulties. Chert is very indurated and can be difficult to core with the XCB system, taking a very long time to penetrate the layer. It is also possible for the XCB cutting shoe to catastrophically fail when coring chert, which would result in the hole being abandoned and require starting a new hole. If chert significantly impacts coring at a site, we can opt to abandon the hole and begin a new hole with the RCB system (although this could result in poor core quality in between chert layers if the sediments are very soft). Another option is to examine the seismic profiles for that site and its alternates to check for any indication that chert might not be present at one of the alternate sites.

Downhole logging risks

Several risks are involved in any downhole logging operations. First, the upper parts of the holes have been open longer before logging, and high rates of fluid circulation might have been used to raise the cuttings and clear the hole. Therefore, the hole could be washed out (wide) over intervals through unconsolidated sediment, and log quality will be reduced for those tools that need good contact with the borehole wall (density, porosity, FMS resistivity images, and VSI check shots). The end of the drill pipe is typically set at ~80 mbsf to help prevent the most unconsolidated sediments at the top of the borehole from collapsing around the tool string. This depth can be adjusted depending on hole conditions. Secondly, there is a risk of bridging where the hole closes up. This would result in either not reaching the total depth of the hole or, in the worst case scenario, getting a tool string stuck in the hole. A good guide to this will be the conditions encountered during drilling and a wiper trip before logging. If the risk is considered to be significant, the radioactive source will not be deployed in the density tool.

Sampling and data sharing strategy

Shipboard and shore-based researchers should refer to the IODP Sample, Data, and Obligations Policy and Implementation Guidelines posted on the Web at **http://www.iodp.org/top-resources/program-documents/policies-and-guidelines**. This document outlines the policy for distributing IODP samples and data to research scientists, curators, and educators. The document also defines the obligations that sample and data recipients incur. The Sample Allocation Committee (SAC; composed of Co-Chief Scientists, Staff Scientist, and IODP Curator on shore and curatorial representative on board ship) will work with the entire scientific party to formulate a formal expedition-specific sampling plan for shipboard and postcruise sampling.

Shipboard scientists are expected to submit sample requests (**http://iodp.tamu.edu/curation/samples.html**) ~6 months before the beginning of the expedition. Based on sample requests (shore based and shipboard) submitted by this deadline, the SAC will prepare a tentative sampling plan, which will be revised on the ship as dictated by core recovery and cruise objectives. The sampling plan will be subject to modification depending upon the actual material recovered and collaborations that may evolve between scientists during the expedition. Modification of the strategy during the expedition must be approved by the Co-Chief Scientists, Staff Scientist, and curatorial representative on board ship.

The minimum permanent archive will be the standard archive half of each core. All sample frequencies and sizes must be justified on a scientific basis and will depend on core recovery, the full spectrum of other requests, and the cruise objectives. Some redundancy of measurements is unavoidable, but minimizing the duplication of measurements among the shipboard party and identified shore-based collaborators will be a factor in evaluating sample requests.

Shipboard sampling will primarily be restricted to acquiring ephemeral data types and shipboard measurements. Limited low-resolution sampling for personal research to help better plan postcruise sampling will be at the discretion of the SAC (and use of shipboard sample residues for this will be encouraged). The data collected during the expedition will be used to produce stratigraphic spliced sections for some intervals and age models for each site, which are critical to the overall objectives of the expedition and for planning for higher resolution sampling postexpedition. Whole-round samples may be taken for interstitial water measurements and physical property measurements as dictated by the shipboard sampling plan that will be finalized during the first few days of the expedition. Most sampling for postcruise research will be postponed until a shore-based sampling party that will be implemented approximately 4–6 months after the end of the expedition at the Gulf Coast Repository in College Station, Texas (United States).

If some critical intervals are recovered, there may be considerable demand for samples from a limited amount of cored material. These intervals may require special handling, a higher sampling density, reduced sample size, or continuous core sampling by a single investigator. Shipboard sampling of critical intervals will be avoided if possible, and a detailed sampling plan coordinated by the SAC may be required for postcruise sampling. The SAC can decide at any stage during the expedition or during the moratorium period which recovered intervals should be considered critical. During the expedition, all archive halves will be permanent archives. Following the expedition, the curator will finalize the archive halves designated as permanent over intervals cored in multiple holes.

Following Expedition 392, cores will be delivered to the IODP Gulf Coast Repository in College Station, Texas, for postcruise X-ray fluorescence core scanning and sampling for postcruise research. Upon completion of these measurements and the sampling party, cores will be sent to the Kochi Core Center in Kochi, Japan, for permanent storage. All collected data and samples will be protected by a 1 y moratorium period following the completion of the postcruise sampling party, during which time data and samples will be available only to the Expedition 392 science party and approved shore-based participants.

Expedition scientists and scientific participants

The current list of participants for Expedition 392 can be found at **http://iodp.tamu.edu/scienceops/expeditions/agulhas_plateau_climate.html**.

References

Ando, A., Woodard, S.C., Evans, H.F., Littler, K., Herrmann, S., Macleod, K.G., Kim, S., Khim, B.-K., Robinson, S.A., and Huber, B.T., 2013. An emerging paleoceanographic 'missing link': multidisciplinary study of rarely recovered parts of deep-sea Santonian–Campanian transition from Shatsky Rise. *Journal of the Geological Society (London, United Kingdom)*, 170(3):381–384. **https://doi.org/10.1144/jgs2012-137**

Arthur, M.A., Dean, W.E., and Schlanger, S.O., 1985. Variations in the global carbon cycle during the Cretaceous related to climate, volcanism, and changes in atmospheric CO_2. *In* Sundquist, E.T., and Broecker, W.S. (Eds.), *The Carbon Cycle and Atmospheric CO_2: Natural Variations Archaen to Present*. Geophysical Monograph, 32:504–529. **https://doi.org/10.1029/GM032p0504**

Arthur, M.A., Schlanger, S.O., and Jenkyns, H.C., 1987. The Cenomanian-Turonian Oceanic Anoxic Event, II. Paleoceanographic controls on organic-matter production and preservation. *In* Brooks, J., and Fleet, A.J. (Eds.), *Marine Petroleum Source Rocks*. Special Publication - Geological Society of London, 26(1):401–420. **https://doi.org/10.1144/GSL.SP.1987.026.01.25**

Beerling, D.J., and Royer, D.L., 2011. Convergent Cenozoic CO_2 history. *Nature Geoscience,* 4(7):418–420. **https://doi.org/10.1038/ngeo1186**

Berner, R.A., Lasaga, A.C., and Garrels, R.M., 1983. The carbonate-silicate geochemical cycle and its effect on atmospheric carbon dioxide over the past 100 million years. *American Journal of Science,* 283(7):641–683. **https://doi.org/10.2475/ajs.283.7.641**

Biastoch, A., Böning, C.W., and Lutjeharms, J.R.E., 2008. Agulhas leakage dynamics affects decadal variability in Atlantic overturning circulation. *Nature,* 456(7221):489–492. **https://doi.org/10.1038/nature07426**

Biastoch, A., Böning, C.W., Scheinert, M., and Lutjeharms, J.R.E., 2009. The Agulhas system as a key region of the global oceanic circulation. *In* Nagel, W.E., Kröner, D.B., and Resch, M.M. (Eds.), *High Performance Computing in Science and Engineering'08*: Heidelberg (Springer), 459–469. **https://doi.org/10.1007/978-3-540-88303-6_32**

Bice, K.L., Birgel, D., Meyers, P.A., Dahl, K.A., Hinrichs, K.-U., and Norris, R.D., 2006. A multiple proxy and model study of Cretaceous upper ocean temperatures and atmospheric CO_2 concentrations. *Paleoceanography and Paleoclimatology*, 21(2):PA2002. **https://doi.org/10.1029/2005PA001203**

Bice, K.L., Huber, B.T., and Norris, R.D., 2003. Extreme polar warmth during the Cretaceous greenhouse? Paradox of the late Turonian $\delta^{18}O$ record at Deep Sea Drilling Project Site 511. *Paleoceanography,* 18(2):1031. **https://doi.org/10.1029/2002PA000848**

Bryan, S.E., and Ernst, R.E., 2008. Revised definition of Large Igneous Provinces (LIPs). *Earth-Science Reviews*, 86(1–4):175–202. **https://doi.org/10.1016/j.earscirev.2007.08.008**

Charvis, P., Recq, M., Operto, S., and Brefort, D., 1995. Deep structure of the northern Kerguelen Plateau and hotspot-related activity. *Geophysical Journal International*, 122(3):899–924. **https://doi.org/10.1111/j.1365-246X.1995.tb06845.x**

Clarke, L.J., and Jenkyns, H.C., 1999. New oxygen isotope evidence for long-term Cretaceous climatic change in the Southern Hemisphere. *Geology*, 27(8):699–702. **https://doi.org/10.1130/0091-7613(1999)027<0699:NOIEFL>2.3.CO;2**

Coffin, M.F., and Eldholm, O., 1994. Large igneous provinces: crustal structure, dimensions, and external consequences. *Reviews of Geophysics*, 32(1):1–36. **https://doi.org/10.1029/93RG02508**

Davy, B., Hoernle, K., and Werner, R., 2008. Hikurangi Plateau: crustal structure, rifted formation, and Gondwana subduction history. *Geochemistry, Geophysics, Geosystems,* 9(7):Q07004. **https://doi.org/10.1029/2007GC001855**

de Ruijter, W.P.M., Biastoch, A., Drijfhout, S.S., Lutjeharms, J.R.E., Matano, R.P., Picheven, T., van Leeuwen, P.J., and Weijer, W., 1999. Indian-Atlantic interocean exchange: dynamics, estimations and impact. *Journal of Geophysical Research: Oceans,* 104(C9):20885–20910. **https://doi.org/10.1029/1998JC900099**

de Ruijter, W.P.M., Brummer, G.-J.A., Drijfhout, S.S., Lutjeharms, J.R.E., Peters, F., Ridderinkhoff, H., van Aken, H., and van Leeuwen, P.J., 2006. Observations of the inter-ocean exchange around South Africa. *Eos, Transactions of the American Geophysical Union*, 87(9):97–101. **https://doi.org/10.1029/2006EO090002**

DeConto, R.M., and Pollard, D., 2003. Rapid Cenozoic glaciation of Antarctica induced by declining atmospheric CO_2. *Nature,* 421(6920):245–249. **https://doi.org/10.1038/nature01290**

Duncan, R., Arndt, N., Hanyu, T., Harada, Y., Harrp, K., Hoernle, K., Kellog, L., et al., 2007. Report from the Hotspot Geodynamics Detailed Planning Group. **https://www.iodp.org/hotspot-geodynamics-detailed-planning-group-dpg-report-january-2007/file**

Expedition 324 Scientists, 2010. Expedition 324 summary. *In* Sager, W.W., Sano, T., Geldmacher, J., and the Expedition 324 Scientists, *Proceedings of the Integrated Ocean Drilling Program,* 324: Tokyo (Integrated Ocean Drilling Program Management International, Inc.). **https://doi.org/10.2204/iodp.proc.324.101.2010**

Fischer, M.D., 2017. The Mozambique Ridge: evolution of a Large Igneous Province and its implication for paleocean circulation [Ph.D. dissertation]. University of Bremen, Germany. (in German) **https://epic.awi.de/id/eprint/45674/1/Dissertation_M_D_Fischer.pdf**

Fischer, M.D., and Uenzelmann-Neben, G., 2018. Late Cretaceous onset of current controlled sedimentation in the African–Southern Ocean gateway. *Marine Geology*, 395:380–396. **https://doi.org/10.1016/j.margeo.2017.11.017**

Fischer, M.D., Uenzelmann-Neben, G., Jacques, G., and Werner, R., 2017. The Mozambique Ridge: a document of massive multistage magmatism. *Geophysical Journal International,* 208(1):449–467. **https://doi.org/10.1093/gji/ggw403**

Forster, A., Schouten, S., Moriya, K., Wilson, P.A., and Sinninghe Damsté, J.S., 2007. Tropical warming and intermittent cooling during the Cenomanian/Turonian Oceanic Anoxic Event 2: sea surface temperature records

from the equatorial Atlantic. *Paleoceanography and Paleoclimatology*, 22(1):PA1219. **https://doi.org/10.1029/2006PA001349**

Frank, M., Reynolds, B.C., and O'Nions, R.K., 1999. Nd and Pb isotopes in Atlantic and Pacific water masses before and after closure of the Panama gateway. *Geology*, 27(12):1147–1150. **https://doi.org/10.1130/0091-7613(1999)027<1147:NAPIIA>2.3.CO;2**

Frank, T.D., and Arthur, M.A., 1999. Tectonic forcings of Maastrichtian ocean-climate evolution. *Paleoceanography,* 14(2):103–117. **https://doi.org/10.1029/1998PA900017**

Friedrich, O., Norris, R.D., Bornemann, A., Beckmann, B., Pälike, H., Worstell, P., Hofmann, P., and Wagner, T., 2008. Cyclic changes in Turonian to Coniacian planktic foraminiferal assemblages from the tropical Atlantic Ocean. *Marine Micropaleontology*, 68(3–4):299–313. **https://doi.org/10.1016/j.marmicro.2008.06.003**

Friedrich, O., Norris, R.D., and Erbacher, J., 2012. Evolution of middle to Late Cretaceous oceans—a 55 m.y. record of Earth's temperature and carbon cycle. *Geology,* 40(2):107–110. **https://doi.org/10.1130/G32701.1**

Geldmacher, J., van den Bogaard, P., Heydolph, K., and Hoernle, K., 2014. The age of Earth's largest volcano: Tamu Massif on Shatsky Rise (northwest Pacific Ocean). *International Journal of Earth Sciences*, 103:2351–2357. **https://doi.org/10.1007/s00531-014-1078-6**

Georgen, J.E., Lin, J., and Dick, H.J.B., 2001. Evidence from gravity anomalies for interactions of the Marion and Bouvet hotspots with the Southwest Indian Ridge: effects of transform offsets. *Earth and Planetary Science Letters,* 187(3–4):283–300. **https://doi.org/10.1016/S0012-821X(01)00293-X**

Gohl, K., and Uenzelmann-Neben, G., 2001. The crustal role of the Agulhas Plateau, southwest Indian Ocean: evidence from seismic profiling. *Geophysical Journal International*, 144(3):632–646. **https://doi.org/10.1046/j.1365-246x.2001.01368.x**

Gohl, K., Uenzelmann-Neben, G., and Grobys, N., 2011. Growth and dispersal of a southeast African Large Igneous Province. *South African Journal of Geology*, 114(3–4):379–386. **https://doi.org/10.2113/gssajg.114.3-4.379**

Gruetzner, J., Jiménez Espejo, F.J., Lathika, N., Uenzelmann-Neben, G., Hall, I.R., Hemming, S.R., LeVay, L.J., and the Expedition 361 Scientists, 2019. A new seismic stratigraphy in the Indian-Atlantic Ocean Gateway resembles major paleo-oceanographic changes of the last 7 Ma. *Geochemistry, Geophysics, Geosystems*, 20(1):339–358. **https://doi.org/10.1029/2018GC007668**

Hall, I.R., Hemming, S.R., LeVay, L.J., and the Expedition 361 Scientists, 2016. *Expedition 361 Preliminary Report: South African Climates (Agulhas LGM Density Profile).* International Ocean Discovery Program. **https://doi.org/10.14379/iodp.pr.361.2016**

Hall, I.R., Hemming, S.R., LeVay, L.J., Barker, S., Berke, M.A., Brentegani, L., Caley, T., Cartagena-Sierra, A., Charles, C.D., Coenen, J.J., Crespin, J.G., Franzese, A.M., Gruetzner, J., Han, X., Hines, S.K.V., Jimenez Espejo, F.J., Just, J., Koutsodendris, A., Kubota, K., Lathika, N., Norris, R.D., Periera dos Santos, T., Robinson, R., Rolinson, J.M., Simon, M.H., Tangunan, D., van der Lubbe, J.J.L., Yamane, M., and Zhang, H., 2017. Expedition 361 summary. *In* Hall, I.R., Hemming, S.R., LeVay, L.J., and the Expedition 361 Scientists, *South African Climates (Agulhas LGM Density Profile).* Proceedings of the International Ocean Discovery Program, 361: College Station, TX (International Ocean Discovery Program). **https://doi.org/10.14379/iodp.proc.361.101.2017**

Hanan, B.B., Blichert-Toft, J., Pyle, D.G., and Christie, D.M., 2004. Contrasting origins of the upper mantle revealed by hafnium and lead isotopes from the Southeast Indian Ridge. *Nature,* 432(7013):91–94. **https://doi.org/10.1038/nature03026**

Hay, W.W., 2011. Can humans force a return to a 'Cretaceous' climate? *Sedimentary Geology*, 235(1–2):5–26. **https://doi.org/10.1016/j.sedgeo.2010.04.015**

Hay, W.W., DeConto, R.M., Wold, C.N., Wilson, K.M., Voigt, S., Schulz, M., Rossby Wold, A., Dullo, W.-C., Ronov, A.B., Balukhovsky, A.N., and Söding, E., 1999. Alternative global Cretaceous paleogeography. *In* Barrera, E., and Johnson, C.C. (Eds.), *Evolution of the Cretaceous Ocean-Climate System*. Special Paper - Geological Society of America, 332:1–47. **https://doi.org/10.1130/0-8137-2332-9.1**

Heydolph, K., Murphy, D.T., Geldmacher, J., Romanova, I.V., Greene, A., Hoernle, K., Weis, D., and Mahoney, J., 2014. Plume versus plate origin for the Shatsky Rise oceanic plateau (NW Pacific): insights from Nd, Pb and Hf isotopes. *Lithos,* 200–201:49–63. **https://doi.org/10.1016/j.lithos.2014.03.031**

Hoernle, K., Hauff, F., van den Bogaard, P., Werner, R., Mortimer, N., Geldmacher, J., Garbe-Schönberg, D., and Davy, B., 2010. Age and geochemistry of volcanic rocks from the Hikurangi and Manihiki oceanic plateaus. *Geochimica et Cosmochimica Acta,* 74(24):7196–7219. **https://doi.org/10.1016/j.gca.2010.09.030**

Huber, B.T., Hobbs, R.W., Bogus, K.A., and the Expedition 369 Scientists, 2018. *Expedition 369 Preliminary Report: Australia Cretaceous Climate and Tectonics.* International Ocean Discovery Program. **https://doi.org/10.14379/iodp.pr.369.2018**

Huber, B.T., Hodell, D.A., and Hamilton, C.P., 1995. Middle–Late Cretaceous climate of the southern high latitudes: stable isotopic evidence for minimal equator-to-pole thermal gradients. *Geological Society of America Bulletin,* 107(10):1164–1191. **https://doi.org/10.1130/0016-7606(1995)107<1164:MLCCOT>2.3.CO;2**

Huber, B.T., Norris, R.D., and MacLeod, K.G., 2002. Deep sea paleotemperature record of extreme warmth during the Cretaceous. *Geology,* 30(2):123–126. **https://doi.org/10.1130/0091-7613(2002)030<0123:DSPROE>2.0.CO;2**

Jackson, M.G., and Carlson, R.W., 2011. An ancient recipe for flood-basalt genesis. *Nature*, 476(7360):316–319. **https://doi.org/10.1038/nature10326**

Jackson, M.G., Carlson, R.W., Kurz, M.D., Kempton, P.D., Francis, D., and Blusztajn, J., 2010. Evidence for the survival of the oldest terrestrial mantle reservoir. *Nature*, 466(7308):853–856. **https://doi.org/10.1038/nature09287**

Jacques, G., Hauff, F., Hoernle, K., Werner, R., Uenzelmann-Neben, G., Garbe-Schönberg, D., and Fischer, M., 2019. Nature and origin of the Mozambique Ridge, SW Indian Ocean. *Chemical Geology*, 507:9–22. **https://doi.org/10.1016/j.chemgeo.2018.12.027**

Jenkyns, H.C., 2003. Evidence for rapid climate change in the Mesozoic-Palaeogene greenhouse world. *Philosophical Transactions of the Royal Society, A: Mathematical, Physical and Engineering Sciences*, 361(1810):1885–1916. **https://doi.org/10.1098/rsta.2003.1240**

Jenkyns, H.C., 2010. Geochemistry of oceanic anoxic events. *Geochemistry, Geophysics, Geosystems,* 11(3):Q03004. **https://doi.org/10.1029/2009GC002788**

Jung, C., Voigt, S., Friedrich, O., Koch, M.C., and Frank, M., 2013. Campanian–Maastrichtian ocean circulation in the tropical Pacific. *Paleoceanography,* 28(3):562–573. **https://doi.org/10.1002/palo.20051**

König, M., and Jokat, W., 2010. Advanced insights into magmatism and volcanism of the Mozambique Ridge and Mozambique Basin in the view of new potential field data. *Geophysical Journal International*, 180(1):158–180. **https://doi.org/10.1111/j.1365-246X.2009.04433.x**

Kump, L.R., and Pollard, D., 2008. Amplification of Cretaceous warmth by biological cloud feedbacks. *Science*, 320(5873):195. **https://doi.org/10.1126/science.1153883**

Lutjeharms, J.R.E., 1996. The exchange of water between the South Indian and South Atlantic Oceans. *In* Wefer, G., Berger, W.H., Siedler, G., and Webb, D.J. (Eds.), *The South Atlantic: Present and Past Circulation:* Berlin (Springer-Verlag), 125–162.

Lutjeharms, J.R.E., 2006. *The Agulhas Current:* Berlin (Springer-Verlag). **https://doi.org/10.1007/3-540-37212-1**

Lutjeharms, J.R.E., and Ansorge, I., 2001. The Agulhas Return Current. *Journal of Marine Systems,* 30(1–2):115–138. **https://doi.org/10.1016/S0924-7963(01)00041-0**

MacLeod, K.G., and Huber, B.T., 1996. Reorganization of deep ocean circulation accompanying a Late Cretaceous extinction event. *Nature*, 380(6573):422–425. **https://doi.org/10.1038/380422a0**

MacLeod, K.G., Isaza Londoño, C., Martin, E.E., Jiménez Berrocoso, Á., and Basak, C., 2011. Changes in North Atlantic circulation at the end of the

Cretaceous greenhouse interval. *Nature Geoscience*, 4:779–782. **https://doi.org/10.1038/ngeo1284**

MacLeod, K.G., Martin, E.E., and Blair, S.W., 2008. Nd isotopic excursion across Cretaceous Oceanic Anoxic Event 2 (Cenomanian–Turonian) in the tropical North Atlantic. *Geology,* 36(10):811–814. **https://doi.org/10.1130/G24999A.1**

Mantyla, A.W., and Reid, J.L., 1995. On the origins of deep and bottom waters of the Indian Ocean. *Journal of Geophysical Research: Oceans,* 100(C2):2417–2439. **https://doi.org/10.1029/94JC02564**

Marks, K.M., and Tikku, A.A., 2001. Cretaceous reconstructions of East Antarctica, Africa and Madagascar. *Earth and Planetary Science Letters*, 186(3–4):479–495. **https://doi.org/10.1016/S0012-821X(01)00262-X**

Murphy, D.P., and Thomas, D.J., 2012. Cretaceous deep-water formation in the Indian sector of the Southern Ocean. *Paleoceanography,* 27(1). **https://doi.org/10.1029/2011PA002198**

Murphy, D.P., and Thomas, D.J., 2013. The evolution of Late Cretaceous deep-ocean circulation in the Atlantic basins: neodymium isotope evidence from South Atlantic drill sites for tectonic controls. *Geochemistry, Geophysics, Geosystems*, 14(12):5323–5340. **https://doi.org/10.1002/2013GC004889**

Niemi, T.M., Ben-Avraham, Z., Hartnady, C.J.H., and Reznikov, M., 2000. Post-Eocene seismic stratigraphy of the deep ocean basin adjacent to the southeast African continental margin: a record of geostrophic bottom current systems. *Marine Geology,* 162(2–4):237–258. **https://doi.org/10.1016/S0025-3227(99)00062-6**

Parsiegla, N., Gohl, K., and Uenzelmann-Neben, G., 2008. The Agulhas Plateau: structure and evolution of a large igneous province. *Geophysical Journal International,* 174(1):336–350. **https://doi.org/10.1111/j.1365-246X.2008.03808.x**

Pietsch, R., and Uenzelmann-Neben, G., 2015. The Manihiki Plateau—a multistage volcanic emplacement history. *Geochemistry, Geophysics, Geosystems*, 16(8):2480–2498. **https://doi.org/10.1002/2015GC005852**

Poulsen, C.J., Gendaszek, A.S., and Jacob, R.L., 2003. Did the rifting of the Atlantic Ocean cause the Cretaceous thermal maximum? *Geology*, 31(2):115–118. **https://doi.org/10.1130/0091-7613(2003)031<0115:DTROTA>2.0.CO;2**

Poulsen, C.J., and Zhou, J., 2013. Sensitivity of Arctic climate variability to mean state: insights from the Cretaceous. *Journal of Climate*, 26(18):7003–7022. **https://doi.org/10.1175/JCLI-D-12-00825.1**

Read, J.F., and Pollard, R.T., 1999. Deep inflow into the Mozambique Basin. *Journal of Geophysical Research: Oceans*, 104(C2):3075–3090. **https://doi.org/10.1029/1998JC900078**

Robinson, S.A., Murphy, D.P., Vance, D., and Thomas, D.J., 2010. Formation of "Southern Component Water" in the Late Cretaceous: evidence from Nd-isotopes. *Geology,* 38(10):871–874. **https://doi.org/10.1130/G31165.1**

Robinson, S.A., and Vance, D., 2012. Widespread and synchronous change in deep-ocean circulation in the North and South Atlantic during the Late Cretaceous. *Paleoceanography,* 27(1):PA1102. **https://doi.org/10.1029/2011PA002240**

Royer, D.L., Berner, R.A., Montañez, I.P., Tabor, N.J., and Beerling, D.J., 2004. CO_2 as a primary driver of Phanerozoic climate. *GSA Today*, 14(3):3–10.

Sager, W.W., Kim, J., Klaus, A., Nakanishi, M., and Khankishieva, L.M., 1999. Bathymetry of Shatsky Rise, northwest Pacific Ocean: implications for ocean plateau development at a triple junction. *Journal of Geophysical Research: Solid Earth*, 104(B4):7557–7576. **https://doi.org/10.1029/1998JB900009**

Sager, W.W., Zhang, J., Korenaga, J., Sano, T., Koppers, A.A.P., Widdowson, M., and Mahoney, J.J., 2013. An immense shield volcano within the Shatsky Rise oceanic plateau, northwest Pacific Ocean. *Nature Geoscience*, 6:976–981. **https://doi.org/10.1038/ngeo1934**

Schlanger, S.O., and Jenkyns, H.C., 1976. Cretaceous oceanic anoxic events: causes and consequences. *Geologie en Mijnbouw,* 55:179–184.

Schlüter, P., and Uenzelmann-Neben, G., 2007. Seismostratigraphic analysis of the Transkei Basin: a history of deep sea current controlled sedimentation. *Marine Geology*, 240(1–4):99–111. **https://doi.org/10.1016/j.margeo.2007.02.015**

Schlüter, P., and Uenzelmann-Neben, G., 2008. Conspicuous seismic reflections in Upper Cretaceous sediments as evidence for black shales off South Africa. *Marine and Petroleum Geology*, 25(10):989–999. **https://doi.org/10.1016/j.marpetgeo.2007.10.003**

Sewall, J.O., van de Wal, R.S.W., van der Zwan, K., van Oosterhout, C., Dijkstra, H.A., and Scotese, C.R., 2007. Climate model boundary conditions for four Cretaceous time slices. *Climate of the Past*, 3:647–657. **https://doi.org/10.5194/cp-3-647-2007**

Sijp, W.P., von der Heydt, A.S., Dijkstra, H.A., Flögel, S., Douglas, P.M.J., and Bijl, P.K., 2014. The role of ocean gateways on cooling climate on long time scales. *Global and Planetary Change*, 119:1–22. **https://doi.org/10.1016/j.gloplacha.2014.04.004**

Sinninghe Damsté, J.S., van Bentum, E.C., Reichart, G.-J., Pross, J., and Schouten, S., 2010. A CO_2 decrease-driven cooling and increased latitudinal temperature gradient during the mid-Cretaceous Oceanic Anoxic Event 2. *Earth and Planetary Science Letters*, 293(1–2):97–103. **https://doi.org/10.1016/j.epsl.2010.02.027**

Smith, W.H.F., and Sandwell, D.T., 1997. Global seafloor topography from satellite altimetry and ship depth soundings. *Science,* 277(5334):1956–1962. **https://doi.org/10.1126/science.277.5334.1956**

Stracke, A., Hofmann, A.W., and Hart, S.R., 2005. FOZO, HIMU, and the rest of the mantle zoo. *Geochemistry, Geophysics, Geosystems*, 6(5):1–20. **https://doi.org/10.1029/2004GC000824**

Taylor, B., 2006. The single largest oceanic plateau: Ontong Java–Manihiki–Hikurangi. *Earth and Planetary Science Letters*, 241(3–4):372–380. **https://doi.org/10.1016/j.epsl.2005.11.049**

Tejada, M.L.G., Mahoney, J.J., Castillo, P.R., Ingle, S.P., Sheth, H.C., and Weis, D., 2004. Pin-pricking the elephant: evidence on the origin of the Ontong Java Plateau from Pb-Sr-Hf-Nd isotopic characteristics of ODP Leg 192 basalts. *In* Fitton, J.G., Mahoney, J.J., Wallace, P.J., and Saunders, A.D. (Eds.), *Origin and Evolution of the Ontong Java Plateau.* Geological Society Special Publication, 229(1):133–150. **https://doi.org/10.1144/GSL.SP.2004.229.01.09**

Tejada, M.L.G., Mahoney, J.J., Duncan, R.A., and Hawkins, M.P., 1996. Age and geochemistry of basement and alkalic rocks of Malaita and Santa Isabel, Solomon Islands, southern margin of Ontong Java Plateau. *Journal of Petrology*, 37(2):361–394. **https://doi.org/10.1093/petrology/37.2.361**

Tejada, M.L.G., Mahoney, J.J., Neal, C.R., Duncan, R.A., and Petterson, M.G., 2002. Basement geochemistry and geochronology of Central Malaita, Solomon Islands, with implications for the origin and evolution of the Ontong Java Plateau. *Journal of Petrology*, 43(3):449–484. **https://doi.org/10.1093/petrology/43.3.449**

Timm, C., Hoernle, K., Werner, R., Hauff, F., van den Bogaard, P., Michael, P., Coffin, M.F., and Koppers, A., 2011. Age and geochemistry of the oceanic Manihiki Plateau, SW Pacific: new evidence for a plume origin. *Earth and Planetary Science Letters*, 304(1–2):135–146. **https://doi.org/10.1016/j.epsl.2011.01.025**

Tomczak, M., and Godfrey, J.S., 1994. Hydrology of the Indian Ocean. *In* Tomczak, M., and Godfrey, J.S. (Eds.), *Regional Oceanography: an Introduction*. Pergamon, Amsterdam (Pergamon), 221–236. **https://doi.org/10.1016/B978-0-08-041021-0.50016-3**

Toole, J.M., and Warren, B.A., 1993. A hydrographic section across the subtropical South Indian Ocean. *Deep-Sea Research, Part I: Oceanographic Research Papers*, 40(10):1973–2019. **https://doi.org/10.1016/0967-0637(93)90042-2**

Toggweiler, J.R., and Russell, J., 2008. Ocean circulation in a warming climate. *Nature*, 451(7176):286–288. **https://doi.org/10.1038/nature06590**

Totterdell, J.M., Struckmeyer, H.I.M., Boreham, C.J., Mitchell, C.H., Monteil, E., and Bradshaw, B.E., 2008. Mid–Late Cretaceous organic-rich rocks from the eastern Bight Basin: implications for prospectivity. *In* Blevin, J.E., Bradshaw, B.E., and Uruski, C. (Eds.), *Eastern Australasian Basins Symposium III.* Petroleum Exploration Society of Australia Special Publication, 137–158.

Tsikos, H., Jenkyns, H.C., Walsworth-Bell, B., Petrizzo, M.R., Forster, A., Kolonic, S., Erba, E., et al., 2004. Carbon-isotope stratigraphy recorded by the Cenomanian–Turonian oceanic anoxic event: correlation and impli-

cations based on three key localities. *Journal of the Geological Society (London, United Kingdom),* 161:711–719. **https://doi.org/10.1144/0016-764903-077**

Tucholke, B.E., and Carpenter, G.B., 1977. Sediment distribution and Cenozoic sedimentation patterns on the Agulhas Plateau. *Geological Society of America Bulletin*, 88(9):1337–1346. **https://doi.org/10.1130/0016-7606(1977)88<1337:SDACSP>2.0.CO;2**

Tucholke, B.E., and Embley, R.E., 1984. Cenozoic regional erosion of the abyssal seafloor off South Africa. *In* Schlee, J.S. (Ed.), *Interregional unconformities and hydrocarbon accumulation*. AAPG Memoir, 36:145–164.

Uenzelmann-Neben, G., 1998. Sedimentation and tectonics of Agulhas Ridge and Agulhas Plateau. *Berichte zur Polar und Meeresforschung,* 273:22.

Uenzelmann-Neben, G., 2001. Seismic characteristics of sediment drifts: an example from the Agulhas Plateau, southwest Indian Ocean. *Marine Geophysical Research,* 22(5):323–343. **https://doi.org/10.1023/A:1016391314547**

Uenzelmann-Neben, G., 2002. Contourites on the Agulhas Plateau, SW Indian Ocean: indications for the evolution of currents since Palaeogene times. *In* Stow, D.A.V., Pudsey, C.J., Howe, J.A., Faugères, J.-C., and Viana, A.R. (Eds.), *Deep-Water Contourite Systems: Modern Drifts and Ancient Series, Seismic and Sedimentary Characteristics.* Memoirs - Geological Society of London, 22(1):271–288. **https://doi.org/10.1144/GSL.MEM.2002.022.01.20**

Uenzelmann-Neben, G., 2005. Southeastern Atlantic and southwestern Indian Ocean: reconstruction of the sedimentary and tectonic development since the Cretaceous AISTEK-1: Agulhas Transect. *Berichte zur Polar- und Meeresforschung*, 73.

Uenzelmann-Neben, G., 2010. Margins of Africa - the interdependency of deep and shallow studies. Inkaba yeAfrica Annual Workshop, Potsdam.

Uenzelmann-Neben, G., 2014. *The Expedition of the Research Vessel "Sonne" to the Mozambique Ridge in 2014 (SO232):* Bremerhaven, Germany (Alfred-Wegener-Institut). **https://doi.org/10.2312/BzPM_0677_2014**

Uenzelmann-Neben, G., Gohl, K., Ehrhardt, A., and Seargent, M., 1999. Agulhas Plateau, SW Indian Ocean: new evidence for extensive volcanism. *Geophysical Research Letters*, 26(13):1941–1944. **https://doi.org/10.1029/1999GL900391**

Uenzelmann-Neben, G., Weber, T., Grützner, J., and Thomas, M., 2017. Transition from the Cretaceous ocean to Cenozoic circulation in the western South Atlantic - a twofold reconstruction. *Tectonophysics*, 716:225–240. **https://doi.org/10.1016/j.tecto.2016.05.036**

van Aken, H.M., Ridderinkhof, H., and de Ruijter, W.P.M., 2004. North Atlantic Deep Water in the south-western Indian Ocean. *Deep Sea Research Part I: Oceanographic Research Papers,* 51(6):755–776. **https://doi.org/10.1016/j.dsr.2004.01.008**

Voigt, S., Jung, C., Friedrich, O., Frank, M., Teschner, C., and Hoffmann, J., 2013. Tectonically restricted deep-ocean circulation at the end of the Cretaceous greenhouse. *Earth and Planetary Science Letters*, 369–370:169–177. **https://doi.org/10.1016/j.epsl.2013.03.019**

You, Y., Lutjeharms, J.R.E., Boebel, O., and de Ruijter, W.P.M., 2003. Quantification of the interocean exchange of intermediate water masses around southern Africa. *Deep-Sea research II: Topical Studies in Oceanography*, 50(1):197–228. **https://doi.org/10.1016/S0967-0645(02)00384-3**

Zhou, J., Poulsen, C.J., Pollard, D., and White, T.S., 2008. Simulation of modern and middle Cretaceous marine $\delta^{18}O$ with an ocean-atmosphere general circulation model. *Paleoceanography and Paleoclimatology*, 23(3):PA3223. **https://doi.org/10.1029/2008PA001596**

Zindler, A., and Hart, S., 1986. Chemical geodynamics. *Annual Review of Earth and Planetary Sciences*, 14:493–570. **https://doi.org/10.1146/annurev.ea.14.050186.002425**

Table T1. Location coordinates, planktonic foraminifer biozones, and ages of sediment piston cores taken on Agulhas Plateau (AP). From Tucholke and Carpenter (1977). E = excellent, G = good, M = moderate, P = poor.

Core	Sample (cm)	Region	Coordinates	Age	Biozone	Preservation	Biomarkers/comments
V16-55	40–41	Central AP	40°14′S, 25°15′E	early Eocene	AE1	G	Foraminifer ooze *Ac. aspensis* *Ac. collactea*
V16-55	150–151	Central AP	40°14′S, 25°15′E	early Eocene	AE1	G	Foraminifer ooze
V16-56	30–31	Southern AP	41°21′S, 26°38′E	late Campanian	*A. australis*	G–E	*Ar. australis* *Ar. mateola* *Gl. planata*
V16-56	190–191	Southern AP	41°21′S, 26°38′E	late Campanian	*A. australis*	G–E	*Ar. australis* *Ar. mateola* *Gl. planata*
V22-124	172–173	Central AP	40°02′S, 25°18′E	late Maastrichtian	*A. mayaroensis*	G	Foraminifer chalk *Ab. mayaroensis* *Ru. circumnodifer* *Gl. subcarinatus*
V22-126	358–359	Central AP	41°10′S, 26°30′E	Paleocene	AP4	G	Foraminifer chalk *Gl. planoconica* *Ac. mckannai* *Ac. soldadoensis* *Morozovella* spp.
V22-134	40–41	Northern AP	39°05′S, 24°09′E	?	?	P	Mn nodules Quaternary to recent
V22-134	140–141	Northern AP	39°05′S, 24°09′E	Cretaceous?	?	P–M	Mn nodules Abundant fish teeth Foraminifers rare Radiolarians
V24-214	30–31	Northern AP	37°03′S, 24°57′E	latest Eocene–early Oligocene	AE10–AO1	G	Foraminifer ooze
V24-214	290–291	Northern AP	37°03′S, 24°57′E	latest Eocene–early Oligocene	AE10–AO1	G	Foraminifer ooze Highly fragmented *Su. angiporoides* *Su. utilisindex*

Table T2. Seismostratigraphic model for Agulhas Plateau. Unit age from Tucholke and Carpenter (1977), Tucholke and Embley (1984), and Uenzelmann-Neben (2001, 2002). OAE = oceanic anoxic event. PETM = Paleocene/Eocene Thermal Maximum.

Unit	Unit age (Ma)	Base reflector	Climatic/Oceanic event of base reflector
6	0–6	LP	Regional hiatus from 10 to 6 Ma due to erosion/redeposition resulting from Circumpolar Deep Water activity; covers Mi6 (9.6 Ma)
5	10–15	MM (wedge-out at seafloor)	Erosion/Redeposition due to Antarctic Bottom Water activity, Miocene Climatic Optimum?; covers Mi2 (16.1 Ma) and Mi3 (13.6 Ma)?
4	15–29	LO (unconformity)	Intensified abyssal currents (Antarctic Circumpolar Current) resulting in a hiatus from 33 to 29 Ma, post-Oi1 (35.8 Ma), covers Oi2 (32.5 Ma)
3	33–47	LE (conformity)	Sea level highstand and low sedimentation rates resulting in hiatus from 56 to 47 Ma, covers PETM (55.8 Ma)?
2	>65	M (erosional unconformity)	Erosion, covers OAE 2 (~93.6 Ma) and OAE 3 (~85.8 Ma)?
1		Top basement	

Table T3. Seismostratigraphic model for Transkei Basin. Unit age from Niemi et al. (2000) and Schlüter and Uenzelmann-Neben (2007, 2008). RMS = root mean square. PETM = Paleocene/Eocene Thermal Maximum. OAE = oceanic anoxic event.

Unit	Unit age (Ma, approximate)	Base reflector	Unit thickness (RMS) (m)	Sedimentation rate (m/My)	Climatic/Oceanic event of base reflector
5	0–6	P (discordance, onlap and downlap)	150.4	25	Pliocene warm phase
4	6–15	M	146.9	16.3	Miocene Climatic Optimum (MCO)?; covers Mi3 (13.6 Ma), Mi4 (12.5 Ma), Mi5 (11.8 Ma), and Mi6 (9.6 Ma)?
3	15–32.5	O (unconformity, downlap)	92.9	5.3	Intensified bottom water flow resulting in a hiatus; post-Oi1 (35.8 Ma), covers Oi2 (32.5 Ma), Mi1 (23.08 Ma), Mi2 (16.1 Ma), MCO
2	32.5–35.8	E	46.2	14	High-amplitude reflection in lower part – black shales, internal reflector separating lower homogeneous from upper faulted part; K/Pg boundary, PETM
1	35.8–90	Basement	854.1	15.8	Erosion, covers OAE 2 (~93.6 Ma) and OAE 3 (~85.8 Ma)?

Table T4. Site information, selection criteria, and science questions to be addressed, Expedition 392. EPSP = Environmental Protection and Safety Panel, CDP = common depth point. OAE = oceanic anoxic event. PETM = Paleocene/Eocene Thermal Maximum, K/Pg = Cretaceous/Paleogene boundary. (Continued on next page.)

Proposed site	Primary seismic line	Latitude, longitude (°)	Water depth (m)	Proposed sediment penetration (mbsf)	Proposed basement penetration (mbsf)	Total proposed penetration (mbsf)	EPSP approved penetration (mbsf)	Drilling targets	Objectives to address	Site information
Primary sites										
TB-01A	AWI-20050008 (CDP 2988)	–35.6805992, 29.6501999	4500	950	0	950	1100	Cretaceous–Neogene sediment Black shales	3–6	150 m Quaternary–Pliocene, 50 m upper Miocene, 70 m middle–lower Miocene to Oligocene, 30 m Eocene, 250 m Eocene–Paleocene, 250 m Maastrichtian–Santonian Black shale (OAE 3?)
AP-10A	AWI-20050201 (CDP 12650)	–39.9510994, 26.2362003	2500	620	50	670	670	Cretaceous–Neogene sediment Basement	1–6	300 m lower Miocene–lower Oligocene, 150 m Eocene, 70 m Paleocene, 100 m Maastrichtian/older Mi1, Oi1, PETM(?), K/Pg, OAE 3, OAE 2 Basement
AP-09B	AWI-98105 (CDP 5750)	–40.7859001, 26.6068993	2620	340	150	490	550	Cretaceous, Paleogene sediment Basement	1–6	200 m Eocene, 20 m Paleocene, 120 m Maastrichtian/older PETM(?), K/Pg, OAE 3, OAE 2 Shallow basement target
AP-07A	AWI-98011 (CDP 2100)	–37.0250015, 24.9953003	3400	100	200	300	300	Cretaceous sediment Basement	1–6	100 m Paleocene/ Maastrichtian (or older) K/Pg, OAE 3, OAE 2 Shallow basement target
AP-08A	AWI-98011 (CDP 1150)	–37.16550105, 24.7980995	3900	400	50	450	500	Cretaceous, Paleogene sediment Basement	1–6	350 m Paleocene, 50 m Maastrichtian/older Shallowly buried oldest sediment K/Pg, OAE 3, OAE 2 Layered basement
Alternate sites										
TB-02A (alt. for TB-01A)	AWI-20050008 (CDP 2068)	–35.4749985, 29.6793995	4300	1050	0	1050	1200	Cretaceous–Neogene sediment Black shales	3–6	230 m Quaternary and Pliocene, 150 m upper Miocene, 70 m middle–lower Miocene and Oligocene, 50 m Eocene, 250 m Eocene–Paleocene, 250 m Maastrichtian–Santonian Black shale (OAE 3?)
AP-01A (alt. for AP-09B)	AWI-98015 (CDP 2850)	–40.8800011, 27.4428997	2700	150	200	350	350	Cretaceous sediment Basement	1–6	100 m Pliocene–upper Miocene, 50 m Maastrichtian/ older Thin sediment sequence K/Pg, OAE 3 Shallow basement
AP-02A (alt. for AP-08A)	AWI-98015 (CDP 3500)	–40.8604012, 27.2537003	2620	650	50	700	700	Cretaceous–Neogene sediment Basement	1–6	200 m upper Miocene, 150 m lower Miocene–Oligocene, 150 m Eocene, 50 m Paleocene, 50 m Maastrichtian/older Mi5, Mi4, Mi1, Oi1, PETM(?), K/Pg, OAE 3
AP-03A (alt. for AP-09B)	AWI-98014 (CDP 6950)	–41.2631989, 26.3272991	3220	300	200	500	500	Cretaceous, Paleogene sediment Basement	1–6	130 m Eocene, 120 m Paleocene, 50 m Maastrichtian/older Shallow burial of older sediments PETM(?), K/Pg, OAE 3
AP-04B (alt. for AP-10A)	AWI-98014 (CDP 6220)	–41.2951012, 26.1151009	3075	850	50	900	900	Cretaceous–Neogene sediment Basement	1–6	170 m upper Miocene, 140 m lower Miocene–lower Oligocene, 300 m Eocene, 160 m Paleocene, 80 m Maastrichtian/older Mi5, Mi4, Mi1, Oi1, PETM(?), K/Pg, OAE 3, OAE 2 Sediment drift structure (high sedimentation rate) Basement
AP-05A (alt. for AP-10A)	AWI-98017 (CDP 4900)	–40.0082626, 25.2681999	2800	450	50	500	500	Cretaceous, Paleogene sediment Basement	1–6	200 m Eocene, 130 m Paleocene, 120 m Maastrichtian/older PETM(?), K/Pg, OAE 3, OAE 2 Good Cretaceous target Basement
AP-06A (alt. for AP-07A)	AWI-98017 (CDP 5700)	–40.0663986, 25.5009003	2550	200	200	400	400	Cretaceous sediment Basement	1–6	100 m Paleocene, 100 m Maastrichtian/older Shallower burial depth for older sediments K/Pg, OAE 2, OAE 3
AP-11A (alt. for AP-10A)	AWI-98017 (CDP 1400)	–40.0671997, 24.2537994	3490	720	50	770	770	Cretaceous–Neogene sediment Basement	1–6	150 m upper Miocene, 170 m lower Miocene–lower Oligocene, 180 m Eocene, 150 m Paleocene, 70 m Maastrichtian/older Mi5, Mi4, Mi1, Oi1, PETM(?), K/Pg, OAE 3
AP-12A (alt. for AP-08A)	AWI-98017 (CDP 2400)	–40.0681992. 24.5436993	3100	750	50	800	800	Cretaceous–Neogene sediment Basement	1–6	200 m upper Miocene, 200 m lower Miocene–lower Oligocene, 180 m Eocene, 100 m Paleocene, 70 m Maastrichtian/older Mi5, Mi4, Mi1, Oi1, PETM(?), K/Pg, OAE 3 Layered basement

Table T4 (continued).

Proposed site	Primary seismic line	Latitude, longitude (°)	Water depth (m)	Proposed sediment penetration (mbsf)	Proposed basement penetration (mbsf)	Total proposed penetration (mbsf)	EPSP approved penetration (mbsf)	Drilling targets	Objectives to address	Site information
AP-13A (alt. for AP-09B)	AWI-98017 (CDP 1180)	–40.0671997, 24.1895008	3850	420	200	620	620	Cretaceous, Paleogene sediment Basement	1–6	200 m Eocene, 150 m Paleocene, 70 m Maastrichtian/older PETM(?), K/Pg, OAE 3 Layered basement
AP-14A (alt. for AP-07A)	AWI-98015 (CDP 7850)	–40.7178993, 26.0069008	2800	650	50	700	700	Cretaceous–Neogene sediment Basement	1–6	200 m lower Miocene–lower Oligocene, 200 m Eocene, 130 m Paleocene, 100 m Maastrichtian/older Mi1, Oi1, PETM(?), K/Pg, OAE 3, OAE 2 Layered basement

Table T5. Operations plan and time estimates for primary sites, Expedition 392. See Drilling, coring, and downhole measurements strategy and Figure AF3 for details about Environmental Protection and Safety Panel (EPSP) approval for proposed Site AP-09B. LWD = logging while drilling, MWD = measurement while drilling. APC = advanced piston corer, XCB = extended core barrel, RCB = rotary core barrel. FMS = Formation MicroScanner, VSI = Versatile Seismic Imager, UBI = Ultrasonic Borehole Imager.

Site No.	Location (Latitude Longitude)	Seafloor Depth (mbrf)	Operations Description	Transit (days)	Drilling Coring (days)	LWD/ MWD Log (days)
Cape Town			Begin Expedition 5.0 port call days			
			Transit ~604 nmi to TB-01A @ 10.5 knots	2.4		
TB-01A	35° 40.8360' S	4511	Hole A - APC to 300 mbsf; XCB to 700 mbsf	0	6.6	0.0
EPSP	29° 39.0120' E		Hole B - Drill to 690 mbsf; RCB to 950 mbsf; Log Triple, FMS, VSI	0	4.8	2.0
to 1100 mbsf						
			Sub-Total Days On-Site: 13.3			
			Transit ~303 nmi to AP-10A @ 10.5 knots	1.2		
AP-10A	39° 57.0660' S	2511	Hole A - APC to 300 mbsf; XCB to 620 mbsf	0	3.9	0.0
EPSP	26° 14.1720' E		Hole B - APC to 300 mbs; XCB to 620 mbsf	0	3.8	0.0
to 670 mbsf			Hole C - Drill to 610 mbsf; RCB to 670 mbsf, Log Quad	0	2.8	0.7
			Sub-Total Days On-Site: 11.2			
			Transit ~53 nmi to AP-09B @ 10.6 knots	0.2		
AP-09B	40° 47.1540' S	2631	Hole A - APC to 300 mbsf; XCB to 340 mbsf	0	2.1	0.0
EPSP	26° 36.4140' E		Hole B - Drill to 200 mbsf; APC to 300 mbsf: XCB to 340 mbsf	0	1.5	0.0
to 550 mbsf			Hole C - Drill to 330 mbsf; RCB to 490 mbsf; Log Triple, FMS, UBI	0	4.5	1.2
			Sub-Total Days On-Site: 9.4			
			Transit ~238 nmi to AP-07A @ 10.5 knots	0.9		
AP-07A	37° 1.5000' S	3411	Hole A - RCB to 300 mbsf; Log Triple, FMS, UBI	0	7.0	1.1
EPSP	24° 59.7180' E					
to 300 mbsf						
			Sub-Total Days On-Site: 8.0			
			Transit ~13 nmi to AP-08A @ 10.1 knots	0.1		
AP-08A	37° 9.9300' S	3911	Hole A - APC to 300 mbsf; XCB to 400 mbsf	0	3.1	0.0
EPSP	24° 47.8860' E		Hole B - APC to 300 mbsf; XCB to 400 mbsf	0	3.0	0.0
to 500 mbsf			Hole C - Drill to 390 mbsf; RCB to 450 mbsf	0	2.6	0.0
			Sub-Total Days On-Site: 8.7			
			Transit ~394 nmi to Cape Town @ 10.5 knots	1.6		
Cape Town			End Expedition	6.4	45.7	4.9

Port Call:	5.0	Total Operating Days:	57.0
Sub-Total On-Site:	50.6	Total Expedition:	62.0

Table T6. Time estimates for alternate sites, Expedition 392. LWD = logging while drilling, MWD = measurement while drilling. EPSP = Environmental Protection and Safety Panel. APC = advanced piston corer, XCB = extended core barrel, RCB = rotary core barrel. FMS = Formation MicroScanner, VSI = Versatile Seismic Imager, UBI = Ultrasonic Borehole Imager.

Site No.	Location (Latitude Longitude)	Seafloor Depth (mbrf)	Operations Description	Drilling Coring (days)	LWD/ MWD Log (days)
TB-02A (TB-01A)	35° 28.4999' S	4311	Hole A - APC to 300 mbsf; XCB to 700 mbsf	6.4	0.0
EPSP	29° 40.7640' E		Hole B - Drill to 690 mbsf; RCB to 1050 mbsf; Log Triple, FMS, VSI	5.7	2.0
to 1200 mbsf					
			Sub-Total Days On-Site: 14.1		
AP-01A (AP-09B)	40° 52.8001' S	2711	Hole A - APC to 150 mbsf	1.5	0.0
EPSP	27° 26.5740' E		Hole B - Drill to 140 mbsf; RCB to 300 mbsf; Log Triple, FMS, UBI	3.8	1.1
to 350 mbsf					
			Sub-Total Days On-Site: 6.4		
AP-02A (AP-08A)	40° 51.6241' S	2631	Hole A - APC to 300 mbsf; XCB to 650 mbsf	4.1	0.0
EPSP	27° 15.2220' E		Hole B - APC to 300 mbsf; XCB to 650 mbsf	4.0	0.0
to 700 mbsf			Hole C - Drill to 640 mbsf; RCB to 700 mbsf	2.7	0.0
			Sub-Total Days On-Site: 10.8		
AP-03A (AP-09B)	41° 15.7919' S	3231	Hole A - APC to 300 mbsf	2.6	0.0
EPSP	26° 19.6379' E		Hole B - Drill to 290 mbsf; RCB to 450 mbsf; Log Triple, FMS, UBI	4.3	1.2
to 500 mbsf					
			Sub-Total Days On-Site: 8.1		
AP-04B (AP-10A)	41° 17.7061' S	3086	Hole A - APC to 300 mbsf; XCB to 850 mbsf	6.3	0.0
EPSP	26° 6.9061' E		Hole B - APC to 300 mbs; XCB to 850 mbsf	6.1	0.0
to 900 mbsf			Hole C - Drill to 840 mbsf; RCB to 900 mbsf; Log Quad	3.6	0.8
			Sub-Total Days On-Site: 16.8		
AP-05A (AP-10A)	40° 0.4958' S	2811	Hole A - APC to 300 mbsf; XCB to 450 mbsf	3.0	0.0
EPSP	25° 16.0919' E		Hole B - APC to 300 mbs; XCB to 450 mbsf	2.8	0.0
to 500 mbsf			Hole C - Drill to 440 mbsf; RCB to 500 mbsf; Log Quad	2.6	0.6
			Sub-Total Days On-Site: 9.0		
AP-06A (AP-07A)	40° 3.9839' S	2561	Hole A - RCB to 400 mbsf; Log Triple, FMS, UBI	7.0	1.1
EPSP	25° 30.0540' E				
to 400 mbsf					
			Sub-Total Days On-Site: 8.1		
AP-11A (AP-10A)	40° 4.0320' N	3501	Hole A - APC to 300 mbsf; XCB to 720 mbsf	5.4	0.0
EPSP	24° 15.2280' E		Hole B - APC to 300 mbs; XCB to 720 mbsf	5.2	0.0
to 770 mbsf			Hole C - Drill to 710 mbsf; RCB to 770 mbsf; Log Quad	3.2	0.8
			Sub-Total Days On-Site: 14.5		
AP-12A (AP-08A)	40° 4.0920' S	3111	Hole A - APC to 300 mbsf; XCB to 750 mbsf	5.4	0.0
EPSP	24° 32.6220' E		Hole B - APC to 300 mbsf; XCB to 750 mbsf	5.3	0.0
to 800 mbsf			Hole C - Drill to 740 mbsf; RCB to 800 mbsf	3.0	0.0
			Sub-Total Days On-Site: 13.7		
AP-13A (AP-09B)	40° 4.0320' S	3861	Hole A - APC to 300 mbsf; XCB to 420 mbsf	3.7	0.0
EPSP	24° 11.3700' E		Hole B - Drill to 410 mbsf; RCB to 570 mbsf; Log Triple, FMS, UBI	5.2	1.4
to 620 mbsf					
			Sub-Total Days On-Site: 10.3		
AP-14A (AP-07A)	40° 43.0740' S	2811	Hole A - RCB to 700 mbsf; Log Triple, FMS	5.9	1.2
EPSP	26° 0.4140' E				
to 700 mbsf					
			Sub-Total Days On-Site: 7.1		

Figure F1. Plate tectonic reconstructions using rotation poles published by Parsiegla et al. (2008). Rotation was performed with respect to Africa. Thick lines sketch estimated location of paleospreading system (black: spreading axis). AFFZ = Agulhas-Falkland Fracture Zone, ANT = Antarctica, FAP = future position of Agulhas Plateau (AP), FI = Falkland Islands, MB = Maurice Ewing Basin, MOZR = Mozambique Ridge. A. 120 Ma. Agulhas Plateau region was still occupied by Falkland Plateau (FP) with Maurice Ewing Bank (MEB) leaving no space for evolution of Agulhas Plateau at this time. B. 105 Ma. Agulhas Plateau region was cleared. This is the first possibility for formation of Agulhas Plateau. C. 100 Ma. Reconstructions of Agulhas Plateau, Northeast Georgia Rise (NEGR), and Maud Rise (MR) (but with recent boundaries) show overlap between Agulhas Plateau and Northeast Georgia Rise, which is due to different dimensions of these structures at 100 Ma. D. 94 Ma. Formation of entire large igneous province (LIP) (AP, NEGR, and MR) is complete. Bouvet triple junction is located at southwest tip of Agulhas Plateau (Marks and Tikku, 2001), and subsequent spreading causes separation of the three fragments of the AP-NEGR-MR LIP. Reproduced from Parsiegla et al. (2008). By permission of Oxford University Press on behalf of the Royal Astronomical Society. This figure is not included under the Creative Commons CC-BY 4.0 license of this publication. For permissions, please email journals.permissions@oup.com.

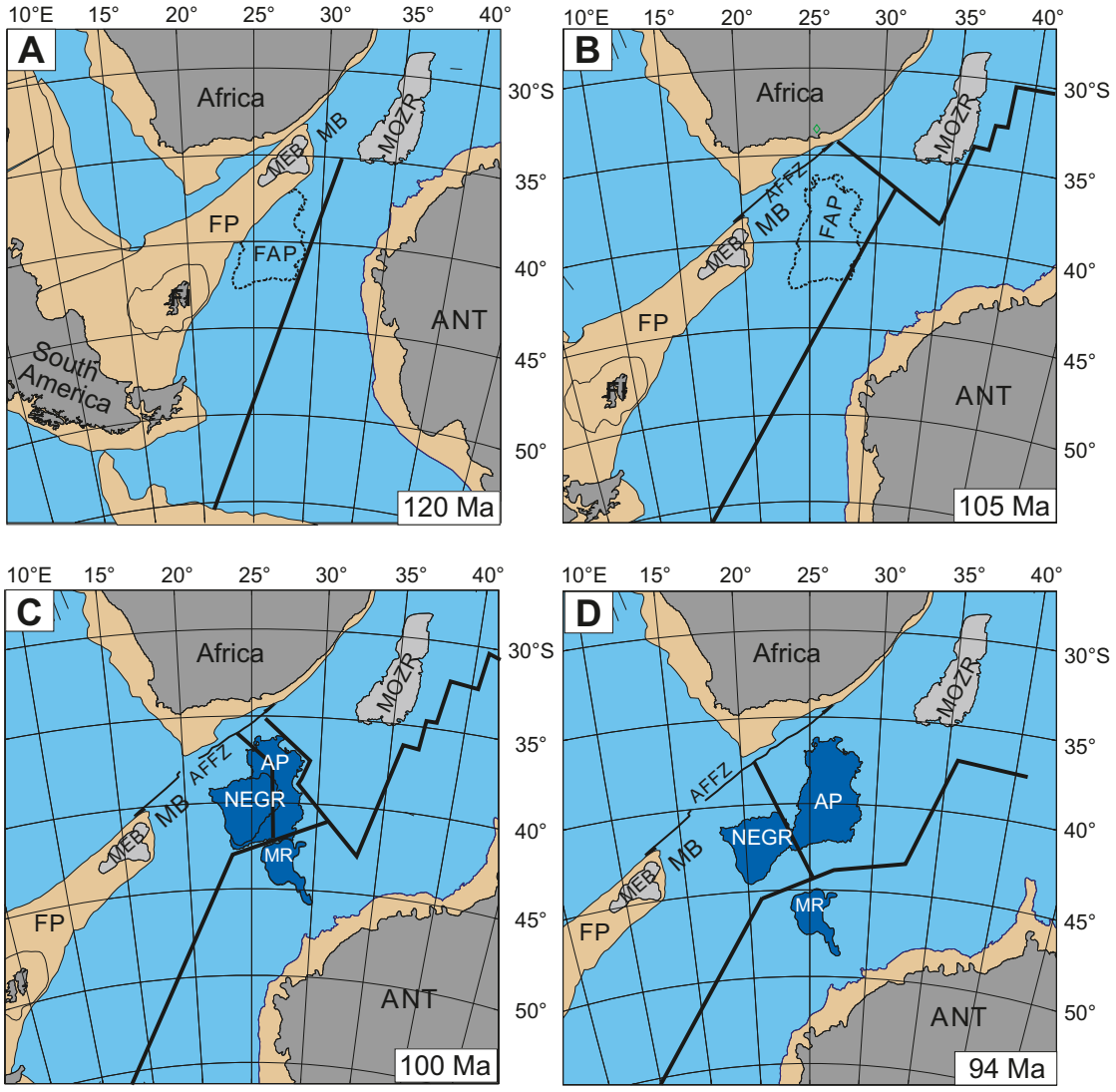

Figure F2. Map of region between Africa and Antarctica showing modern circulation (colored arrows; AABW = Antarctic Bottom Water, AC = Agulhas Current, ACC = Antarctic Circumpolar Current, NADW = North Atlantic Deep Water) and main tectonic elements (AP = Agulhas Plateau, AR = Astrid Ridge, GR = Gunnerus Ridge, MadR = Madagascar Ridge, MozR = Mozambique Ridge, MR = Maud Rise, SWIR = Southwest Indian Ridge) in African–Southern Ocean gateway.

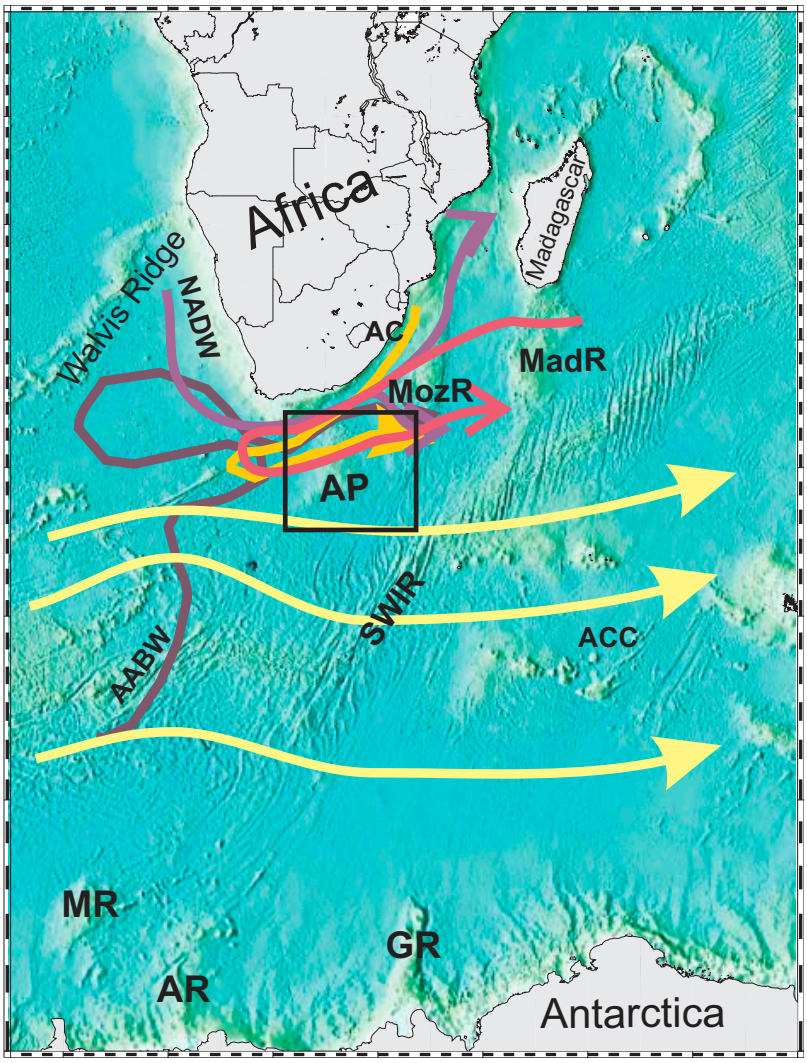

Figure F3. Satellite-derived bathymetry (Smith and Sandwell, 1997) of Agulhas Plateau and Transkei Basin. Proposed sites (A: red stars = primaries, B: pink stars = alternates) and existing sediment cores (triangles) on seismic lines (black lines) collected in 1998, 2005, and 2014 (Uenzelmann-Neben, 1998, 2005, 2014). Green diamond = Expedition 361 Site U1475 (Gruetzner et al., 2019; Hall et al., 2016).

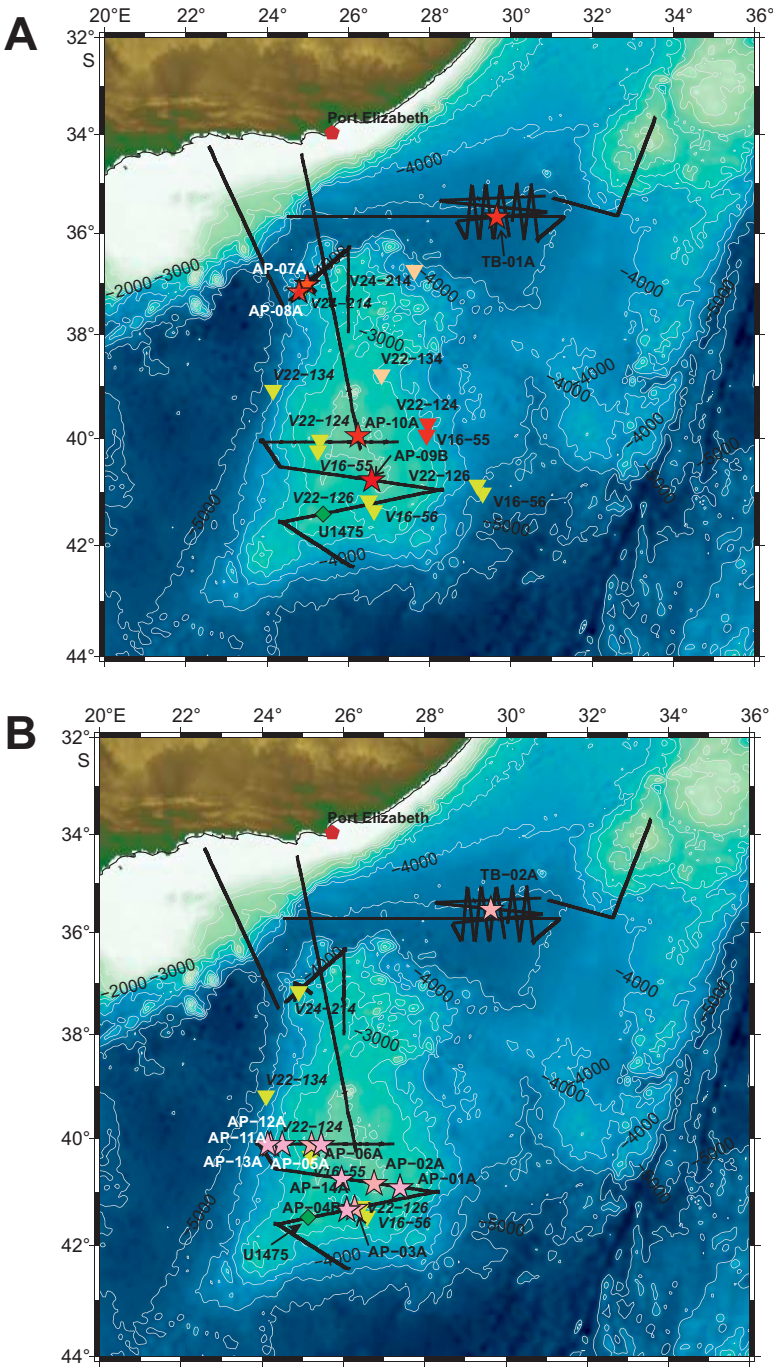

Figure F4. Seismic Profile AWI-98015 showing proposed Sites AP-09B and AP-14A from central Agulhas Plateau. Yellow arrow and line show interval approved for coring along Seismic Line AWI-98015 for proposed Site AP-09B (see Drilling, coring, and downhole measurements strategy for details). Inset map shows seismic line (white line) location. LE = lower Eocene, LO = lower Oligocene, M = Maastrichtian, MM = middle Miocene. CDP = common depth point. TWT = two-way traveltime.

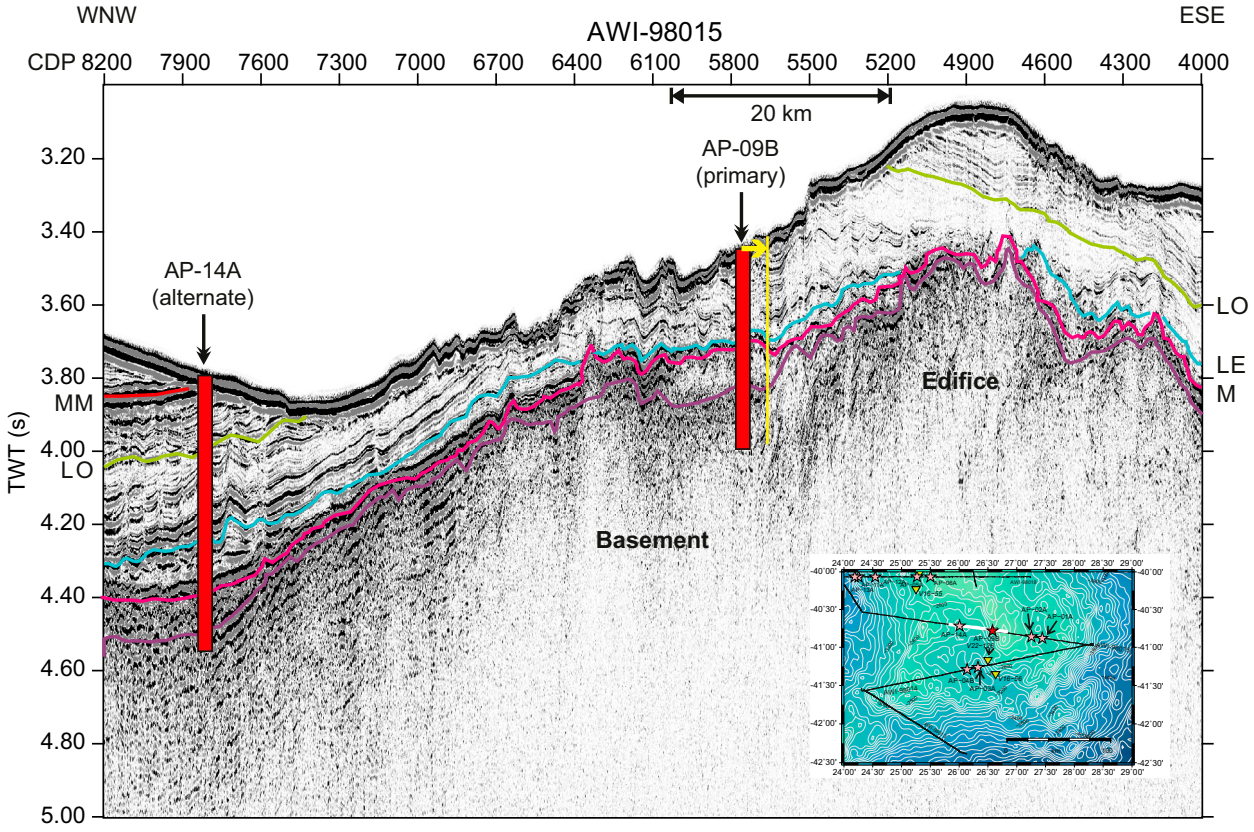

Figure F5. Seismic Profile AWI-98017 showing proposed Sites AP-05A and AP-06A and sediment piston core locations from central Agulhas Plateau. Inset map shows seismic line (white line) location. LE = lower Eocene, LO = lower Oligocene, M = Maastrichtian, MM = middle Miocene. For details of sediment core ages see Table T1. CDP = common depth point. TWT = two-way traveltime.

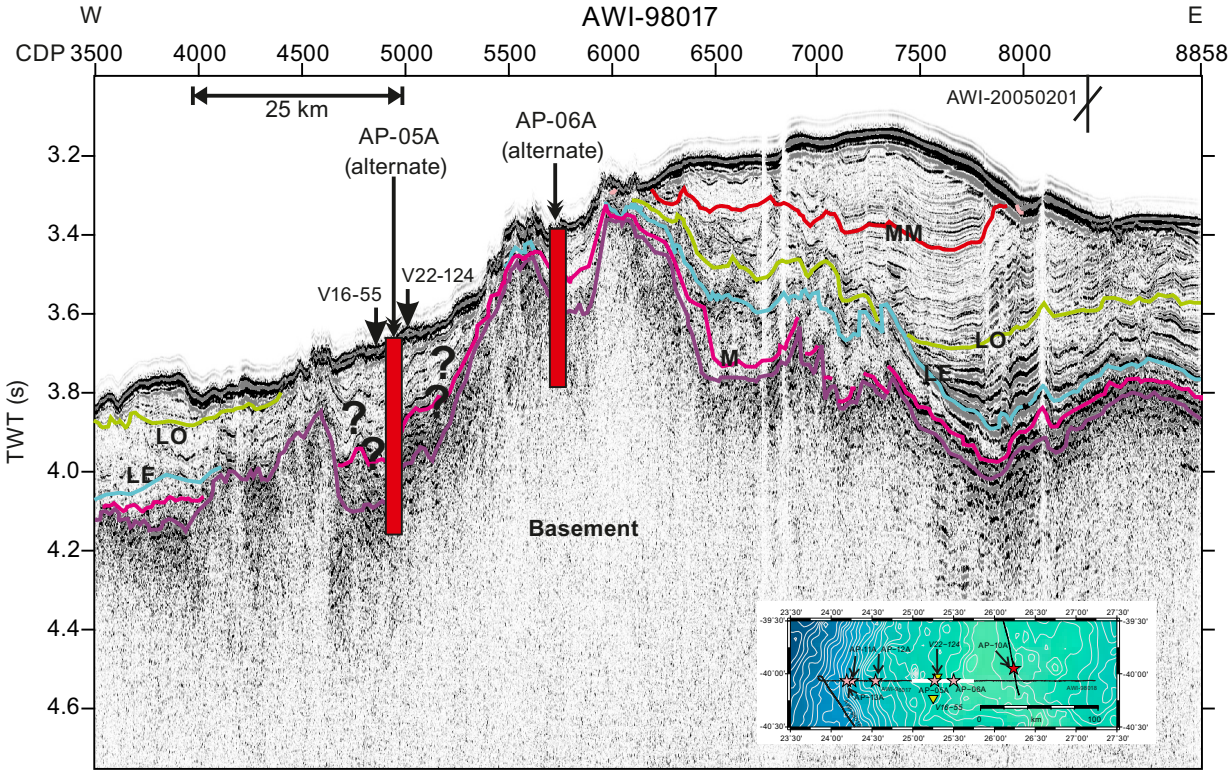

Figure F6. Seismic Profile AWI-98011 showing proposed Sites AP-07A and AP-08A and sediment piston core locations from northern Agulhas Plateau. Inset map shows seismic line (white line) location. LE = lower Eocene, LO = lower Oligocene, M = Maastrichtian, MM = middle Miocene. For details of sediment core ages (lE-lO = latest Eocene–latest Oligocene) see Table T1. CMP = common midpoint. TWT = two-way traveltime.

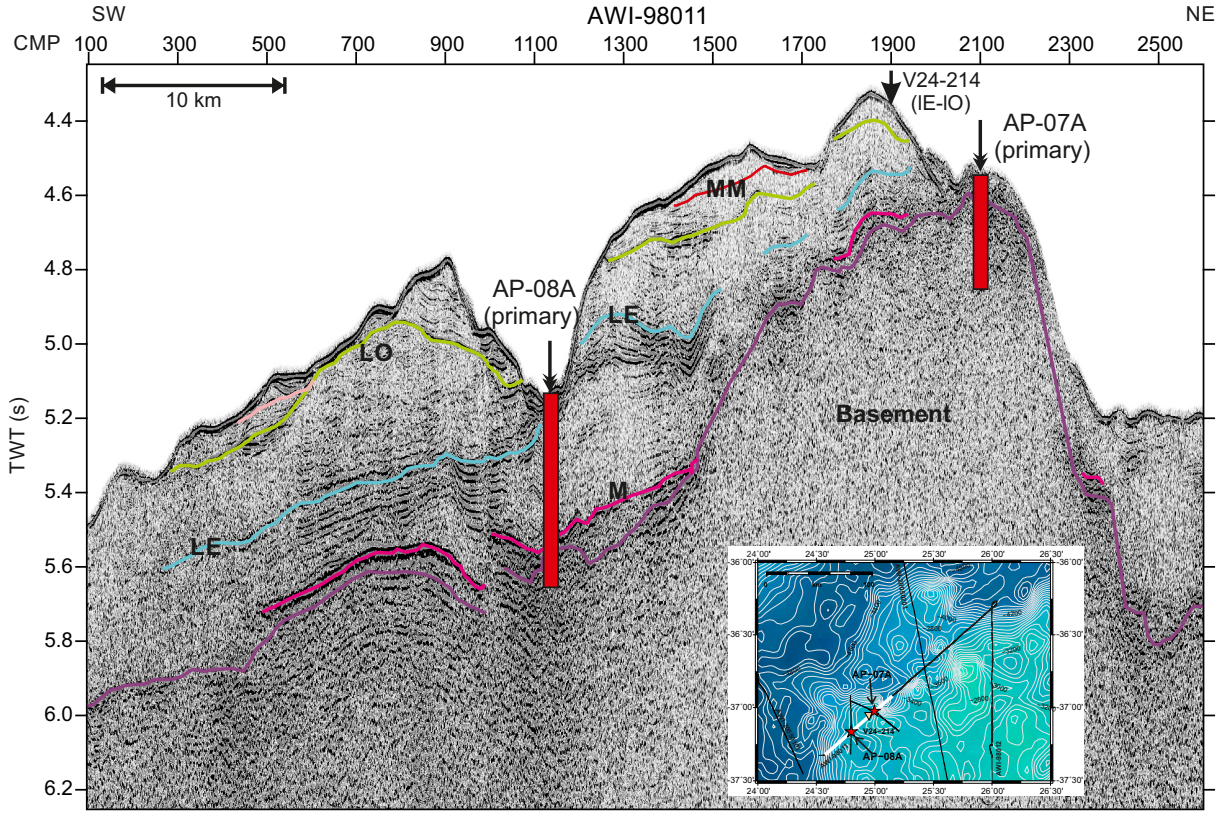

Figure F7. Seismic Profile AWI-20050201 with proposed Site AP-10A from central Agulhas Plateau. Inset map shows seismic line (white line) location. LE = lower Eocene, LO = lower Oligocene, M = Maastrichtian, MM = middle Miocene. CDP = common depth point. TWT = two-way traveltime.

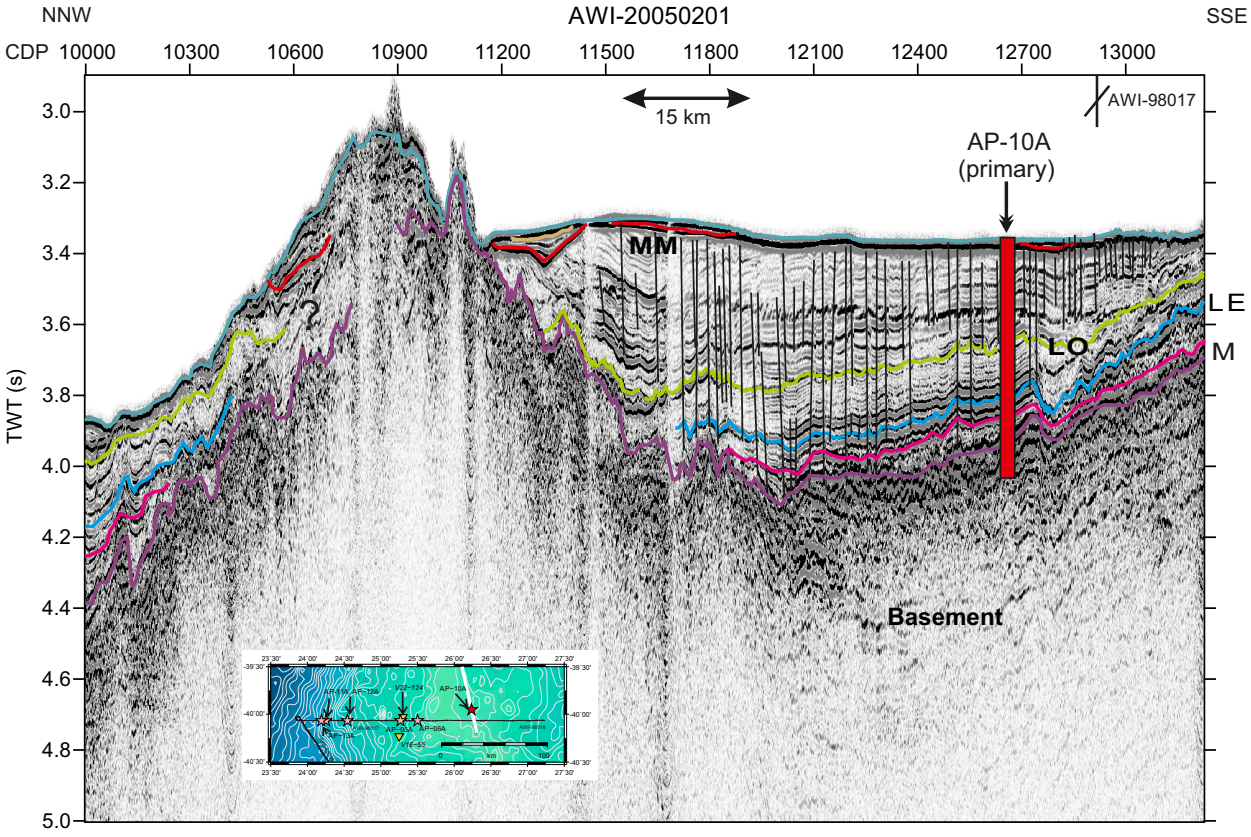

Figure F8. Seismic Profile AWI-20050008 showing proposed Site TB-01A from Transkei Basin. Inset map shows seismic line (white line) location. B = black shales, E = Paleocene/Eocene boundary, K-T = Cretaceous/Paleogene boundary, M = Oligocene/Miocene boundary, O = Eocene/Oligocene boundary, P = Miocene/Pliocene boundary. CDP = common depth point. TWT = two-way traveltime.

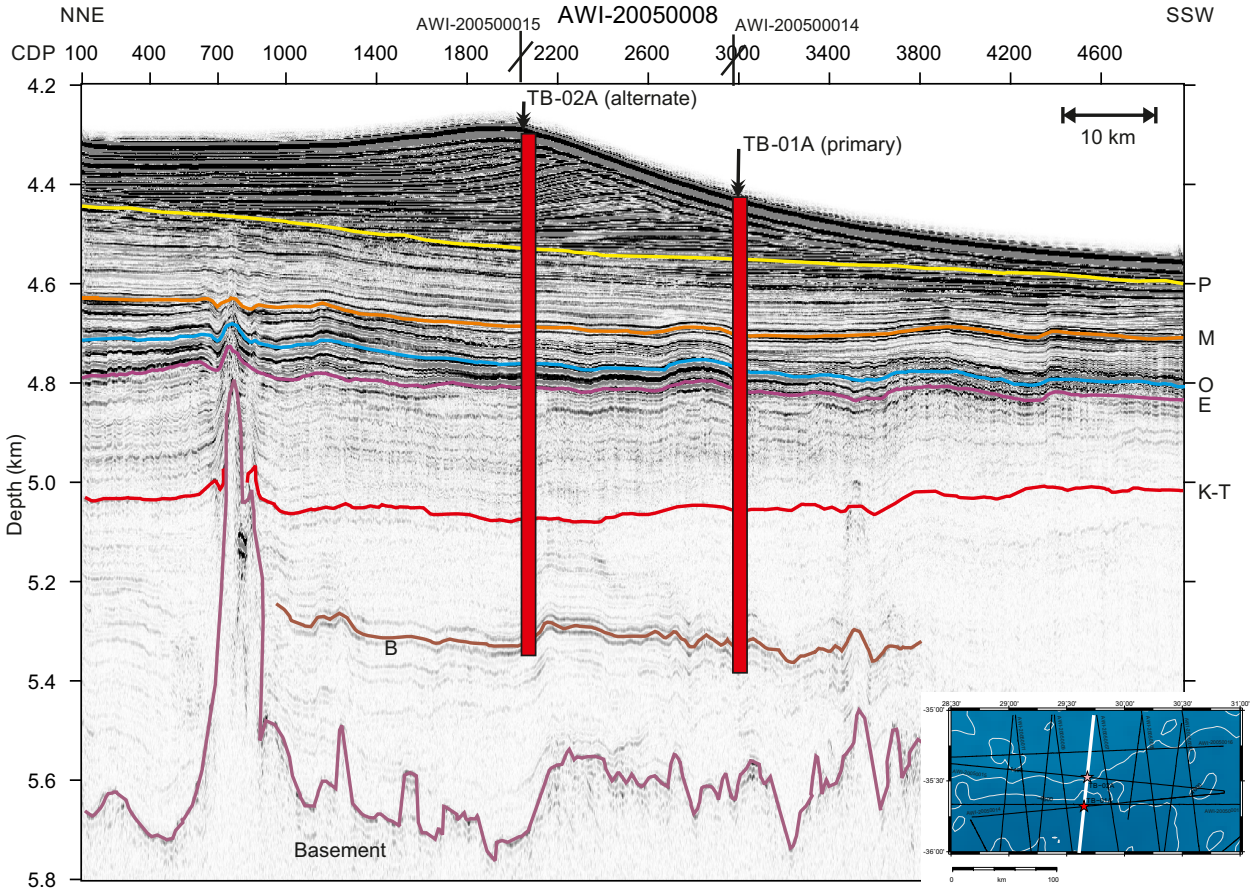

Figure F9. 3-D bathymetric map of Agulhas Plateau region showing primary and alternate site locations.

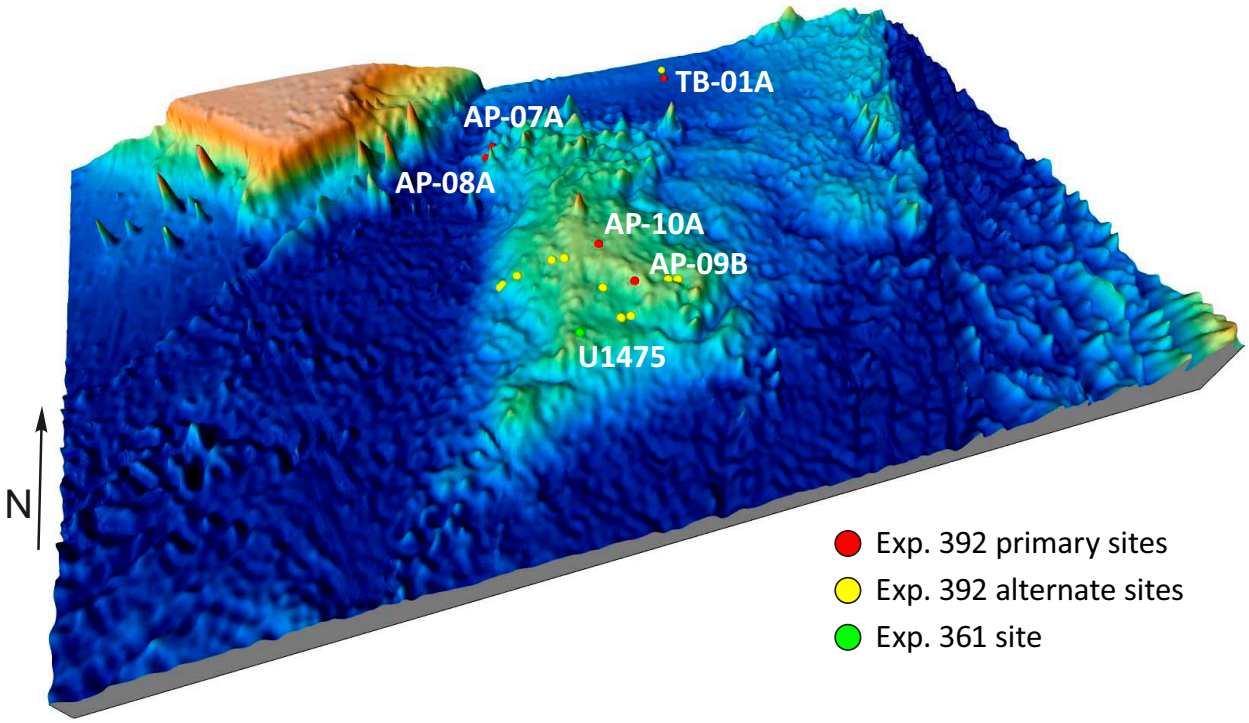

Figure F10. Proposed operations plan for the five primary sites. For each site, predicted age of sequences is shown with proposed coring and logging plan for each hole. Total depth of penetration is listed below each hole. Note that at Site AP-09B, the operations plan includes rotary core barrel (RCB) coring to 490 mbsf (~150 m into basement); however, we have permission to core to 550 mbsf and may do so if additional basement penetration is needed to meet the expedition objectives. AP = Agulhas Plateau. APC = advanced piston corer, XCB = extended core barrel.

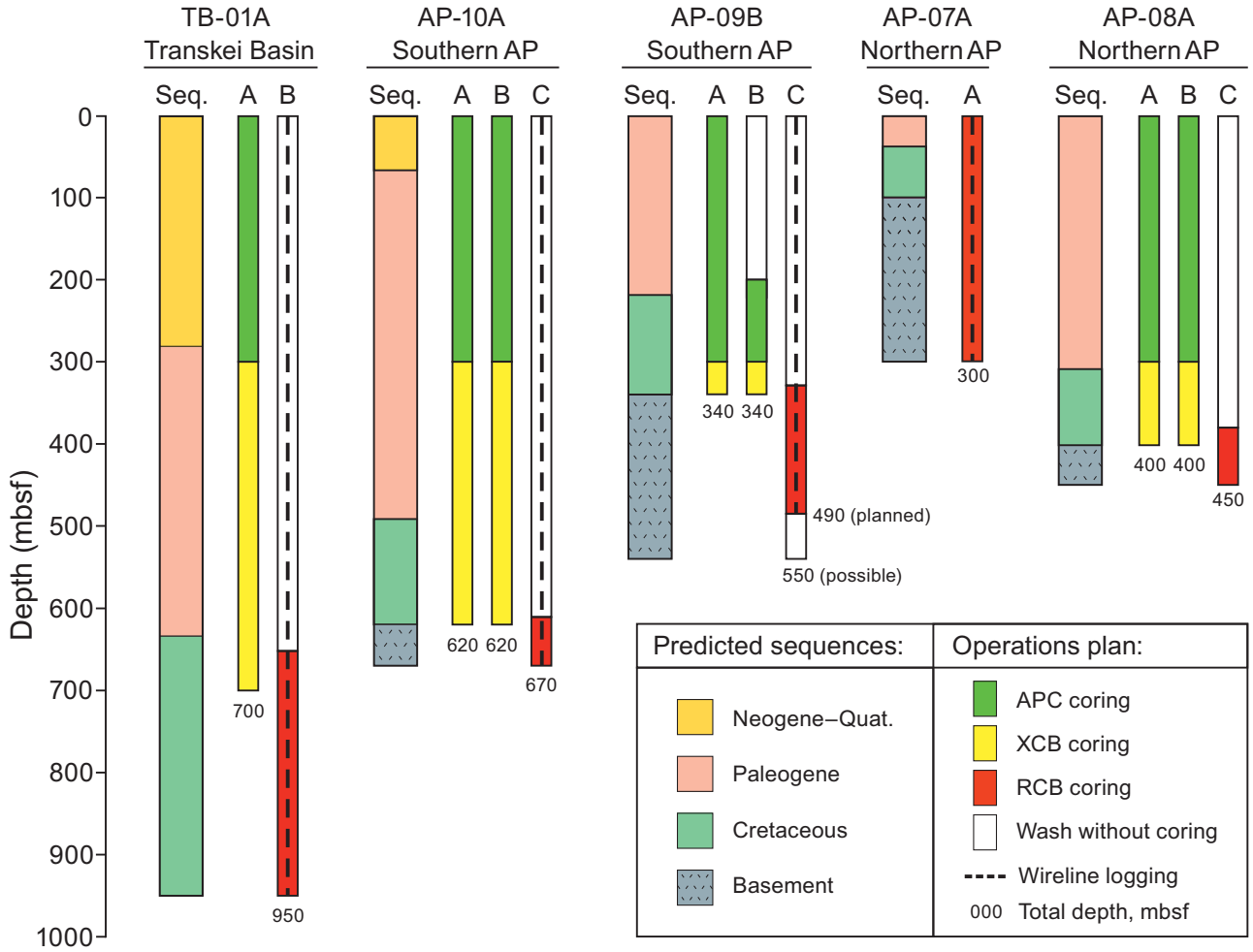

Figure F11. Late Campanian planktonic foraminifers, Vema Core V16-56. Scale bars = 100 µm. 1. *Planoheterohelix globulosa* Ehrenberg (Sample V16-56, 190–191 cm). 2. *Globigerinelloides multispina* Ehrenberg (Sample V16-56, 30–31 cm). 3. *Archaeoglobigerina mateola* Huber (Sample V16-56, 190–191 cm). 4: *Archaeoglobigerina australis* Huber (Sample V16-56, 30–31 cm).

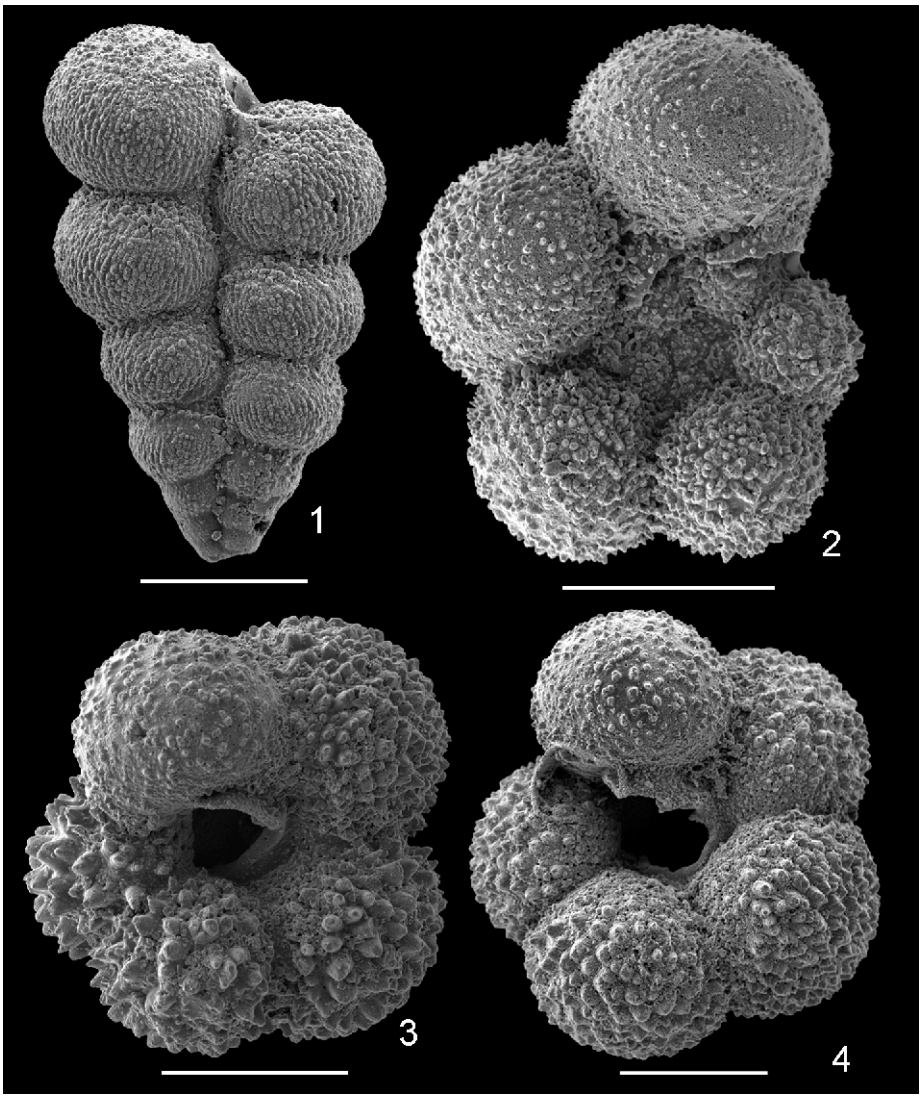

Site summaries

Figure AF1. Top: map of proposed primary Site TB-01A with multibeam swath bathymetry, multichannel seismic (MCS) tracks and common depth point (CDP) numbers. Multibeam swaths have 50 m resolution. Bottom: MCS Lines AWI-20050008 and AWI-20050014 across Site TB-01A. B = black shale, K-T = Cretaceous/Paleogene boundary, E = Eocene, O = Oligocene, M = Miocene, P= Pliocene, purple = top basement.

Site TB-01A

Priority:	Primary
Position:	35.6805992°S, 29.6501999°E
Water depth (m):	4500
Target drilling depth (mbsf):	950
Approved maximum penetration (mbsf):	1100
Survey coverage (track map; seismic profile):	Bathymetric and seismic track map MCS data: • Primary line: CDP 2988 on AWI-20050008 • Crossing line: CDP 3631 on AWI-20050014
Objective(s):	• Cretaceous to Neogene record • Date the age ranges of the observed unconformities and interpret their causes • Recover high-latitude paleotemperature records of the transition from the Cretaceous supergreenhouse and through the Paleogene • Recover critical intervals of ocean–climate transitions (OAE 3) • Sample black shales
Coring program:	Hole A: APC to 300 mbsf, XCB to 700 mbsf Hole B: drill to 690 mbsf, RCB to 950 mbsf
Downhole measurements program:	Hole B: • Triple combo • FMS-sonic • VSI
Nature of rock anticipated:	Foraminifer ooze, black shales

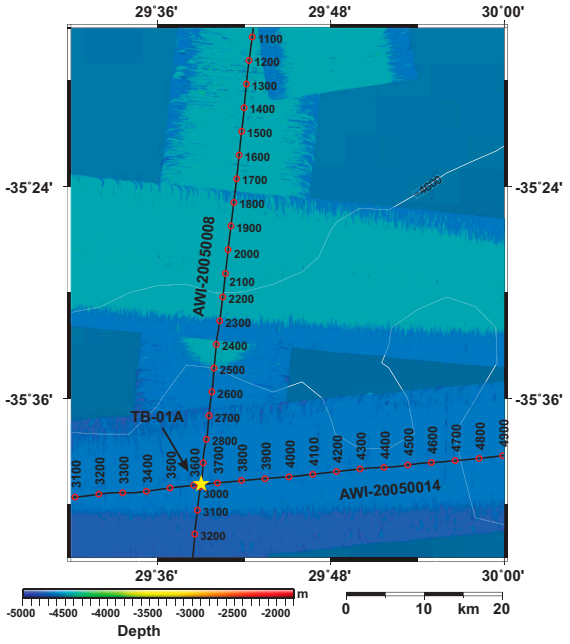

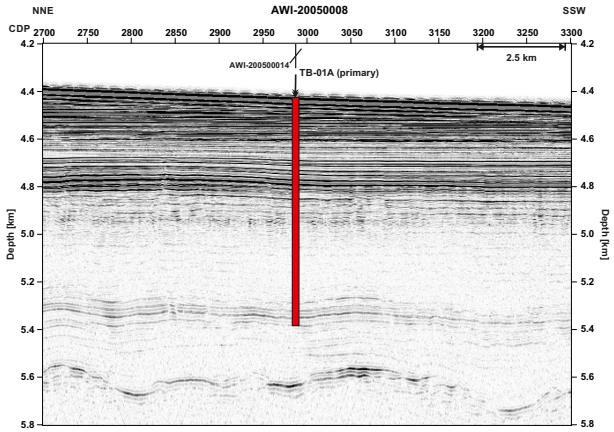

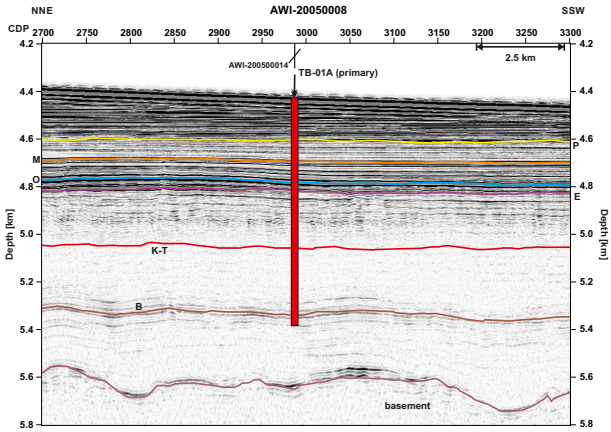

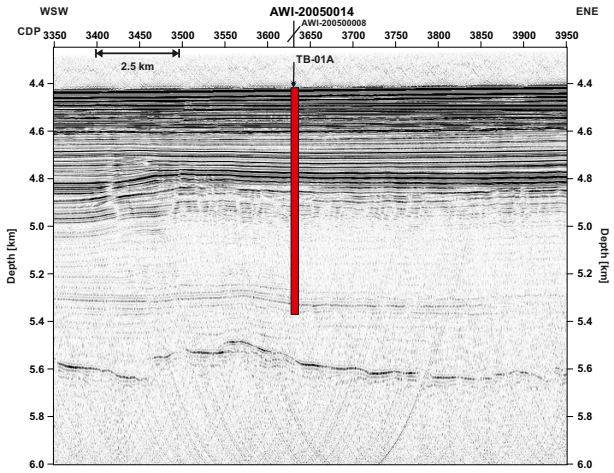

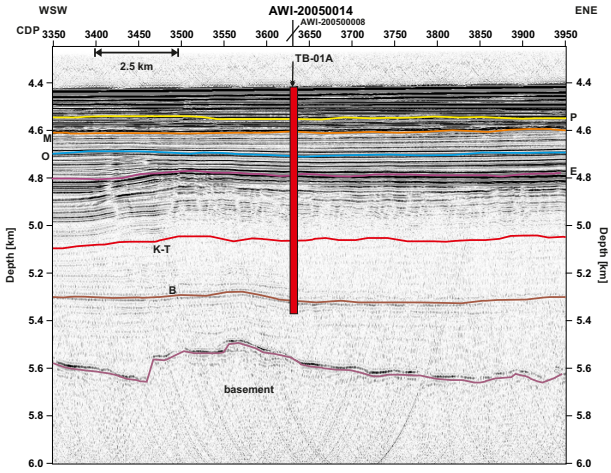

Figure AF2. Top: map of proposed primary Site AP-10A with multibeam swath bathymetry, multichannel seismic (MCS) tracks and common depth point (CDP) numbers. Multibeam swaths have 50 m resolution. Bottom: MCS Line AWI-20050201 across Site AP-10A. M = Maastrichtian, LE = lower Eocene, LO = lower Oligocene, MM = middle Miocene, purple = top basement. TWT = two-way traveltime.

Site AP-10A

Priority:	Primary
Position:	39.9510994°S, 26.2362003°E
Water depth (m):	2500
Target drilling depth (mbsf):	670
Approved maximum penetration (mbsf):	670
Survey coverage (track map; seismic profile):	Bathymetric and seismic track map MCS data: • Primary line: CDP 12650 on AWI-20050201
Objective(s):	• Cretaceous to Paleogene record • Date the age ranges of the observed unconformities and interpret their causes (M, LE, LO) • Date oldest sediment overlying crust and determine paleodepth and paleoenvironment • Recover high-latitude paleotemperature records of the transition from the Cretaceous supergreenhouse and through the Paleogene • Recover critical intervals of ocean–climate transitions (Oi1, PETM, K/Pg boundary, OAE 2, OAE 3) • Unravel the nature of Agulhas Plateau basement
Coring program:	Hole A: APC to 300 mbsf, XCB to 620 mbsf Hole B: APC to 300 mbsf, XCB to 620 mbsf Hole C: drill to 610 mbsf, RCB to 670 mbsf
Downhole measurements program:	Hole C: • Quad combo
Nature of rock anticipated:	Foraminifer ooze, basalt

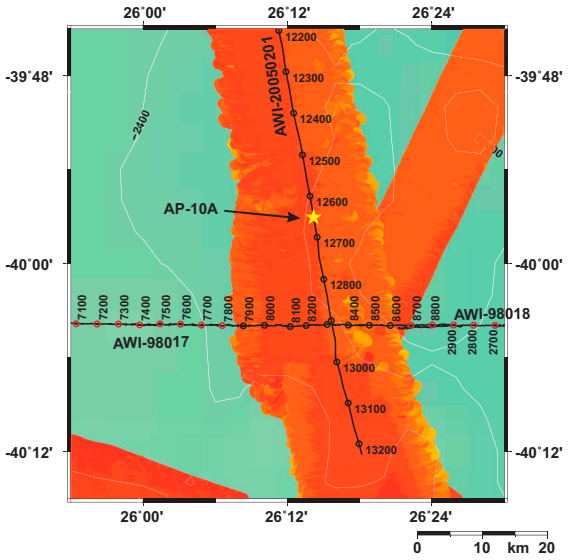

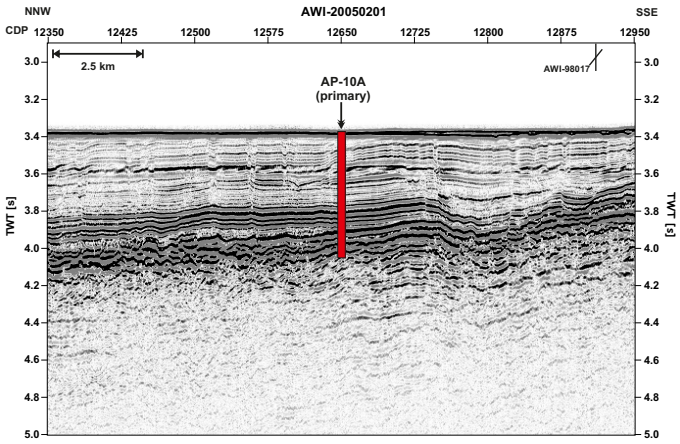

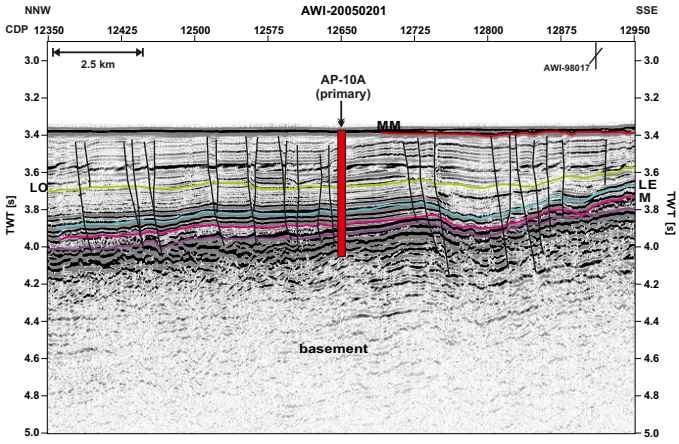

Figure AF3. Top: map of proposed primary Site AP-09B with multibeam swath bathymetry, multichannel seismic (MCS) tracks and common depth point (CDP) numbers. Horizontal yellow line = 3 km interval of seismic line approved for coring between CDP 5750 (star) and CDP 5665 (vertical yellow line). Multibeam swaths have 50 m resolution. Bottom: MCS Line AWI-98015 across Site AP-09B. Red bar = position of CDP 5750 (yellow star on map), yellow bar = position of CDP 5665 (vertical yellow line on map). Coring is approved at any position along the seismic line between these two points in a 50 m wide swath on either side of the seismic line. M = Maastrichtian, LE = lower Eocene, purple = top basement. TWT = two-way traveltime.

Site AP-09B

Priority:	Primary
Position:	40.7859001°S, 26.60689939°E
Water depth (m):	2620
Target drilling depth (mbsf):	490
Approved maximum penetration (mbsf):	550 (at any point along Seismic Line AWI-98015 between CDP 5750 and CDP 5665 [40.7873993°S, 26.6243992°E])
Survey coverage (track map; seismic profile):	Bathymetric and seismic track map MCS data: • Primary line: CDP 5750 on AWI-98015
Objective(s):	• Cretaceous to Neogene record • Date the age ranges of the observed unconformities and interpret their causes (M, LE) • Date oldest sediment overlying crust and determine paleodepth and paleoenvironment • Recover high-latitude paleotemperature records of the transition from the Cretaceous supergreenhouse and through the Paleogene • Recover critical intervals of ocean–climate transitions (PETM, K/Pg boundary, OAE 2, OAE 3) • Unravel the nature of Agulhas Plateau basement
Coring program:	Hole A: APC to 300 mbsf, XCB to 340 mbsf Hole B: drill to 200 mbsf, APC to 300 mbsf, XCB to 340 mbsf Hole C: drill to 330 mbsf, RCB to 490 mbsf
Downhole measurements program:	Hole C: • Triple combo • FMS-sonic • UBI
Nature of rock anticipated:	Foraminifer ooze, basalt

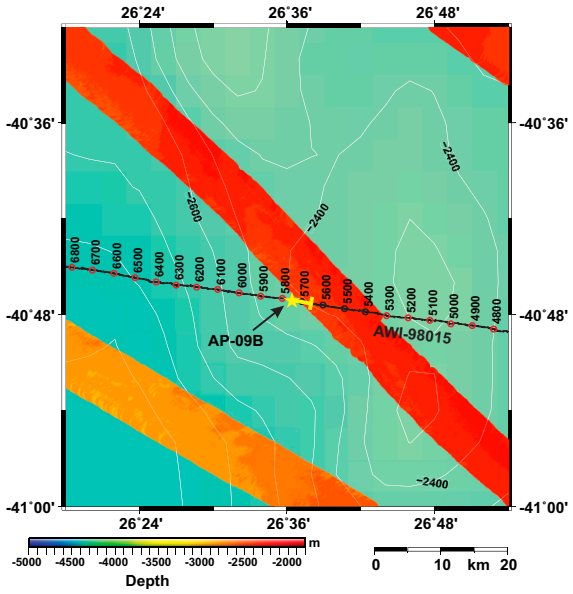

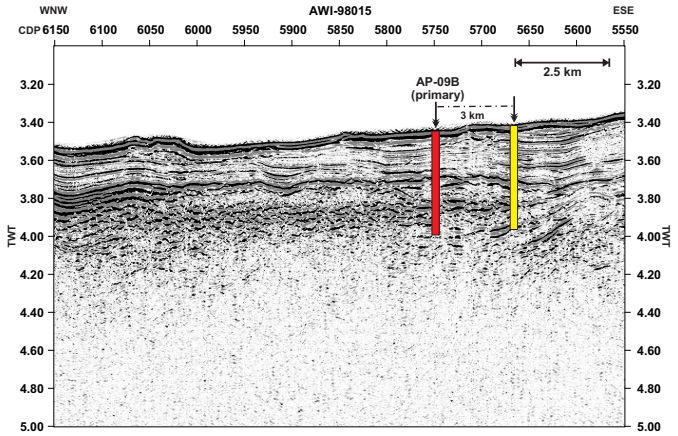

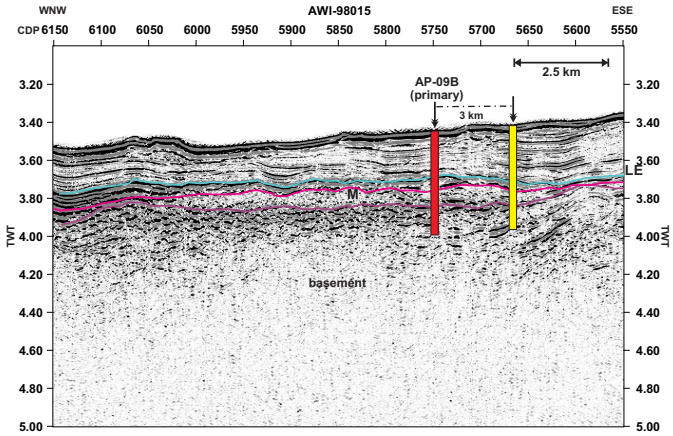

Figure AF4. Top: map of proposed primary Site AP-07A with multibeam swath bathymetry, multichannel seismic (MCS) tracks and common depth point (CDP) numbers. Multibeam swaths have 50 m resolution. Bottom: MCS Lines AWI-98011 and AWI-20140232 across Site AP-07A. M = Maastrichtian, LE = lower Eocene, LO = lower Oligocene, purple = top basement. TWT = two-way traveltime.

Site AP-07A

Priority:	Primary
Position:	37.0250015°S, 24.9953003°E
Water depth (m):	3400
Target drilling depth (mbsf):	300
Approved maximum penetration (mbsf):	300
Survey coverage (track map; seismic profile):	Bathymetric and seismic track map MCS data: • Primary line: CDP 2100 on AWI-98011 • Crossing line: CDP 908 on AWI-20140232
Objective(s):	• Cretaceous record • Date the age ranges of the observed unconformities and interpret their causes (M) • Date oldest sediment overlying crust and determine paleodepth and paleoenvironment • Recover high-latitude paleotemperature records of the transition from the Cretaceous supergreenhouse and through the Paleogene • Recover critical intervals of ocean–climate transitions (K/Pg boundary, OAE 2, OAE 3) • Unravel the nature of Agulhas Plateau basement
Coring program:	Hole A: RCB to 300 mbsf
Downhole measurements program:	Hole A: • Triple combo • FMS-sonic • UBI
Nature of rock anticipated:	Foraminifer ooze, basalt

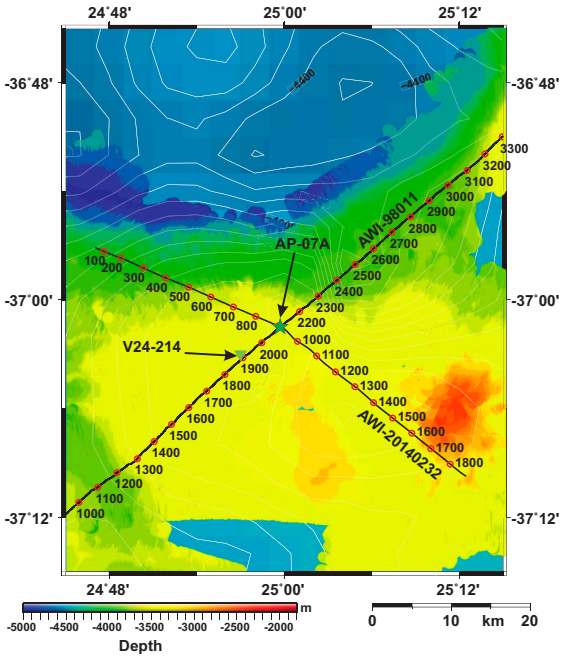

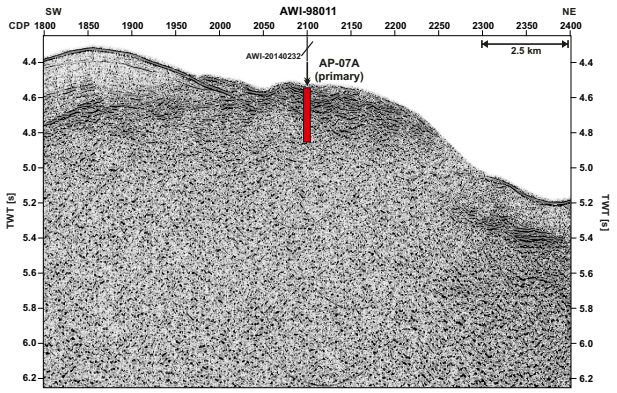

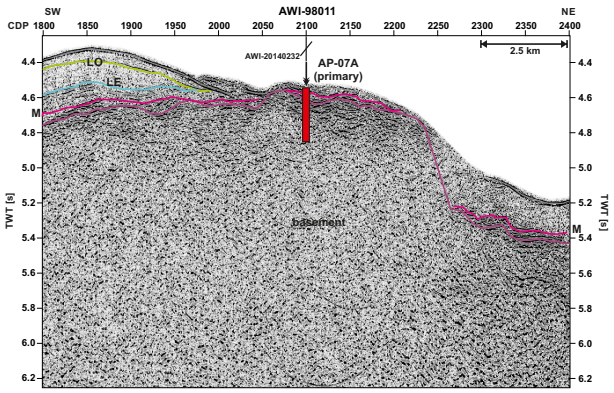

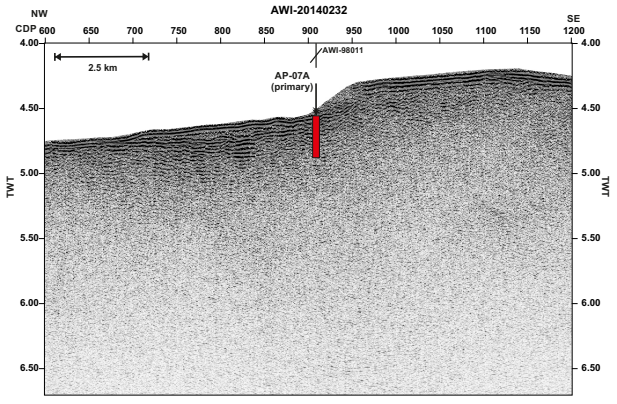

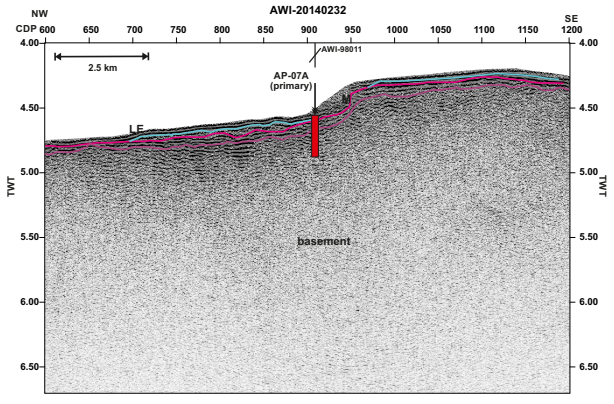

Figure AF5. Top: map of proposed primary Site AP-08A with multibeam swath bathymetry, multichannel seismic (MCS) tracks and common depth point (CDP) numbers. Multibeam swaths have 50 m resolution. Bottom: MCS Lines AWI-98011 and AWI-20140231 across Site AP-08A. M = Maastrichtian, LE = lower Eocene, LO = lower Oligocene, purple = top basement. TWT = two-way traveltime.

Site AP-08A

Priority:	Primary
Position:	37.16550105°S, 24.7980995°E
Water depth (m):	3900
Target drilling depth (mbsf):	450
Approved maximum penetration (mbsf):	500
Survey coverage (track map; seismic profile):	Bathymetric and seismic track map MCS data: • Primary line: CDP 1150 on AWI-98011 • Crossing line: CDP 806 on AWI-20140231
Objective(s):	• Cretaceous record • Date the age ranges of the observed unconformities and interpret their causes (M and LE) • Date oldest sediment overlying crust and determine paleodepth and paleoenvironment • Recover high-latitude paleotemperature records of the transition from the Cretaceous supergreenhouse and through the Paleogene • Recover critical intervals of ocean–climate transitions (K/Pg boundary, OAE 2, OAE 3) • Unravel the nature of Agulhas Plateau basement
Coring program:	Hole A: APC to 300 mbsf, XCB too 400 mbsf Hole B: APC to 300 mbsf, XCB too 400 mbsf Hole C: drill to 390 mbsf, RCB to 450 mbsf
Downhole measurements program:	None
Nature of rock anticipated:	Foraminifer ooze, basalt

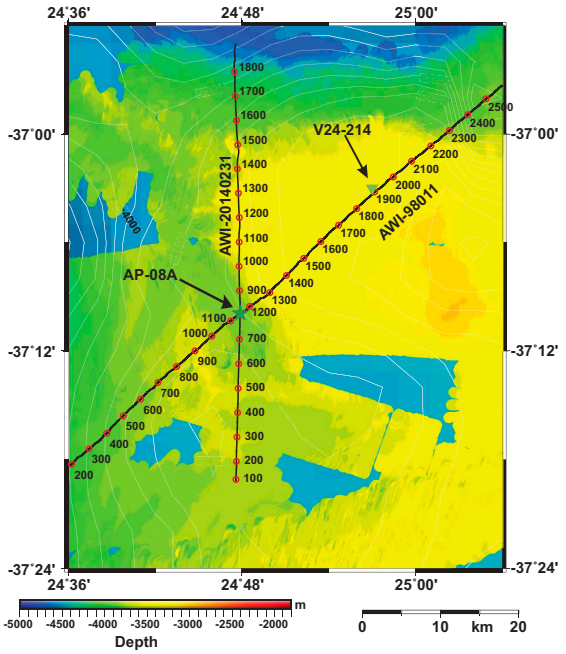

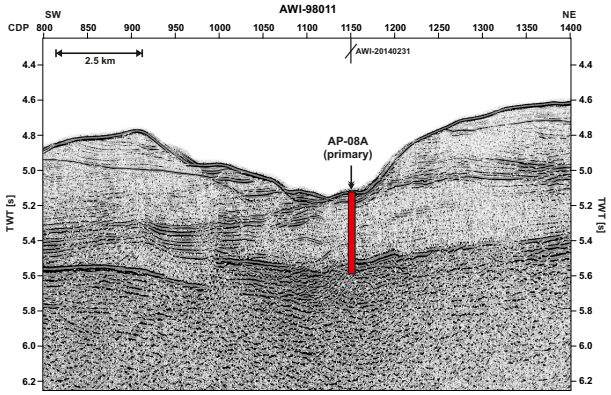

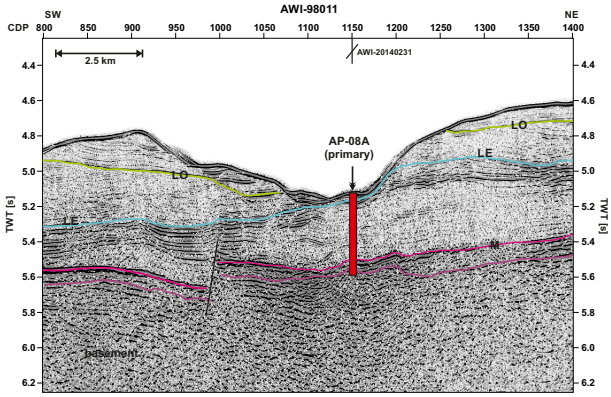

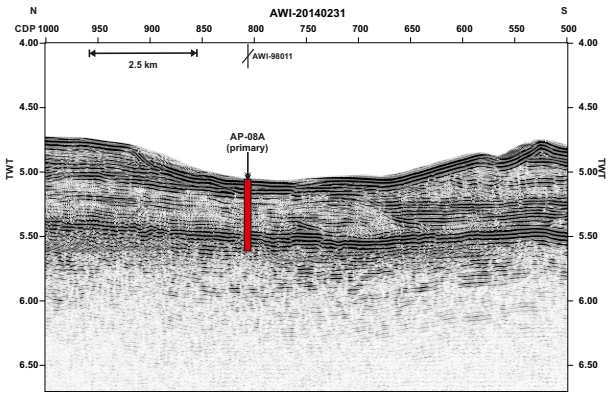

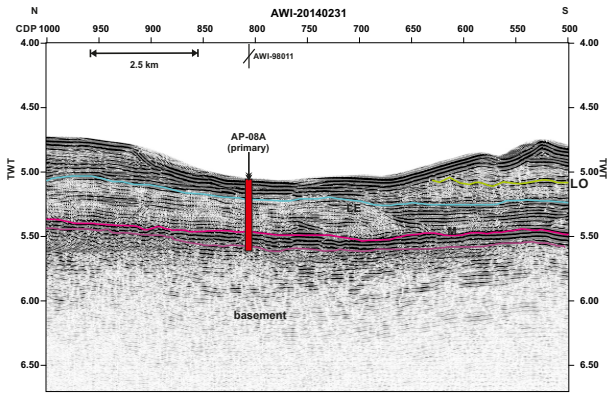

Figure AF6. Top: map of proposed alternate Site TB-02A with multibeam swath bathymetry, multichannel seismic (MCS) tracks and common depth point (CDP) numbers. Multibeam swaths have 50 m resolution. Bottom: MCS Lines AWI-20050008 and AWI-20050015 across Site TB-02A. B = black shale, K-T= Cretaceous/Paleogene boundary, E = Eocene, O = Oligocene, M = Miocene, P = Pliocene, purple = top basement.

Site TB-02A

Priority:	Alternate for Site TB-01A
Position:	35.4749985°S, 29.6793995°E
Water depth (m):	4300
Target drilling depth (mbsf):	1050
Approved maximum penetration (mbsf):	1200
Survey coverage (track map; seismic profile):	Bathymetric and seismic track map MCS data: • Primary line: CDP 2068 on AWI-20050008 • Crossing line: CDP 4397 on AWI-20050015
Objective(s):	• Cretaceous to Neogene record • Date the age ranges of the observed unconformities and interpret their causes • Recover high-latitude paleotemperature records of the transition from the Cretaceous supergreenhouse and through the Paleogene • Recover critical intervals of ocean–climate transitions (OAE 3) • Sample black shales
Coring program:	Hole A: APC to 300 mbsf, XCB to 700 mbsf Hole B: drill to 690 mbsf, RCB to 1050 mbsf
Downhole measurements program:	Hole B: • Triple combo • FMS-sonic • VSI
Nature of rock anticipated:	Foraminifer ooze, black shales

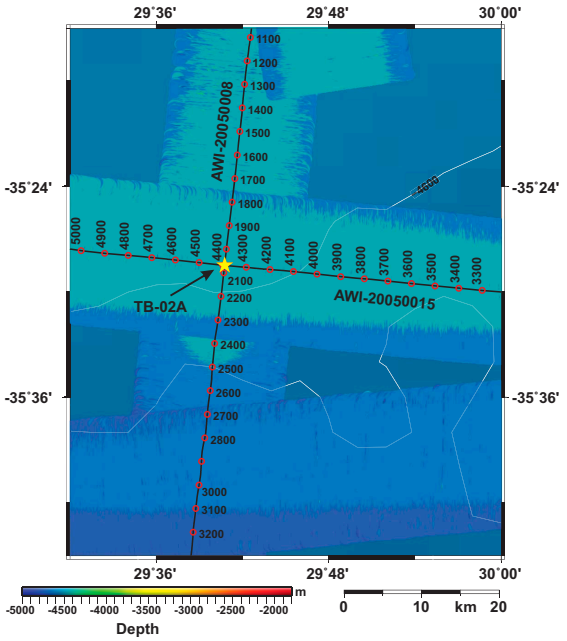

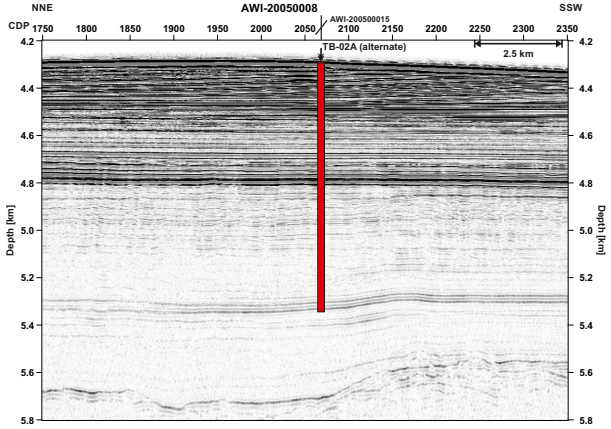

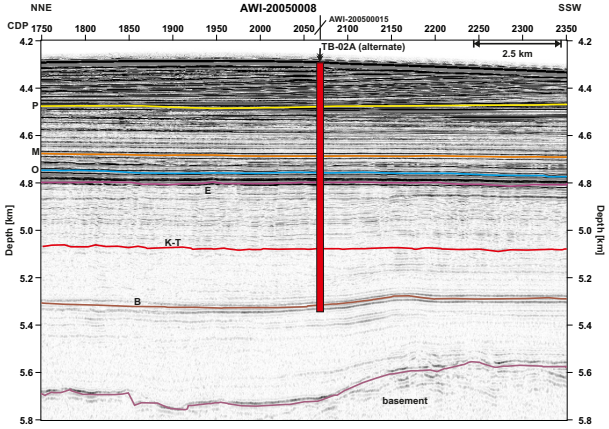

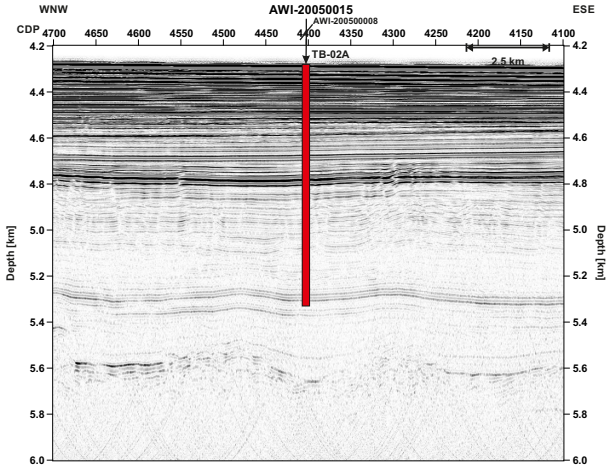

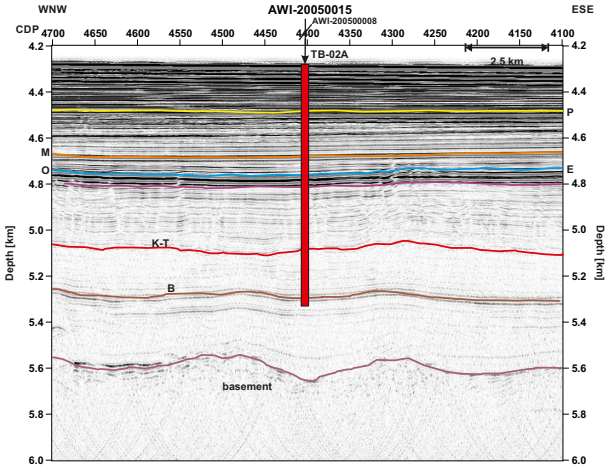

Figure AF7. Top: map of proposed alternate Site AP-04B with multibeam swath bathymetry, multichannel seismic (MCS) tracks and common depth point (CDP) numbers. Multibeam swaths have 50 m resolution. Bottom: MCS Line AWI-98014 across Site AP-04B. M = Maastrichtian, LE = Lower Eocene, LO = Lower Oligocene, MM = middle Miocene, purple = top basement. TWT = two-way traveltime.

Site AP-04B

Priority:	Alternate for Site AP-10A
Position:	41.2951012°S, 26.1151009°E
Water depth (m):	3075
Target drilling depth (mbsf):	900
Approved maximum penetration (mbsf):	900
Survey coverage (track map; seismic profile):	Bathymetric and seismic track map MCS data: • Primary line: CDP 6220 on AWI-98014
Objective(s):	• Cretaceous to Neogene record • Date the age ranges of the observed unconformities and interpret their causes (M, LE, LO, MM) • Date oldest sediment overlying crust and determine paleodepth and paleoenvironment • Recover high-latitude paleotemperature records of the transition from the Cretaceous supergreenhouse and through the Paleogene • Recover critical intervals of ocean–climate transitions (Mi5, Mi4, Mi1, Oi1, PETM[?], K/Pg boundary, OAE 2, OAE 3) • Unravel the nature of Agulhas Plateau basement
Coring program:	Hole A: APC to 300 mbsf, XCB to 850 mbsf Hole B: APC to 300 mbsf, XCB to 850 mbsf Hole C: drill to 840 mbsf, RCB to 900 mbsf
Downhole measurements program:	Hole C: • Quad combo
Nature of rock anticipated:	Foraminifer ooze, basalt

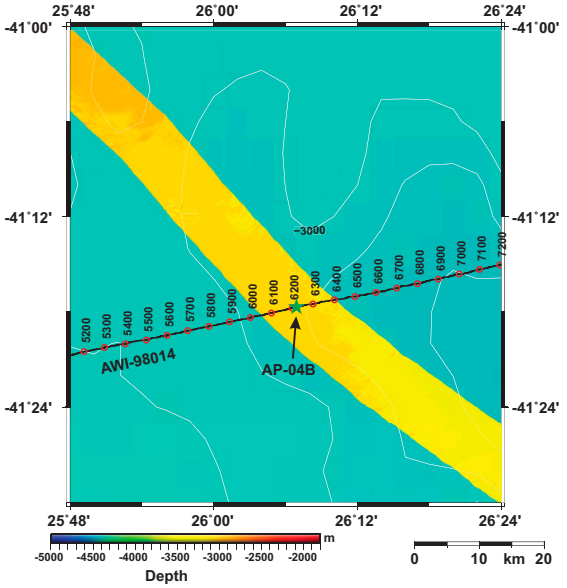

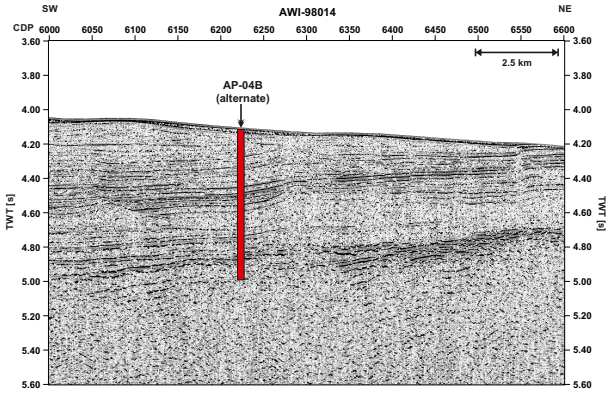

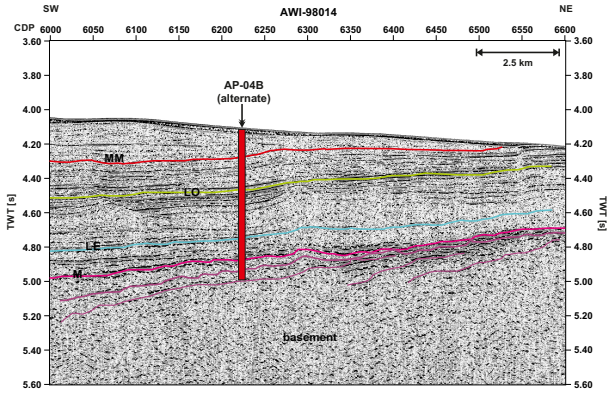

Figure AF8. Top: map of proposed alternate Site AP-05A with multibeam swath bathymetry, multichannel seismic (MCS) tracks and common depth point (CDP) numbers. Multibeam swaths have 50 m resolution. Bottom: MCS Line AWI-98017 across Site AP-05A. M = Maastrichtian, LE = lower Eocene, purple = top basement. TWT = two-way traveltime.

Site AP-05A

Priority:	Alternate for Site AP-10A
Position:	40.0082626°S, 25.2681999°E
Water depth (m):	2800
Target drilling depth (mbsf):	500
Approved maximum penetration (mbsf):	500
Survey coverage (track map; seismic profile):	Bathymetric and seismic track map MCS data: • Primary line: CDP 4900 on AWI-98017
Objective(s):	• Cretaceous to Paleogene record • Date the age ranges of the observed unconformities and interpret their causes (M, LE) • Date oldest sediment overlying crust and determine paleodepth and paleoenvironment • Recover high-latitude paleotemperature records of the transition from the Cretaceous supergreenhouse and through the Paleogene • Recover critical intervals of ocean–climate transitions (Oi1, PETM, K/Pg boundary, OAE 2, OAE 3) • Unravel the nature of Agulhas Plateau basement
Coring program:	Hole A: APC to 300, XCB to 450 mbsf Hole B: APC to 300, XCB to 450 mbsf Hole C: drill to 440 mbsf, RCB to 500 mbsf
Downhole measurements program:	Hole C: • Quad combo
Nature of rock anticipated:	Foraminifer ooze, basalt

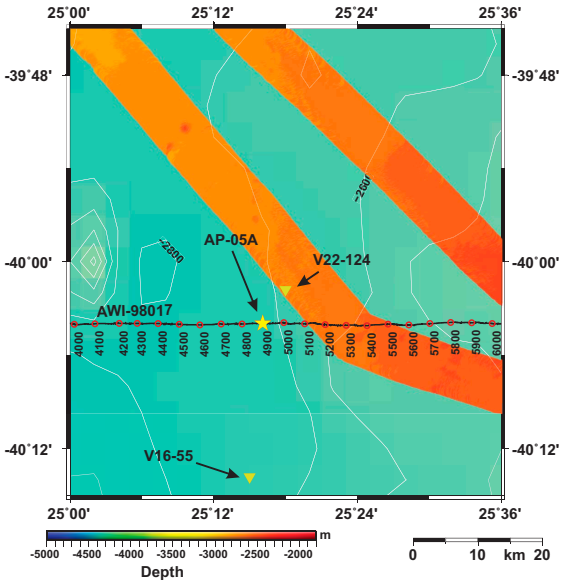

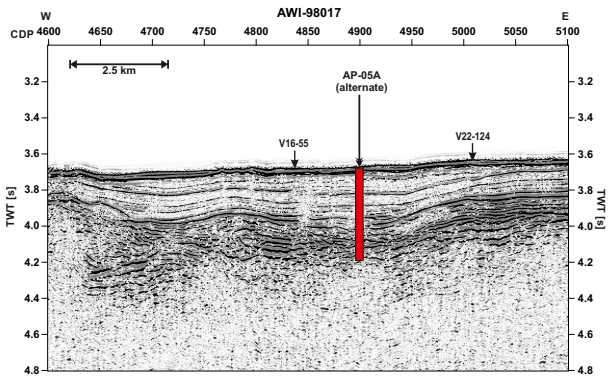

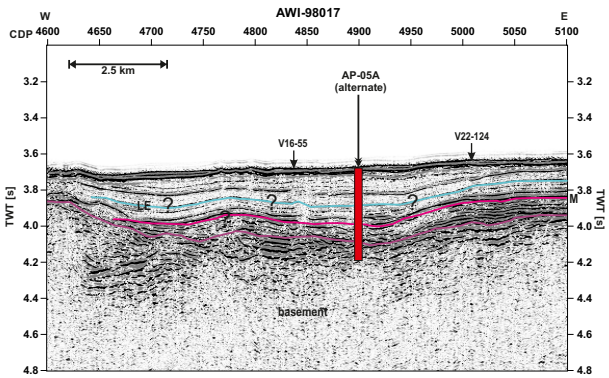

Figure AF9. Top: map of proposed alternate Site AP-11A with multibeam swath bathymetry, multichannel seismic (MCS) tracks and common depth point (CDP) numbers. Multibeam swaths have 50 m resolution. Bottom: MCS Line AWI-98017 across Site AP-11A. M = Maastrichtian, LE = lower Eocene, LO = lower Oligocene, MM = middle Miocene, purple = top basement. TWT = two-way traveltime.

Site AP-11A

Priority:	Alternate for Site AP-10A
Position:	40.0671997°S, 24.2537994°E
Water depth (m):	3490
Target drilling depth (mbsf):	770
Approved maximum penetration (mbsf):	770
Survey coverage (track map; seismic profile):	Bathymetric and seismic track map MCS data: • Primary line: CDP 1400 on AWI-98017
Objective(s):	• Cretaceous to Neogene record • Date the age ranges of the observed unconformities and interpret their causes (M, LE, LO, MM) • Date oldest sediment overlying crust and determine paleodepth and paleoenvironment • Recover high-latitude paleotemperature records of the transition from the Cretaceous supergreenhouse and through the Paleogene • Recover critical intervals of ocean–climate transitions (Mi5, Mi4, Mi1, Oi1, PETM[?], K/Pg boundary, OAE 2) • Unravel the nature of Agulhas Plateau basement
Coring program:	Hole A: APC to 300 mbsf, XCB to 720 mbsf Hole B: APC to 300 mbsf, XCB to 720 mbsf Hole C: drill to 710 mbsf, RCB to 770 mbsf
Downhole measurements program:	Hole C: • Quad combo
Nature of rock anticipated:	Foraminifer ooze, basalt

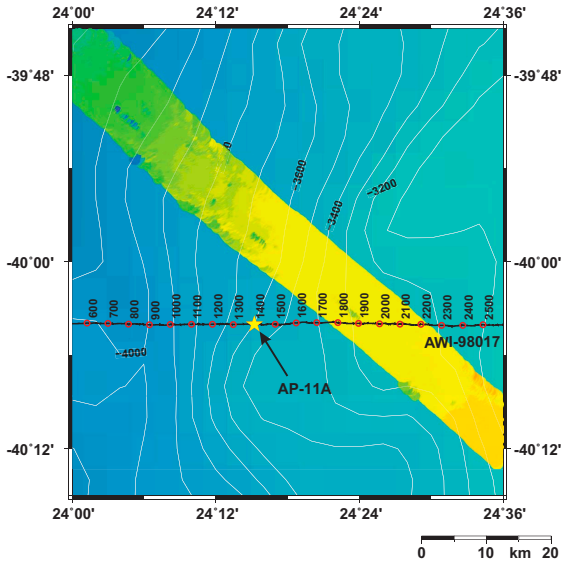

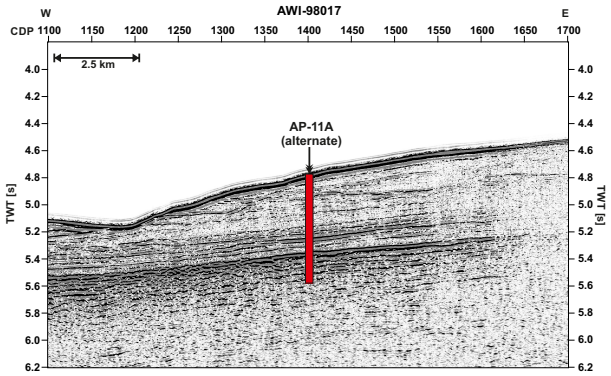

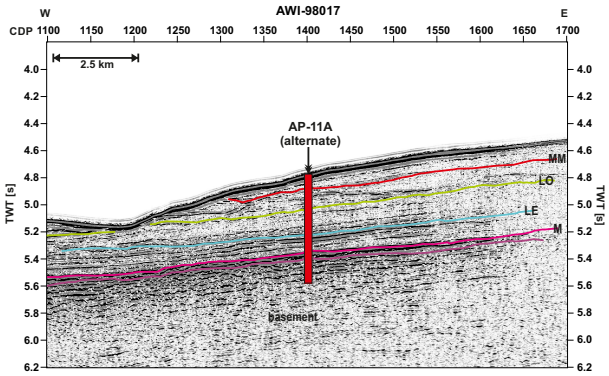

Figure AF10. Top: map of proposed alternate Site AP-01A with multibeam swath bathymetry, multichannel seismic (MCS) tracks and common depth point (CDP) numbers. Multibeam swaths have 50 m resolution. Bottom: MCS Line AWI-98015 across Site AP-01A. M = Maastrichtian, LO = lower Oligocene, MM = middle Miocene, purple = top basement. TWT = two-way traveltime.

Site AP-01A

Priority:	Alternate for Site AP-09B
Position:	40.8800011°S, 27.4428997°E
Water depth (m):	2700
Target drilling depth (mbsf):	350
Approved maximum penetration (mbsf):	350
Survey coverage (track map; seismic profile):	Bathymetric and seismic track map MCS data: • Primary line: CDP 2850 on AWI-98015
Objective(s):	• Cretaceous and Neogene record • Date the age ranges of the observed unconformities and interpret their causes (M) • Date oldest sediment overlying crust and determine paleodepth and paleoenvironment • Recover high-latitude paleotemperature records of the transition from the Cretaceous supergreenhouse and through the Paleogene • Recover critical intervals of ocean–climate transitions (K/Pg boundary, OAE 3) • Unravel the nature of Agulhas Plateau basement
Coring program:	Hole A: APC to 150 mbsf Hole B: drill to 140 mbsf, RCB to 300 mbsf
Downhole measurements program:	Hole B: • Triple combo • FMS-sonic • UBI
Nature of rock anticipated:	Foraminifer ooze, basalt

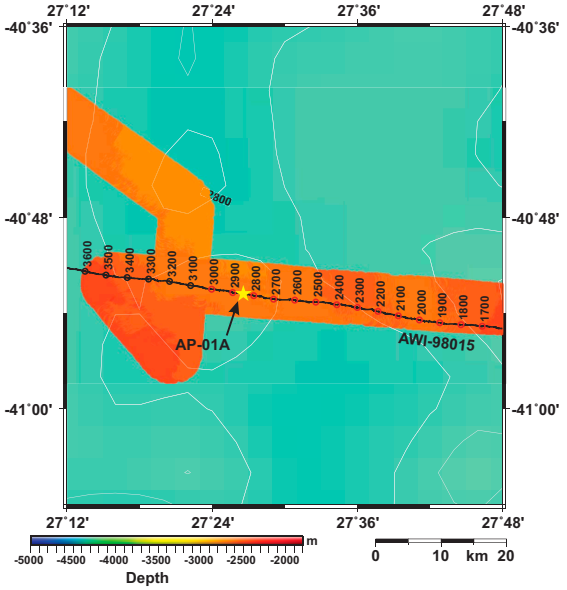

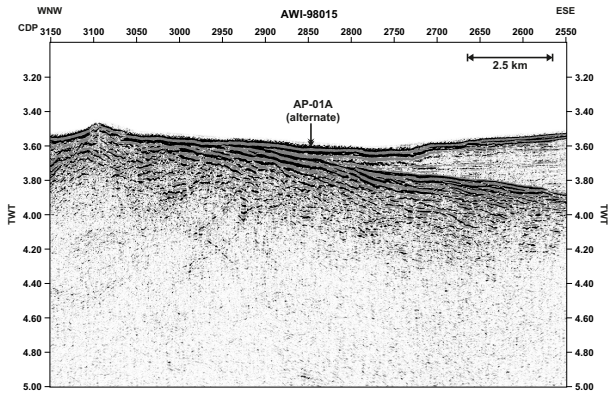

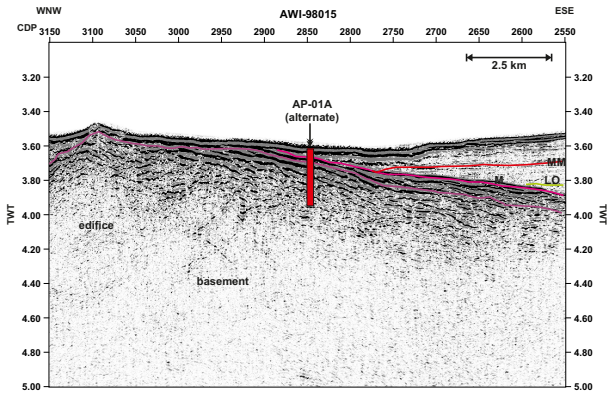

Figure AF11. Top: map of proposed alternate Site AP-03A with multibeam swath bathymetry, multichannel seismic (MCS) tracks and common depth point (CDP) numbers. Multibeam swaths have 50 m resolution. Bottom: MCS Line AWI-98014 across Site AP-03A. M = Maastrichtian, LE = lower Eocene, LO = lower Oligocene, purple = top basement. TWT = two-way traveltime.

Site AP-03A

Priority:	Alternate for Site AP-09B
Position:	41.2631989°S, 26.3272991°E
Water depth (m):	3220
Target drilling depth (mbsf):	500
Approved maximum penetration (mbsf):	500
Survey coverage (track map; seismic profile):	Bathymetric and seismic track map MCS data: • Primary line: CDP 6950 on AWI-98014
Objective(s):	• Cretaceous to Paleogene record • Date the age ranges of the observed unconformities and interpret their causes (M, LE) • Date oldest sediment overlying crust and determine paleodepth and paleoenvironment • Recover high-latitude paleotemperature records of the transition from the Cretaceous supergreenhouse and through the Paleogene • Recover critical intervals of ocean–climate transitions (PETM, K/Pg boundary, OAE 3) • Unravel the nature of Agulhas Plateau basement
Coring program:	Hole A: APC to 300 mbsf Hole B: drill to 290 mbsf, RCB to 450 mbsf
Downhole measurements program:	Hole B: • Triple combo • FMS-sonic • UBI
Nature of rock anticipated:	Foraminifer ooze, basalt

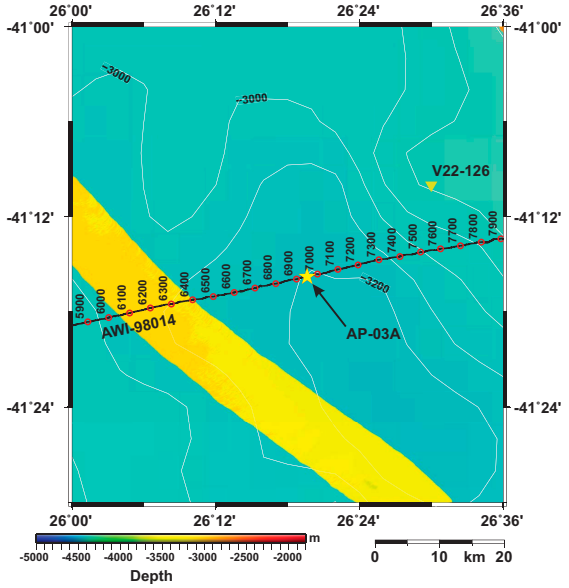

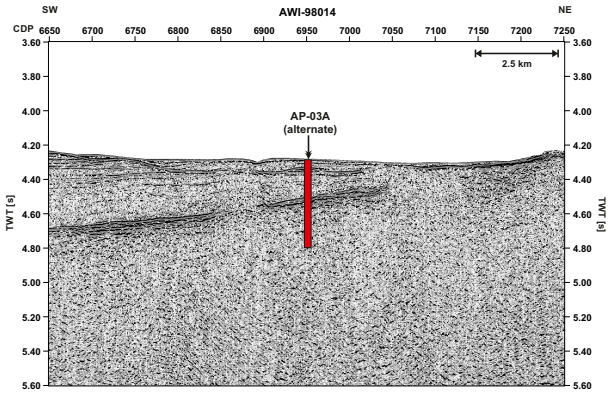

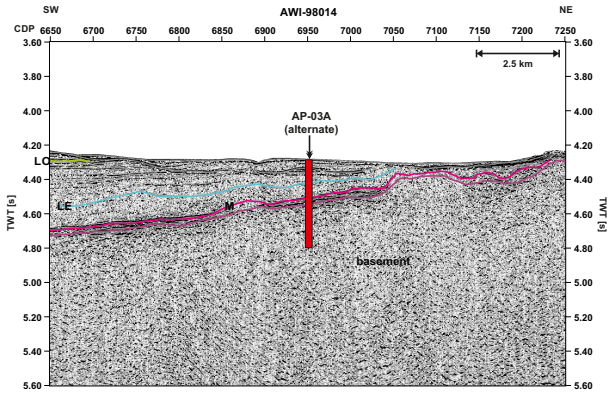

Figure AF12. Top: map of proposed alternate Site AP-13A with multibeam swath bathymetry, multichannel seismic (MCS) tracks and common depth point (CDP) numbers. Multibeam swaths have 50 m resolution. Bottom: MCS Line AWI-98017 across Site AP-13A. M = Maastrichtian, LE = lower Eocene, LO = lower Oligocene, MM = middle Miocene, purple = top basement. TWT = two-way traveltime.

Site AP-13A

Priority:	Alternate for Site AP-09B
Position:	40.0671997°S, 24.1895008°E
Water depth (m):	3850
Target drilling depth (mbsf):	620
Approved maximum penetration (mbsf):	620
Survey coverage (track map; seismic profile):	Bathymetric and seismic track map MCS data: • Primary line: CDP 1180 on AWI-98017
Objective(s):	• Cretaceous to Paleogene record • Date the age ranges of the observed unconformities and interpret their causes (M, LE) • Date oldest sediment overlying crust and determine paleodepth and paleoenvironment • Recover high-latitude paleotemperature records of the transition from the Cretaceous supergreenhouse and through the Paleogene • Recover critical intervals of ocean–climate transitions (PETM, K/Pg boundary, OAE 3) • Unravel the nature of Agulhas Plateau basement
Coring program:	Hole A: APC to 300 mbsf, XCB to 420 mbsf Hole B: drill to 410 mbsf, RCB to 570 mbsf
Downhole measurements program:	Hole B: • Triple combo • FMS-sonic • UBI
Nature of rock anticipated:	Foraminifer ooze, basalt

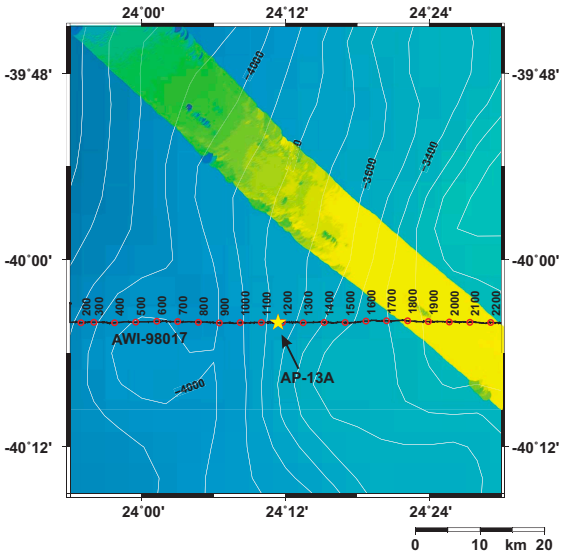

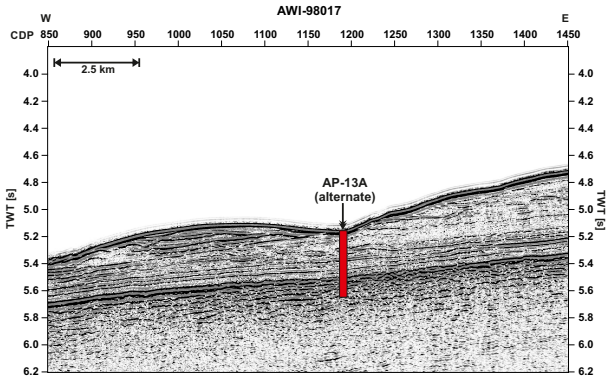

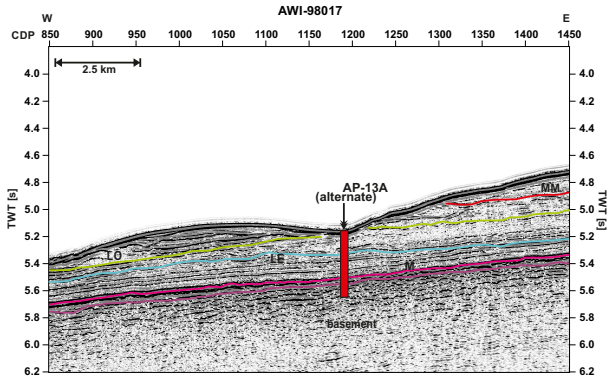

Figure AF13. Top: map of proposed alternate Site AP-06A with multibeam swath bathymetry, multichannel seismic (MCS) tracks and common depth point (CDP) numbers. Multibeam swaths have 50 m resolution. Bottom: MCS Line AWI-98017 across Site AP-06A. M = Maastrichtian, LE = lower Eocene, purple = top basement. TWT = two-way traveltime.

Site AP-06A

Priority:	Alternate for Site AP-07A
Position:	40.0663986°S, 25.5009003°E
Water depth (m):	2550
Target drilling depth (mbsf):	400
Approved maximum penetration (mbsf):	400
Survey coverage (track map; seismic profile):	Bathymetric and seismic track map MCS data: • Primary line: CDP 5700 on AWI-98017
Objective(s):	• Cretaceous to Paleogene record • Date the age ranges of the observed unconformities and interpret their causes (M) • Date oldest sediment overlying crust and determine paleodepth and paleoenvironment • Recover high-latitude paleotemperature records of the transition from the Cretaceous supergreenhouse and through the Paleogene • Recover critical intervals of ocean–climate transitions (K/Pg boundary, OAE 2) • Unravel the nature of Agulhas Plateau basement
Coring program:	Hole A: RCB to 400 mbsf
Downhole measurements program:	Hole A: • Triple combo • FMS-sonic • UBI
Nature of rock anticipated:	Foraminifer ooze, basalt

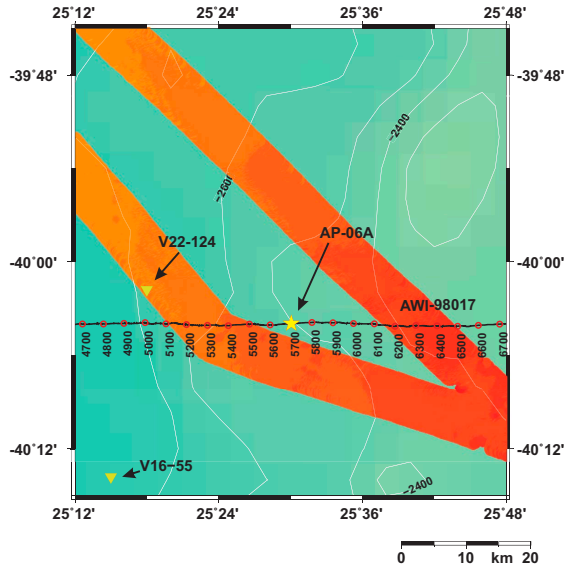

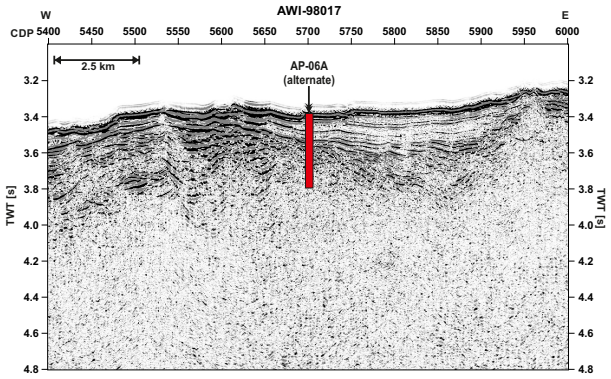

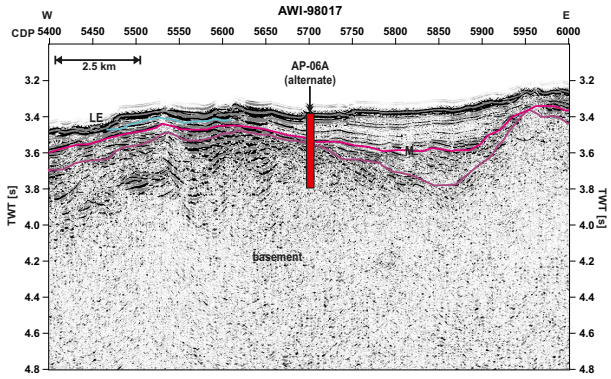

Figure AF14. Top: map of proposed alternate Site AP-14A with multibeam swath bathymetry, multichannel seismic (MCS) tracks and common depth point (CDP) numbers. Multibeam swaths have 50 m resolution. Bottom: MCS Line AWI-98015 across Site AP-14A. M = Maastrichtian, LE = lower Eocene, LO = lower Oligocene, MM = middle Miocene, purple = top basement. TWT = two-way traveltime.

Site AP-14A

Priority:	Alternate for Site AP-07A
Position:	40.7178993°S, 26.0069008°E
Water depth (m):	2800
Target drilling depth (mbsf):	700
Approved maximum penetration (mbsf):	700
Survey coverage (track map; seismic profile):	Bathymetric and seismic track map MCS data: • Primary line: CDP 7850 on AWI-98015
Objective(s):	• Cretaceous to Neogene record • Date the age ranges of the observed unconformities and interpret their causes (M, LE, LO, MM[?]) • Date oldest sediment overlying crust and determine paleodepth and paleoenvironment • Recover high-latitude paleotemperature records of the transition from the Cretaceous supergreenhouse and through the Paleogene • Recover critical intervals of ocean–climate transitions (Mi1, Oi1, PETM, K/Pg boundary, OAE 2, OAE 3) • Unravel the nature of Agulhas Plateau basement
Coring program:	Hole A: RCB to 700 mbsf
Downhole measurements program:	Hole A: • Triple combo • FMS-sonic
Nature of rock anticipated:	Foraminifer ooze, basalt

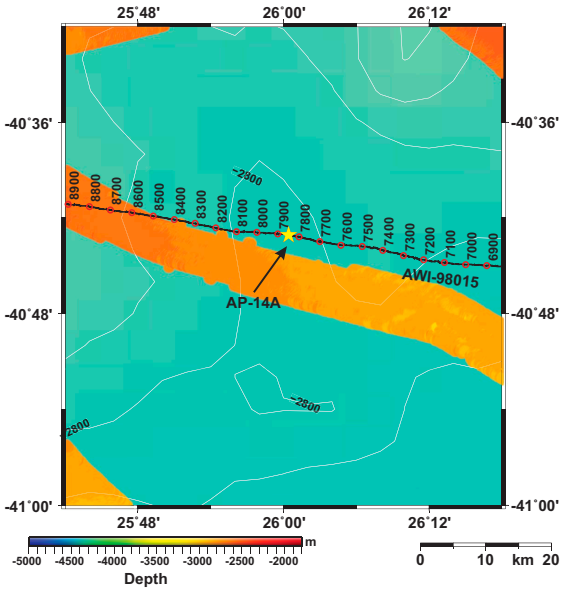

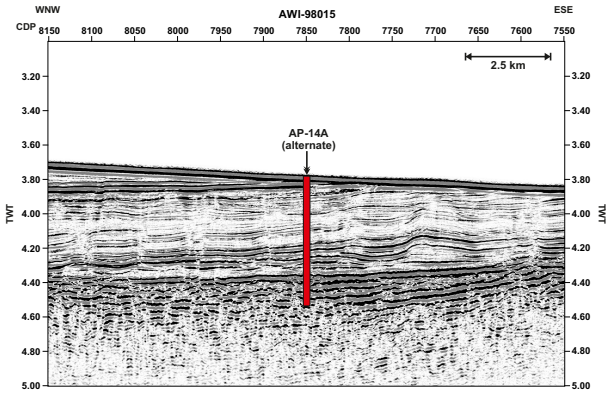

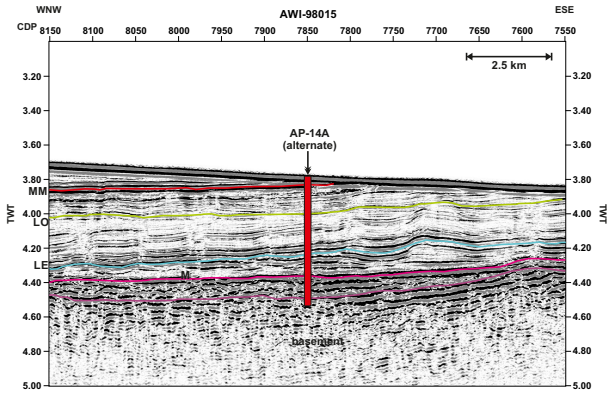

Figure AF15. Top: map of proposed alternate Site AP-02A with multibeam swath bathymetry, multichannel seismic (MCS) tracks and common depth point (CDP) numbers. Multibeam swaths have 50 m resolution. Bottom: MCS Line AWI-98015 across Site AP-02A. M = Maastrichtian, LE = lower Eocene, LO = lower Oligocene, MM = middle Miocene, purple = top basement. TWT = two-way traveltime.

Site AP-02A

Priority:	Alternate for Site AP-08A
Position:	40.8604012°S, 27.2537003°E
Water depth (m):	2620
Target drilling depth (mbsf):	700
Approved maximum penetration (mbsf):	700
Survey coverage (track map; seismic profile):	Bathymetric and seismic track map MCS data: • Primary line: CDP 3500 on AWI-98015
Objective(s):	• Cretaceous to Neogene record • Date the age ranges of the observed unconformities and interpret their causes (M, LE, LO, MM) • Date oldest sediment overlying crust and determine paleodepth and paleoenvironment • Recover high-latitude paleotemperature records of the transition from the Cretaceous supergreenhouse and through the Paleogene • Recover critical intervals of ocean–climate transitions (Mi5, Mi4, Mi1, Oi1, PETM[?], K/Pg boundary, OAE 3) • Unravel the nature of Agulhas Plateau basement
Coring program:	Hole A: APC to 300 mbsf, XCB to 650 mbsf Hole B: APC to 300 mbsf, XCB to 650 mbsf Hole C: drill to 640 mbsf, RCB to 700 mbsf
Downhole measurements program:	None
Nature of rock anticipated:	Foraminifer ooze, basalt

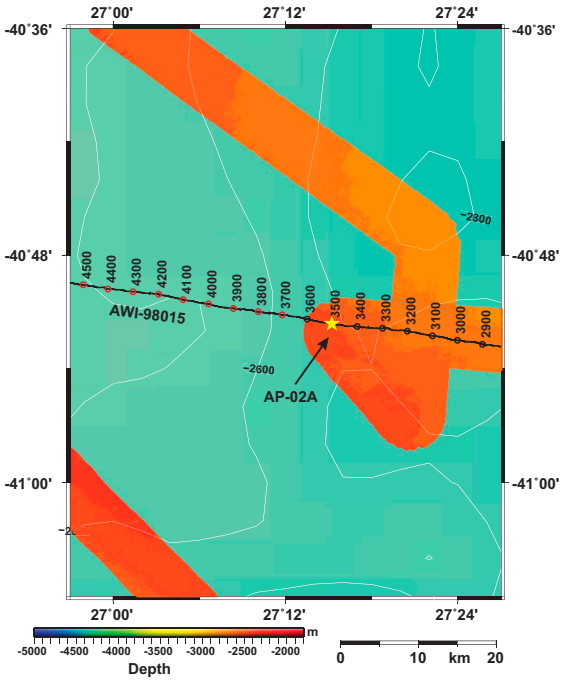

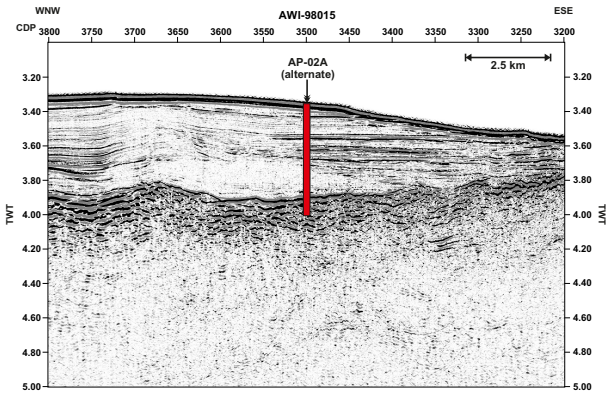

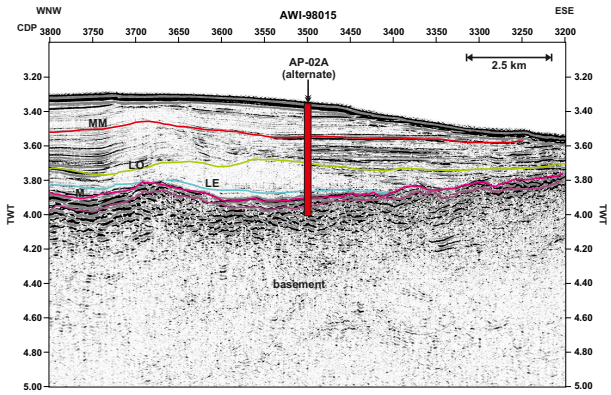

Figure AF16. Top: map of proposed alternate Site AP-12A with multibeam swath bathymetry, multichannel seismic (MCS) tracks and common depth point (CDP) numbers. Multibeam swaths have 50 m resolution. Bottom: MCS Line AWI-98017 across Site AP-12A. M = Maastrichtian, LE = lower Eocene, LO = lower Oligocene, MM = middle Miocene, purple = top basement. TWT = two-way traveltime.

Site AP-12A

Priority:	Alternate for Site AP-08A
Position:	40.0681992°S, 24.5436993°E
Water depth (m):	3100
Target drilling depth (mbsf):	800
Approved maximum penetration (mbsf):	800
Survey coverage (track map; seismic profile):	Bathymetric and seismic track map MCS data: • Primary line: CDP 2400 on AWI-98017
Objective(s):	• Cretaceous to Neogene record • Date the age ranges of the observed unconformities and interpret their causes (M, LE, LO, MM) • Date oldest sediment overlying crust and determine paleodepth and paleoenvironment • Recover high-latitude paleotemperature records of the transition from the Cretaceous supergreenhouse and through the Paleogene • Recover critical intervals of ocean–climate transitions (Mi5, Mi4, Mi1, Oi1, PETM[?], K/Pg boundary, OAE 3) • Unravel the nature of Agulhas Plateau basement
Coring program:	Hole A: APC to 300 mbsf, XCB to 750 mbsf Hole B: APC to 300 mbsf, XCB to 750 mbsf Hole C: drill to 740 mbsf, RCB to 800 mbsf
Downhole measurements program:	None
Nature of rock anticipated:	Foraminifer ooze, basalt